WOOD AND FIBER SCIENCE

The Sustainable Natural Materials Journal

Volume 58, Number 1, 2026 (ISSN 0735-6161)

Open Access

JOURNAL OF THE

SWST – International Society of Wood Science and Technology

EDITORIAL AND PUBLICATION POLICY

Wood and Fiber Science as the official publication of the Society of Wood Science and Technology publishes open access papers with both professional and technical content. Original papers of professional concern, or based on research of international interest dealing with the science, processing, and manufacture of wood and composite products of wood or wood fiber origin will be considered.

All manuscripts are to be written in US English, the text should be proofread by a native speaker of English prior to submission. Any manuscript submitted must be unpublished work not being offered for publication elsewhere.

Papers will be reviewed by referees selected by the editor and will be published in approximately the order in which the final version is received. Research papers will be judged on the basis of their contribution of original data, rigor of analysis, and interpretations of results; in the case of reviews, on their relevancy and completeness.

Color photos/graphics will be offered at no additional cost to authors. The Open Access fee will be $1800/article for SWST members and $2000/article for nonmembers. Reduced rates are available for authors based in developing countries.

Technical Notes

Authors are invited to submit Technical Notes to the Journal. A Technical Note is a concise description of a new research finding, development, procedure, or device. The length should be **no more than two printed pages in WFS**, which would be five pages or less of double-spaced text (TNR12) with normal margins on 8.5 x 11 paper, including space for figures and tables. In order to meet the limitation on space, figures and tables should be minimized, as should be the introduction, literature review and references. The Journal will attempt to expedite the review and publication process. As with research papers, Technical Notes must be original and go through a similar double-blind, peer review process.

On-line Access to *Wood and Fiber Science* Back Issues

SWST is providing readers with a means of searching all articles in *Wood and Fiber Science* from 1968 to present.

Visit the SWST website at https://www.swst.org and go to Wood & Fiber Science Online. Click on either SWST Member Publication access (SWST members) or Subscriber Publication access (Institution Access). All must login with their email and password on the https://www.swst.org site or use their ip authentication if they have a site license.

As an added benefit to our current subscribers, you can now access the electronic version of every printed article along with exciting enhancements that include:

- IP authentication for institutions (only with site license)
- Enhanced search capabilities
- Email alerting of new issues
- Custom links to your favorite titles

(ISSN 0735-6161)

WOOD AND FIBER SCIENCE

JOURNAL OF THE SOCIETY OF WOOD SCIENCE AND TECHNOLOGY

VOLUME 58 JANUARY 2026 NUMBER 1

CONTENTS

Editorial: The New and Improved Wood and Fiber Science

At its June meeting, the SWST Executive Board reviewed the status of this journal since the selection of a new editor and the move to open access in 2022. The journal is currently struggling to obtain a suitable number of quality submissions, and this has resulted in a declining impact factor that has further eroded our submissions rate. The journal is an important component of the Society, but many Professional Society-based journals are struggling to attract papers and remain financially viable.

The Board concluded that it needed more vigorous leadership in order to move forward. As a result, Professor Eric Hansen from Oregon State University will become Editor and Dr. Ling Li, Associate Professor of Sustainable Bioenergy Systems at the University of Maine; Professor Andreja Kutnar, University of Primorksa; and Professor Arijit Sinha, Oregon State University will serve as Associate Editors. They look forward to your manuscripts as they work to reverse a three-year decline of the journal in terms of submissions and turn-around times.

We recognize that there are many potential outlets for your scholarly work, but the journal depends on your support. We would encourage you to consider Wood and Fiber Science in your publication plans and look forward to an increase in submissions under the new leadership.

Wood and Fiber Science, 58(1), 2026, pp. 1–1
https://doi.org/10.22382/wfs-2026-01

Competitiveness and cost structure analysis of selected wood-processing industries in Ethiopia

Busha Teshome *
PhD, Researcher
Center for International Forestry Research (CIFOR), Addis Ababa, Ethiopia
Email: b.teshome@cifor-icraf.org/ bayush051@yahoo.com

Habtemariam Kassa
PhD, Principal Scientist
Center for International Forestry Research (CIFOR), Addis Ababa, Ethiopia
Email: h.kassa@cifor-icraf.org

Tsegaye Bekele
Professor
Wondo Genet College of Forestry and Natural Resource, Hawassa University, Hawassa Ethiopia
Email: bekele57@yahoo.com

Jürgen Pretzsch
Professor
Technische Universität Dresden, Institute of International Forestry and Forest Product, Germany
Email: pretzsch@forst.tu-dresden.de

(Received 12 July 2025)

Abstract: Wood-processing industries contribute to economic and social development by producing a variety of wood products, yet limited information exists on their competitiveness and cost structures in Ethiopia. In this study we examined their competitiveness by using diamond model and cost structures of chipboard, plywood, and sawn wood industries using a survey of 29 large and medium firms and detailed cost analysis of three case studies. We used both qualitative and quantitative data to ensure a comprehensive analysis; quantitative data were examined using descriptive statistics including frequencies, means, and percentages to identify measurable patterns and trends, while qualitative data provided contextual depth and insights into the operational and strategic challenges faced by respondents. Findings revealed that limited support from government was a key constraint to competitiveness, while growing demand for wood products had a positive effect. Cost structures varied by industry type: raw materials were the largest expense for chipboard (43%) and plywood (51%) producers, while overhead costs dominated (76%) for the sawn wood (sawmill) respondent from 2019 to 2024. Profitability improved across all products: chipboard margins rose from 6.9% to 7.1%, plywood from 9.6% to 22.8%, and sawn woods from 3.8% to 13.3%. Enhancing the competitiveness of Ethiopia's wood-processing sector requires addressing industry-specific challenges and costs.

Keywords: Chipboard; Diamond model; Plywood; Sawn wood; Wood products

Introduction

Trade of wood and wood products is growing across Africa (AFF 2019), with wood-processing industries playing a key role in producing diverse products that support both economic and social development (Gordeev 2020; Weiss et al. 2011). In Ethiopia, demand for forest products has steadily increased, but the supply gap continues to widen despite efforts to develop the sector. Wood product imports rose sharply from 17,750 m^3 in 1997 to 128,914 m^3 in 2017, while the trade deficit grew from USD 37.2 million to USD 263.4 million over the same period. On average, Ethiopia's annual wood product imports were about USD 118.7 million, compared to just USD 1.5 million in exports, resulting in an annual trade deficit of roughly USD 117.2 million (Tolera 2021). This highlights the need to enhance the competitiveness of wood-processing industries by developing high-quality, value-added products and promoting sustainable forestry practices (Kolev et al. 2020; Milicevic et al. 2017). To succeed in an unpredictable economic environment,

* Corresponding author

these industries must strengthen their competitive advantage, which depends on factors such as the macroeconomic context, business environment, and operational strategies (Deewong et al. 2013; Wethyavivorn et al. 2009; Porter 1990). Moreover, wood-processing industries face competition both domestically and internationally (Milicevic et al. 2017).

Competitiveness refers to a firm's ability to deliver products more effectively and efficiently than its rivals (Porter 2000). To analyze the factors that contribute to competitive advantage in an industry, Porter (2000) introduced the diamond model. Industrial competitiveness is shaped by four interrelated and mutually reinforcing elements: factor conditions, demand conditions, the presence of related and supporting industries, and the nature of firm strategy (Porter 1990). Consequently, it is essential to identify the factors influencing competitiveness to understand the positioning of wood-processing industries. This understanding will enable the formulation of targeted measures and strategies aimed at enhancing competitiveness of these industries.

In addition to the factors identified in Porter's diamond model, a firm's competitiveness is strongly influenced by how effectively it utilizes its inputs (Porter, 1998). Companies seek to maximize profit per unit, either by reducing production costs or increasing output, depending on their strategic goals (Gordeev 2020; Sujová et al. 2015; Drury 2007). A thorough understanding of a company's cost structure supports better cost management by revealing how costs behave (Akyuz et al. 2020; Siadat et al. 2007). This structure is shaped by operational efficiency and strategic cost management, directly impacting profitability and shareholder returns. However, the wood-processing industry in Ethiopia continues to face low productivity, limiting its competitiveness (Gebreeyesus 2013). Globally, the forest sector is under growing pressure to respond to challenges such as climate change, ecosystem services, recreation, renewable energy, and bioeconomy demands, while meeting strict sustainability requirements. Tackling these issues requires improved sector performance, innovation in products and technologies, and greater adaptability to changing market conditions. This study aims to address these gaps by identifying the key factors influencing competitiveness and analyzing the cost structures of wood-processing industries, categorized by clusters of wood product types. We focused specifically on the chipboard, plywood, and sawn wood sectors. By generating insights into industry dynamics and cost structure, the research seeks to inform strategies and policy interventions that could enhance the competitiveness of Ethiopia's wood-processing industries and reduce import dependency.

Methodology

Study area

We conducted the study across four regional states in Ethiopia: Oromia, Amhara, Sidama, and Tigray, as well as in the Addis Ababa city administration. In the Oromia region, we focused on the towns of Shashemene, Jimma, and Arsi Negelle, and in the Amhara region, Bahirdar, Injibara, and Debrebirhan. Additionally, Hawassa city was included from the Sidama region, along with Maichew town from Tigray. The selection criteria for the wood-processing industries involved several factors: the volume of wood products produced; regional distribution to capture the diverse contexts of resource access and marketing; ownership types, both state and privately owned; and the willingness of factory owners and experts to provide accurate information. According to the Ethiopian Central Statistical Authority (CSA), the manufacturing sector is categorized into three groups: large- and medium-scale, small-scale, and cottage and handicraft industries. This classification is based on the number of individuals employed in manufacturing and the level of production means available at each establishment. Large- and medium-scale manufacturing operations employ 10 or more individuals and utilize power-driven machinery (CSA 2014). Figure 1 illustrates the locations of the cities where the studied wood-processing industries are situated. The selected sample industries produced a variety of wood products, including chipboards from 6 industries, plywood from 3 industries, and sawn wood operations from 20 industries.

Methods of data collection and analysis

Secondary data for this study were gathered from both published and unpublished sources, including reports from relevant government agencies and other organizations at both federal and regional levels. Following this, a formal survey was conducted involving 29 wood-processing industries, which represented 30% of the total of 96 large- and medium-sized wood-processing industries in Ethiopia, as reported by CSA in 2016. Notably, 78% of these industries were sawmills (Indufor 2016). From the sample of 29 wood-processing industries, 20 sawmills were randomly selected for further analysis. Additionally, the sample included six chipboard processing manufacturers and three plywood-processing industries, accounting for 60% and 27% of the categories, respectively. The survey questions were crafted to align with the diamond model, focusing on production factors, demand, firm strategy and rivalry, related and supporting sectors, and government support conditions to evaluate industry competitiveness.

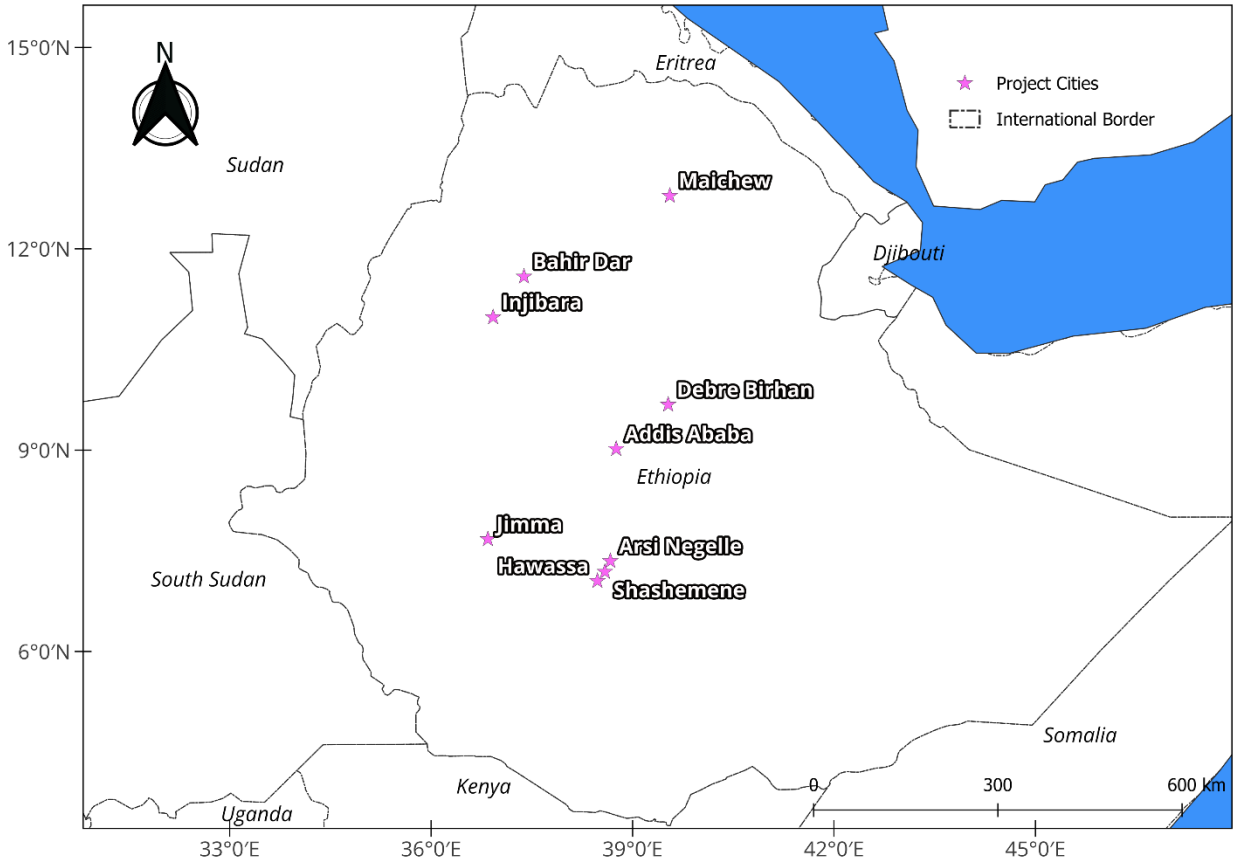

Figure 1. Map of Ethiopia showing nine urban centers where respondent wood-processing manufacturers were located.

Respondents utilized a five-point Likert scale to rate their perceptions, with scores ranging from 1 (most constraining) to 5 (most enhancing). To gain deeper insights into the cost structures of the manufacturers, case studies were also conducted for three wood-processing manufacturers. The cost-structure analysis is based on revenue and expense data collected from wood-processing industries for two fiscal years: 2019, covering the period from July 8, 2018, to July 7, 2019, and 2024, covering July 8, 2023, to July 7, 2024. Data collection involved both surveys and case studies. The initial survey was conducted between April and June 2017, while in-depth case studies were carried out in October 2019 and June 2025 to gather detailed and relevant cost structure information. Analyzing a firm's competitiveness necessitates examining the underlying factors that influence individual firms and industries (Porter 1998). Consequently, this descriptive study employed Porter's framework to identify the factors impacting the competitiveness of Ethiopia's wood-processing industries. The quantitative data obtained from the survey were analyzed using descriptive statistics, including means, frequencies, and percentages using Microsoft Excel®.

Results and Discussion

Descriptive analysis of wood-processing industries

The surveyed wood-processing industries, specifically chipboard manufacturers, have been established for 6 to 55 years and employ between 26 and 350 people. Of the six manufacturers, four (67%) are privately owned and two (33%) are state-owned. Four (67%) manufacturers plan to expand, while two (33%) wish to maintain their current operations. All manufacturers primarily use Eucalyptus logs, with three also utilizing sawdust from nearby sawmills. They mainly produce various sizes of chipboard products, relying on bank loans and profits for capital, with reinvestment of profits being the primary source. Decision-making differs in privately owned manufacturers, the owner decides, while in state-influenced or state-owned manufacturers, the general manager makes decisions, subject to board approval.

Among the three plywood manufacturers, two were established in the 1960s, while the Debrebirhan plywood factory opened in 2017. Employee numbers are 76 at Jimma plywood factory,

82 at Debrebirhan, and 89 at Ethiopian Plywood Enterprise. Two (67%) manufacturers plan to expand, while one (33%) intends to maintain its current status. All manufacturers stock raw materials before the rainy season due to forest inaccessibility in winter, using Eucalyptus logs and urea-formaldehyde for production. They primarily produce various sizes of plywood, relying on reinvested profits and bank loans for capital. Decision-making is led by general managers, with oversight from boards in two (67%) manufacturers and a private owner in one (33%).

The analysis of 20 medium- and large-sized sawmills reveals that their establishment dates range from 2 to 20 years, with employee numbers varying from 12 to 162. Among these, three (15%) are state-owned and 17 (85%) are privately owned. Eleven (55%) sawmills plan to expand, five (25%) intend to maintain their current status, and four (20%) aim to downsize and close.

The primary log species used include *Cupressus lusitanica* (all sawmills), *Juniperus procera* (13 sawmills), *Cordia africana* (11 sawmills), and *Pinus patula* (10 sawmills), with some also using *Persea americana*. Financial capital comes from bank loans, home equity loans, and reinvested profits. Decision-making is led by general managers, with oversight from boards in state-owned mills and primarily by the owners in private mills. Key characteristics of the manufacturers are summarized in Table 1.

Factors affecting competitiveness of wood-processing industries

The competitiveness of the wood-processing industries is a prerequisite for developing high-quality and value-added products and contribute to sustainable forestry (Milicevic et al. 2017). Competitiveness is the firm's ability to provide products more effectively and efficiently compared to its competitors (Porter 2000). Firms in each nation compete in both domestic and global markets (Porter 1998). Porter (2000) developed the diamond model to identify factors affecting the competitive advantage of industry. According to Porter (1990: Figure 2.), industrial competitiveness is determined by four interdependent and mutually reinforcing attributes and by the level of government support. These are production factor conditions, demand conditions, presence of related and supporting sectors, and the nature of firm strategy.

Table 1. Description of respondent wood-processing manufacturers.

Factors		Chipwood	Plywood	Sawmill
		Shares in number (%)		
Ownership	Private	4 (67%)	1 (33%)	17 (85%)
	Shareholder	2 (33%)	2 (67%)	3 (15%)
Expansion	Plan to expand	4 (67%)	2 (67%)	11 (55%)
	Maintain the status	2 (33%)	1 (33%)	5 (25%)
	Plan to close			4 (20%)
Employment	Minimum	26	76	12
	Maximum	350	91	162
Raw material	Urea-formaldehyde	6 (100%)	3 (100%)	
	Log	6 (100%)	3 (100%)	20 (100%)

Production factors

Chipboard manufacturers face several constraints impacting competitiveness, as shown in Table 2. Five manufacturers primarily struggle with limited physical resources, particularly forest and land availability. Meanwhile, four manufacturers identify human resources, capital, infrastructure, and knowledge gaps as significant hindrances. Key informants indicate a scarcity of modern machinery and spare parts in the domestic market, leading to reliance on imports. Additionally, investments in chipboard production and forest resource development encounter difficulties in securing loans, as banks prioritize export-oriented agricultural and manufacturing sectors over forestry investments due to the latter's longer gestation period.

We identified key production factors affecting the competitiveness of plywood, including human capital, land, capital resources, and infrastructure (Table 2). Respondents from two of the three manufacturers emphasized that the availability of human resources enhances competitiveness, while limitations in physical resources, capital, infrastructure, knowledge, and skills serve as significant constraints.

Out of 20 sawmills surveyed, 17 respondents identified the availability of low-cost human resources as a key factor enhancing competitiveness (Table 2). However, limitations in physical resources, lack of knowledge, and capital shortages were noted as constraints by 14, 12, and 11 sawmills, respectively. Key informants highlighted that government control over most forest resources restricts raw material supply, particularly for privately owned sawmills.

Demand factors

The results indicate that demand factor conditions significantly enhance the competitiveness of chipboard manufacturers, with respondents from five manufacturers highlighting market size as crucial. Additionally, four manufacturers emphasized the importance of customer satisfaction regarding service and product quality, as well as the adoption of new products. This suggests that effectively responding to consumer needs

Table 2. Factors affecting respondent competitiveness.

Categories of factors		Chipwood		Plywood		Sawmill	
		Enhancing (n)	Constraining (n)	Enhancing (n)	Constraining (n)	Enhancing (n)	Constraining (n)
Production factor condition	Human	2	4	2	1	17	3
	Physical	1	5	1	2	6	14
	Capital	2	4	1	2	9	11
	Knowledge	2	4	1	2	8	12
Demand condition	Market size	5	1	2	1	14	6
	Adoption of new product	4	2	3	-	14	6
	Satisfaction with products	4	2	1	2	7	13
Firm strategy, structure, and rivalry	Work plan	4	2	3	-	17	3
	Innovation activity	3	3	2	1	6	14
	Age of establishment	4	2	2	1	17	3
	Competition in the market	3	3	1	2	15	5
Related and supporting sector	Energy supplier	2	4	1	2	11	9
	Research institutions	2	4	1	2	6	14
	Higher learning institutions	2	4	1	2	4	16
Government support	Incentives	4	2	2	1	13	7
	Availability of foreign currency	1	5	-	3	8	12
	Illegal forest harvest	2	4	1	2	5	15

through innovative offerings can lead to increased business size and profitability.

For all the plywood manufacturers, adoption of new products was identified as a factor that positively affects competitiveness. Respondents in two of the plywood manufacturers identified market size as enhancing factor, and the lack of satisfaction of customer in terms of product quality, prices, and services as constraining factors for competitiveness (Table 2).

The respondents in the 14 sawmills considered the availability of a relatively large wood product market and customer adoption of new products as sources of competitive advantage for the sawmills. Field level observations helped reveal that in local markets, products from the Shashemene sawmill had much higher demand. A low level of customer satisfaction on price, product quality, and customer services was identified as a constraining factor by 13 sawmills. Key informant interviews revealed that the lack of customer satisfaction is due to a lack of standard dimensions and defects in the products.

Firm strategy, structure, and rivalry

Results revealed that four chipboard manufacturers viewed work planning and establishment time as key factors for enhancing competitiveness, suggesting that longer establishment periods correlate with increased profits and competitive advantages. Additionally, these manufacturers emphasized the importance of securing raw materials before the rainy season. While three manufacturers identified innovation and market competition as enhancing factors, the other three viewed them as constraints.

The competitiveness of plywood manufacturers is influenced by several factors, including the factory work plan, innovation activity, presence and strength of competitors, and age of establishment. All manufacturers recognized the importance of a work plan, while two identified innovation activity and age of establishment as enhancing factors. Additionally, only two manufacturers noted the lack of certification and weak competition as constraints negatively impacting their competitiveness.

Respondents from 17 sawmills identified work plan and age of establishment as enhancing factors of competitiveness, while 15 sawmills highlighted market competition as a key factor. Key informants noted that a flexible work plan boosts competitiveness, but limited technical support and a lack of skilled workforce in wood technologies hinder innovation, which was recognized as a constraining factor by 14 sawmills.

Related and supporting sectors

The competitiveness of four manufacturers is constrained by the limited involvement of energy suppliers, research institutions,

and universities in supporting the wood-processing industry. Key informants noted that higher education and research institutions contribute insufficiently to innovation and new technology development, while frequent power interruptions significantly disrupt production processes.

In this study, electricity generating companies and research institutions were identified as key supporting sectors for plywood manufacturers; however, two manufacturers viewed their current roles as constraints to competitiveness due to the lack of a reliable power supply in Ethiopia. Additionally, the insufficient engagement of research institutions and universities in wood-processing technology research and training has led to a low level of human resource capacity within the industry.

Universities, research institutions, and electric suppliers were identified as related and supporting sectors for sawmills (Table 2). Inadequate support universities and research institutions were reported as constraining factors by respondents from 16 and 14 sawmills, respectively. This is mainly because these institutions have had limited links with sawmills to make a meaningful contribution in making them more competitive. Electricity supply was considered as an enhancing factor by respondents from 11 sawmills, while 9 sawmills identified it as constraining factor. Key informants revealed that frequent blackouts and voltage fluctuations were common affecting production processes and capacities of sawmills, and thereby their profitability.

Government support

The results indicated that the main constraints faced by chipboard manufacturers are a lack of foreign currency and illegal wood product harvesting, identified by five and four manufacturers, respectively. A key informant noted that the foreign currency shortage particularly impacts the import of raw materials like urea-formaldehyde. Conversely, tax incentives for imported machinery and plantation development offered by the government are viewed as beneficial by four manufacturers.

To enhance the competitiveness of plywood manufacturers, government support conditions include providing incentives for wood-processing, improving foreign currency availability, and controlling illegal wood harvesting. While two manufacturers view government incentives, such as low tariff rates on imported machinery, as beneficial, all manufacturers identify foreign currency access as a significant constraint, essential for importing chemicals, spare parts, machines, and equipment.

Government support conditions identified to enhance the competitiveness of sawmills include incentives for wood-processing, improved foreign currency availability, and control of illegal wood harvesting. Out of 20 sawmills surveyed, 13 respondents viewed these conditions positively, particularly appreciating tax incentives for establishing sawmills, while 7 considered them constraining. Key informants noted that the low 5% tariff on lumber imports (ERCA 2016), intended to curb illegal harvesting, has not effectively addressed the issue, as restrictions on legal harvesting from natural forests have led to increased illegal logging and deforestation. Respondents from 15 sawmills identified the failure to control illegal harvesting and the restrictions on legal harvesting from forests as significant constraints, while 12 sawmills highlighted limitations in accessing foreign currency for importing essential raw materials, spare parts, machines, and equipment. Additionally, specific species like *J. procera, Podocarpus falcatus*, *Hagenia abyssinica,* and *Cordia africana* are scarce in the market due to the requirement of permits for their cutting and harvesting.

Production process and cost structure analysis

The cost structure of the three manufacturers' production system encompasses three main steps: inputs, production, and outputs. The inputs stage includes raw materials, direct labor, and overhead costs (such as insurance, salaries, electricity, maintenance, and depreciation), while the production stage involves transforming raw materials into finished products through various processing operations. Finally, the output stage entails producing different categories of wood products, which includes labor charges for loading and unloading, as well as cutting the wood to meet buyer specifications.

Production and the associated cost structure of Ethiopian Chipboard and Furniture Company (ECAFCO)

The company produces 1st- and 2nd-grade chipboard using the same process, with grading based on quality factors like smoothness and defects. Internal quality control determines the grade. Production volume declined from 2,458 m^3 in 2019 to 846 m^3 in 2024. Ethiopian Chipboard and Furniture Company factory generated a total revenue of USD 922,231, primarily from 1st-grade chipboard, which contributed 97% of sales, while 2nd-grade chipboard and labor charges accounted for 0.5% and 2.5%, respectively. Despite both chipboard grades undergoing the same production process, they are differentiated by quality through internal controls. Table 3 compares key financial figures between the years 2019 and 2024, highlighting changes in sales, expenses, and profitability. Gross sales revenue saw a significant decrease from USD 922,231 in 2019 to USD 362,381 in 2024, indicating a sharp decline in business volume or pricing. Correspondingly, total operating expenses also dropped from USD 830,742 to USD 325,531, showing that cost-cutting measures were likely implemented to align with

reduced revenue. Despite the fall in absolute figures, operating profit before tax decreased less dramatically, from USD 91,488 to USD 36,850, suggesting improved operational efficiency. Similarly, net profit declined from USD 64,042 to USD 25,795. Interestingly, the net profit margin slightly increased from 6.9% in 2019 to 7.1% in 2024, which indicates that the company became marginally more profitable relative to its revenue, despite the overall contraction in financial performance. The decline in total revenue production for 2024 can be primarily attributed to a series of operational challenges faced by the factory. One of the main reasons was a shortage of essential raw materials, particularly formaldehyde, which is critical for the factory's manufacturing processes. This shortage disrupted production schedules and limited the volume of chipwood product that could be produced and sold. Additionally, the company faced repeated mechanical breakdowns due to aging equipment, which further hampered production efficiency. These machines, being outdated, frequently required maintenance, but sourcing spare parts became increasingly difficult, causing prolonged downtimes. Furthermore, the factory was in the process of relocating its operations to a new production center, which introduced additional disruptions. Collectively, these issues significantly affected the company's ability to maintain previous levels of output, leading to a notable drop in revenue for 2024, although the net profit margin slightly increased in 2024.

The total estimated production cost for ECAFCO was allocated as follows: 43% for raw materials, 20% for direct labor, and 37% for overhead (Figure 2). ECAFCO's production of chipboard relies on raw materials, primarily round logs and urea-formaldehyde resin powder, with a total raw material cost of which 55% is attributed to glue and the remainder to eucalyptus logs. The direct labor cost, predominantly consisting of salaries (76%), followed by wages (13%) and overtime payments (11%), benefited from Ethiopia's high labor supply that helps lower overall production costs. Overhead costs made up 37% of total input costs, with administrative expenses representing 74% of the overhead, covering customer service, production scheduling, transport planning, and vendor costs.

Production and the associated cost structure of the Ethiopian Plywood Enterprise

The Ethiopian Plywood Enterprise primarily produces plywood, with production decreasing from 670 m³ in 2019 to 129 m³ in 2024. The analysis presents a comparison of financial performance between 2019 and 2024 (Table 4). Gross sales revenue declined significantly from USD 450,463 in 2019 to USD 113,420 in 2024, reflecting a major reduction in overall sales. Correspondingly, total operating expenses also decreased from USD 388,638 to USD 76,433, indicating cost reductions aligned with the lower production. Despite the decline in revenue and expenses, operating profit before tax decreased only moderately, from USD 61,825 to USD 36,986, showing improved efficiency in managing costs. Tax expenses fell from USD 18,547 to USD 11,095, while net profit declined from USD 43,277 to USD 25,890. Notably, the net profit margin increased sharply from 9.6% in 2019 to 22.8% in 2024, suggesting that the factory became significantly more profitable relative to its revenue, successfully enhancing profitability despite the drop in sales. The decline in 2024 revenue was mainly due to raw material shortages, especially formaldehyde, frequent breakdowns of aging equipment, and the factory having been

Table 3. Revenue and profit of the Ethiopian Chipboard and Furniture Company.

Activity cost in USD	2019	2024
Gross sales revenue	922,231	362,381
Total operating expenses	830,742	325,531
Operating profit before tax	91,488	36,850
Expense on tax	27,447	11,055
Net profit	64,042	25,795
Net profit margin (%)	6.9%	7.1%

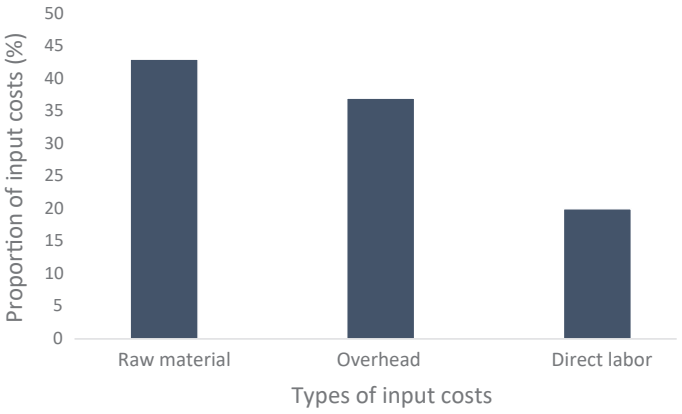

Figure 2. Percentage share of production input costs (ECAFCO).

Table 4. Revenue and profit of the Ethiopian Plywood Enterprise.

Activity cost in USD	2019	2024
Gross sales revenue	450,463	113,420
Total operating expenses	388,638	76,433
Operating profit before tax	61,825	36,986
Expense on tax	18,547	11,095
Net profit	43,277	25,890
Net profit margin (%)	9.6%	22.8%

affected by a government infrastructure development road in the factory campus. These challenges disrupted production and reduced output. Despite the lower revenue, the net profit margin slightly improved in 2024.

The total annual production costs for Ethiopian Plywood Enterprise are illustrated in Figure 3. Raw materials, costing 51%, include logs, glue, hardener, wheat flour, and imported adhesive chemicals like urea-formaldehyde resin, which alone make up 32.82% of raw material costs due to their high import expense. Direct labor, costing (13%), is mostly salary-based (74%), with additional costs for wages (16%), overtime (1%), and performance-based incentives (9%). Overhead costs total (36%), covering administrative expenses (44%), depreciation (35%), and indirect labor (20%).

Production and the associated cost structure of the Arsi Negelle Sawmill

At the Arsi Negelle Sawmill (ANS), logs are crosscut and sawn to produce lumber as the main product, with by-products such as firewood, sawdust, slabs, and resizing leftovers. In 2019, the sawmill produced 10,886.5 m³ of output, including 4,020.5 m³ of lumber and 6,866 m³ of by-products like firewood, sawdust, and slabs. By 2024, total output dropped to 5,699.8 m³, with 2,699 m³ of lumber and 3,000 m³ of by-products. Lumber prices vary by grade, size, species, and use, and are set by the enterprise. In 2019, the factory generated a gross revenue of USD 1,396,463, with 93% from lumber sales, 4% from slabs, and the rest from other products and services, mainly serving the domestic market (Table 5). With total operating expenses of USD 1,319,488, the factory achieved a profit before tax of USD 76,974 and paid USD 23,092 (30%) in income tax, resulting in a net profit of USD 53,882. Access to raw materials from its own plantations and the high quality of its lumber support the factory's full production capacity and strong market preference.

The total annual production costs for ANS, as shown in Figure 4, were dominated by overhead costs (76.3%), followed by raw materials (15.7%) and direct labor (8%). Direct labor was the lowest cost component, with salaries and wages making up 79.5% and 19.5%, respectively, reflecting low daily labor rates. Overhead costs, mainly from administrative expenses (49.2%) and indirect labor (44.9%), also include depreciation (5.5%) and electricity (0.3%), highlighting the factory's cost structure as heavily overhead-driven.

Comparison of the production costs of the three case study manufacturers

The analysis of the three case study manufacturers (ECAFCO, EPE, and ANS) reveals both similarities and differences in their production cost structures, particularly in the input costs for chipboard, plywood, and sawmill operations (Table 6). Notably, raw materials constituted a significant portion of costs in the chipboard and plywood manufacturers, with urea-formaldehyde accounting for about half of these expenses due to its high market price as an imported material. Conversely, ANS had the lowest raw material costs, primarily utilizing logs sourced from nearby plantations, which minimizes transportation expenses and contributes to its cost efficiency.

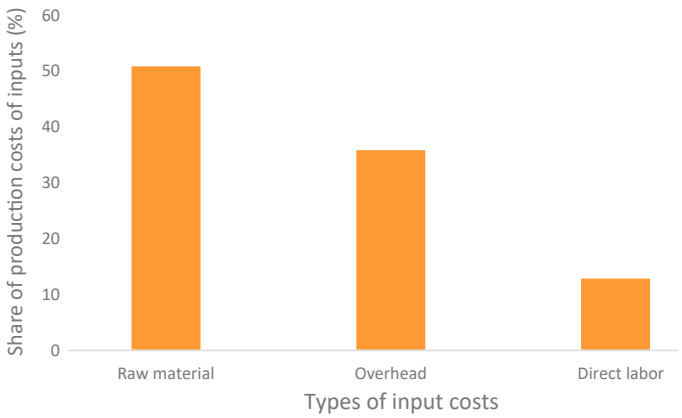

Figure 3. Percentage share of production input costs of the Ethiopian Plywood Enterprise.

Table 5. Revenue and profit of the Arsi Negelle Sawmill.

Activity cost in USD	2019	2024
Gross sales revenue	1,396,463	791,956
Total operating expenses	1,319,488	641,303
Operating profit before tax	76,974	150,653
Expense on tax	23,092	45,195
Net profit	53,882	105,457
Net profit margin (%)	3.8%	13.3%

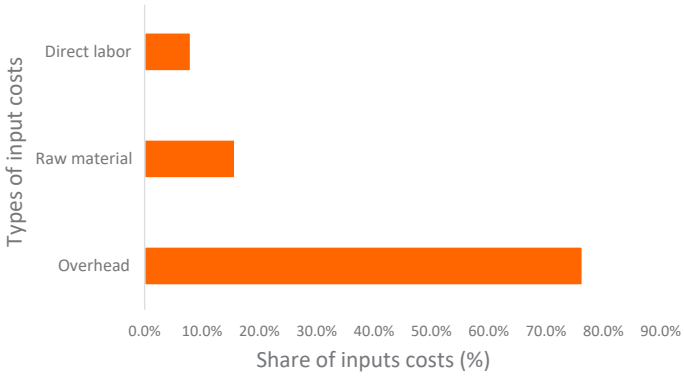

Figure 4. Percentage share of production input costs of the Arsi Negelle Sawmill.

Table 6. Comparison of the production costs of the three case study enterprises

	Production cost in % share		
Input costs	Case study-ECAFCO	Case study-EPE	Case study-ANS
Raw material	43	51	15.7
Direct labor	20	13	8
Overhead	37	36	76.3

The overhead cost constituted the second largest part of the total production costs for the chipboard and plywood manufacturers. The overhead cost of the chipboard and plywood manufacturers included depreciation, electricity, indirect labor, and intermediate inputs. Of the manufacturers, the highest overhead cost (76.3%) was observed in the sawmill, accounted for mainly by the indirect labor cost. This may be associated with the largest number of employees in this sawmill to support the production activities.

We found that all three manufacturers had relatively low direct labor costs, but they differ in net profit margins, with EPE achieving the highest at 9.6% of gross sales, followed by ECAFCO at 6.9%, and ANS at 3.8% in 2019. This suggests that ownership status may influence profitability, as privately owned firms like EPE and ECAFCO tend to maximize profits by minimizing costs, unlike the state-owned ANS, which aligns with findings from empirical studies indicating that private firms often outperform state-owned ones in profit generation (Goldeng et al. 2008).

Discussion

In Ethiopia, the manufacturing sub-sector faces several challenges that hinder its contribution to the national economy (Gebreeyesus 2013). This study identified key factors affecting the competitiveness of wood-processing industries through the lens of Porter's diamond model (Porter 1990). Among these factors, production conditions emerged as the most significant constraint on the competitiveness of wood manufacturers. The limited availability of raw material supply consisting of forest resources in the market, inadequate human resource capacity, and underdeveloped infrastructure are critical barriers. These findings resonate with the work of Ogunwusi and Olife (2012), Chamshama et al. (2009), and Asumadu (2004), who noted that technological limitations, a lack of skilled labor, insufficient access to machinery, and scarce forest resources can impede productivity and growth in forest industries across developing nations. Additionally, there is a notable shift in industrial wood production from natural forests to plantations (Kok et al. 2014). The positive factor identified in this study is the increasing demand for wood products within the country, which reflects a broader trend of rising wood product consumption across African nations (AFF 2019; GEF 2013; Huang et al. 2013). The levels of access to energy, government support, and firm strategy varied among the three wood-processing industries. Sawmill and chipboard manufacturers, in particular, suffer from low levels of government assistance, corroborated by reports indicating that only 8% of enterprises in Ethiopia have received such support (Gebreeyesus and Mohnen 2013). Furthermore, a lack of collaboration among wood-processing industries undermines their competitive advantages. To enhance competitiveness, it is essential to foster strong relationships and cooperation between producers and users of raw materials, as well as with technology providers and market information sources (Porter 2000).

We highlighted notable differences in the cost structures among the three wood-processing industries due to the types of inputs utilized. Ethiopian Chipboard and Furniture Company and the Ethiopian Plywood Enterprise incurred relatively high raw material costs, comprising 43% and 51% of their total expenses, respectively. This finding aligns with the observations of Ogunwusi (2012) and Asumadu (2004), who noted challenges such as a scarcity of domestic raw material suppliers and inadequate infrastructure for wood product inputs in sub-Saharan Africa. Additionally, other research has emphasized the necessity for the forest industry to explore alternative processes that leverage more affordable raw materials, while maintaining product quality (Dieter and Englert 2006; Lantz 2005). These insights can be applied to other wood-processing industries, taking into account the unique circumstances and contexts of each factory.

The findings reveal that the Arsi Negelle Sawmill experienced the highest overhead cost component, accounting for 76.3% of its total expenses. Studies indicate that elevated overhead costs often stem from inaccurate decision-making, ineffective production planning, low plant productivity, and increased production costs within the industry (Golub et al. 2017). This significant overhead suggests that the factory employs a considerable number of staff who are not directly involved in lumber production. Conversely, the sawmill benefits from lower costs for log raw materials due to its proximity to its own plantation. This trend is reflected in the direct labor costs, which represent the smallest expense across all three wood-processing industries. Previous studies (e.g., Ogunwusi and Olife 2012; Ukrainski and Varblane 2005) have highlighted that low labor costs in the forest industry can bolster competi-

tiveness. However, a predominant portion of the workforce consists of unskilled laborers, which ultimately constrains the industry's capacity for innovation and, consequently, its overall competitiveness (Tether et al. 2005).

We also assessed the profitability of three wood product-processing manufacturers, revealing that the EPE achieved the highest net profit margin at 9.6% of gross sales revenue, followed by ECAFCO with 6.9%. In contrast, the ANS exhibited the lowest net profit share at 3.8%, primarily attributed to high overhead costs. This indicates that the private plywood factory outperformed both the shareholder chipboard company and the state-owned sawmill in terms of profitability. To enhance competitiveness within the industry, it is crucial for the government to facilitate access to raw materials, particularly urea-formaldehyde, which is essential for cost-effective panel production. Additionally, managing overhead costs is recommended as a strategy for the sawmill to achieve its profit maximization objectives. The insights gained from this study could be valuable for other countries facing similar challenges in their wood-processing sectors, provided that the unique contexts of each factory are considered. Furthermore, a recommendation for future research includes employing the same research design over an extended period and with a larger sample size to gain a deeper understanding of the cost structures within wood-processing industries. The findings related to competitiveness, cost structure, and profit analysis can serve as a foundation for further studies in Ethiopia.

Conclusion and policy implications

The findings of this study indicate that the wood-processing industry in Ethiopia faces significant constraints that hinder its competitiveness. Utilizing Porter's determinants, it is evident that factors such as production conditions, related and supporting industries, and government support are critical barriers impacting the competitiveness of chipboard, plywood, and sawmill manufacturers. Conversely, the strategies, structures, and rivalry among firms, along with the growing demand for wood products, positively influence the competitiveness of these industries. The finding by Avenyo (2018) and Jacobson et al. (2008) highlights that key elements affecting the competitiveness of forest industries in sub-Saharan Africa include the availability of raw materials, energy resources, and well-developed infrastructure. These results underscore the urgent need to transform the current state of the sector into a more competitive environment. It is essential for the business landscape to enable wood-processing companies to operate effectively, thereby fostering competitiveness. Additionally, government regulations and services should facilitate competitive success rather than impose constraints. Access to reliable and efficient services from related and supporting industries must be equitable for all firms in terms of cost. Ultimately, collaboration among all stakeholders including input suppliers, producers, processors, manufacturers, marketers, distributors, service providers, and government is crucial to cultivating a competitive environment that benefits the entire sector.

We aimed to analyze the cost structure of wood-processing industries, concluding that the financial performance of the manufacturers was favorable. The cost structure analysis encompassed raw material costs, direct labor costs, and overhead costs within the production cycle of the wood-processing sector. Notably, raw material costs accounted for approximately 50% of total production expenses in both chipboard and plywood manufacturers, with a significant portion attributed to the imported urea-formaldehyde. A comparative analysis revealed that the Arsi Negelle Sawmill had an exceptionally high overhead cost share, comprising 76.3% of its total expenses, primarily due to substantial indirect labor costs that do not directly contribute to lumber production. Interestingly, direct labor, a crucial input, represented the lowest cost among the three wood-processing industries examined. This finding aligns with similar observations made by Adenikinju et al. (2002) regarding other African countries. The evidence suggests that reducing overhead costs at the sawmill and enabling cost-effective access to urea-formaldehyde for chipboard and plywood manufacturers could enhance the sector competitiveness and its contribution to the national economy. ECAFCO's net profit margin modestly increased from 6.9% in 2019 to 7.1% in 2024, reflecting a slight rise in profitability despite a general financial downturn. Conversely, Ethiopia Plywood's margin jumped from 9.6% to 22.8%, showing a substantial improvement in profitability despite reduced sales. Despite high production costs, all studied industries remain profitable; however, they must focus on improving competitiveness and sustaining profits through effective cost management and output maximization. Our scope was limited to three case study industries due to insufficient financial data from a larger sample of wood-processing firms. Additionally, the reliance on a single year of data restricted a more comprehensive longitudinal analysis of costs, revenues, and production volumes in the industry. Given the rising demand for wood products in Ethiopia and their potential economic impact, further quantitative research is essential across the wood-processing sector nationwide. The current lack of understanding poses a significant barrier for policymakers aiming to effectively integrate wood-processing

industries into the Ethiopian economy. The insights derived from this study may provide valuable information for assessing the competitiveness of selected wood-processing industries within the country.

Acknowledgement

We are sincerely grateful to the Rufford Small Grants Foundation and the Center for International Forestry Research (CIFOR) for their support of this study. We also extend our special thanks to the experts from the wood-processing industries for their time and participation in the interviews, as well as to the industries themselves for providing access to valuable data.

References

Adenikinju A, Söderling L, Soludo C, Varoudakis A (2002) Manufacturing Competitiveness in Africa: Evidence from Cameroon, Cote d'Ivoire, Nigeria, and Senegal. EDCC 50(3):643–665.

AFF (African Forest Forum) (2019) The State of Forestry in Africa: Opportunities and Challenges. African Forest Forum, Nairobi Kenya. 186 p. https://afforum.org/wp-content/uploads/2019/06/THE-STATE-OF-FORESTRY-IN-AFRICAweb.pdf

Akyuz KC, Yildirim I, Ersen N, Akyuz I, Memis D (2020) Competitiveness of the forest products industry in Turkey. The revealed comparative advantage index. Drewno. Prace Naukowe. Doniesienia. Komunikaty 63(205).

Asumadu K (2004) Development of wood-based industries in Sub-Saharan Africa. East Brighton, Australia. https://afforum.org/new/web/sites/default/files/English_126.pdf

Avenyo EK (2018) Innovations and firm performance in sub-Saharan Africa: Empirical analyses. https://doi.org/10.26481/dis.20180524ea

Chamshama S, Nwonwu F, Lundgren B, Kowero G (2009) Plantation forestry in sub-Saharan Africa: Silvicultural, ecological, and economic aspects. Discov Innov 21(3). https://doi.org/10.4314/dai.v21i3.48210

CSA (Central Statistical Agency of Ethiopia) (2014) Report on Large and Medium Manufacturing and Electricity Industries Survey. Central Statistical Agency. Addis Ababa, Ethiopia.

CSA (Central Statistical Agency) (2016). Report on Demographic and Health Survey. Central Statistical Agency. Addis Ababa, Ethiopia. http://catalog.ihsn.org/index.php/catalog/6783

Deewong W, Leungbootnak N, Aksorn P, Manu P (2013) Competitiveness Factors of Thai Construction Industry within the AEC Context: A Qualitative Approach. Int Transact J Eng Manage Appl Sci Technol 8(3), https://www.tuengr.com/V08/209M.pdf

Dieter M, Englert H (2006) Competitiveness in the global forest industry sector: an empirical study with special emphasis on Germany. Eur J For Res 126(3):401–412. https://doi.org/10.1007/s10342-006-0159-x

Drury C (2007) Management and Cost Accounting, Sixth Edition, Thomson Learning.

ERCA (Ethiopia Revenue and Customs Authority) (2016) Ethiopia Revenue and Customs Authority https://www.mor.gov.et/

Gebreeyesus M (2013) Industrial policy and development in Ethiopia: Evolution and present experimentation (No. 2013/125). WIDER working paper. https://www.econstor.eu/handle/10419/93684

Gebreeyesus M, Mohnen P (2013) Innovation performance and Embeddedness in networks: Evidence from the Ethiopian footwear cluster. World Dev 41:302–316. https://doi.org/10.1016/j.worlddev.2012.05.029

GEF (Global Environment Fund) (2013) Africa will import—not export—wood. https://www.criterionafrica.com/wp-content/uploads/2017/06/Africa-will-Import-not-Export-Wood.pdf

Goldeng E, Grünfeld LA, Benito GR (2008) The performance differential between private and state-owned enterprises: The roles of ownership, management, and market structure. J Manag Stud 45(7):1244–1273. https://doi.org/10.1111/j.1467-6486.2008.00790.x

Golub SS, Ceglowski J, Mbaye AA, Prasad V (2017) Can Africa Compete with China in Manufacturing? The Role of Relative Unit Labor Costs. World Econ 41(6):1508–1528. https://doi.org/10.1111/twec.12603

Gordeev RV (2020) Assessing competitiveness of forest industry: theoretical and empirical aspects. J Sib Fed Univ Humanit Soc Sci 13(4):507-516. https://elib.sfu-kras.ru/handle/2311/142656 https://doi.org/10.1007/s10668-012-9413-1

Huang W, Wilkes A, Sun X, Terheggen A. (2013). Who is importing forest products from Africa to China? An analysis of implications for initiatives to enhance legality and sustainability. Environment, development and sustainability, 15(2), 339-354.

Indufor (2016) Ethiopia Commercial Plantation Forest Industry Investment Plan. Technical Report. Addis Ababa, Ethiopia.

Jacobson MG, Ham C, Ackerman PA (2008) Forest management educational needs in South African forestry companies. South For 70(3):269–274. https://doi.org/10.2989/SF.2008.70.3.10.671

Kok M, Alkemade R, Bakkenes M, Boelee E, Christensen V, van Eerdt M, van der Esch S, Karlsson-Vinkhuyzen S, Kram T, Lazarova T, Linderhof V, Lucas P, Mandryk M, Meijer J, van Oorschot ML, van Hoof L, Westhoek H, Zagt R (2014) How Sectors can Contribute to Sustainable Use and Conservation of Biodiversity. Secretariat of the Convention on Biological Diversity (Ed.), CBD Technical Series, PBL Netherlands Environmental Assessment Agency, The Hague.

Kolev K, Tsoklinova M, Delkov A (2020) Factor analysis of forestry competitiveness. Forest Science (0861-007X) 56(2). https://www.researchgate.net/publication/345901894_factor_analysis_of_forestry_competitiveness

Lantz V (2005) Measuring scale, technology, and price effects on value-added production across Canadian forest industry sectors. For Policy Econ 7(3):333–344. https://doi.org/10.1016/s1389-9341(03)00074-1

Lundmark R, Lundgren T, Olofsson E, Zhou W (2021) Meeting challenges in forestry: Improving performance and competitiveness. Forests 12(2):208. https://doi.org/10.3390/f12020208

Milicevic S, Nikolic M, Cvetanovic S (2017) The competitiveness of the wood-processing industry in the Republic of Serbia during the period 1995-2015. Industrija 45(3):131–150. https://doi.org/10.5937/industrija45-14579

Ogunwusi AA (2012) The forest products industry in Nigeria. Afr Res Rev 6(4):191–205. https://doi.org/10.4314/afrrev.v6i4.13

Ogunwusi AA, Olife I. (2012). Enhancing productivity of forest industry through industrial clusters concept. Ind Eng Lett 2(8):19. https://www.iiste.org/Journals/index.php/IEL/article/view/3249/3296

Porter ME (1990) The competitive advantage of nations: with a new introduction. New York: Free Press.

Porter ME (1998) Competitive advantage: Creating and Sustaining Superior Performance: with a new introduction. New York: Free Press.

Porter ME (2000) Location, competition, and economic development: local clusters in a global economy. Econ Dev Q 14(1):15–34. https://doi.org/10.1177/089124240001400105

Siadat A, Dantan J, Mauchand M, Martin P (2007) A cost estimation system for manufacturing products using ontology and expert system. IFAC Proceedings 40(18):37–42. https://doi.org/10.3182/20070927-4-ro-3905.00008

Sujová A, Hlaváčková P, Marcineková K (2015) Evaluating the competitiveness of wood processing industry. Drvna industrija 66(4):281–288. https://doi.org/10.5552/drind.2015.1432

Tether B, Mina A, Consoli D, Gagliardi D (2005) How does successful innovation impact the demand for skills and how do skills drive innovation? In, A Literature Review on Skills and Innovation. Department of Trade and Industry, ESRC Centre for Research on Innovation and Competition, University of Manchester. https://research.manchester.

ac.uk/en/publications/how-does-successful-innovation-impact-on-the-demand-for-skills-an

Tolera BT (2021). Cluster analysis for forest and wood-processing industry sector development in Ethiopia [Doctoral dissertation, Technische Universität Dresden].

Ukrainski K, Varblane U (2005) Sources of innovation in the Estonian forest and wood Cluster. University of Tartu Estonian. https://mjtoimetised.ut.ee/febpdf/febawb36.pdf

Viitamo E (2003) Knowledge-intensive services and competitiveness of the forest cluster: Case Finland (No. 845). ETLA Discussion Papers. https://www.etla.fi/wp-content/uploads/2012/09/dp845.pdf

Weiss G, Pettenella D, Ollonqvist P, Slee B (eds.) (2011) Innovation in forestry: territorial and value chain relationships. Wallingford Oxford; Cambridge MA CABI.

Wethyavivorn P, Charoenngam C, Teerajetgul W (2009) Strategic assets driving organizational capabilities of Thai construction firms. J Constr Eng Manag 135(11):1222–1231. https://doi.org/10.1061/(ASCE)CO.1943-7862.000009

Stem position and root infection influence heartwood formation in Douglas-fir plantations

Emmanuel A. Boakye *
Natural Resources Canada, Canadian Forest Service, Edmonton, AB T6H 3S5, Canada
Email: emmanuel.boakye@nrcan-rncan.gc.ca / eaaboakye@yahoo.com

Cyriac S. Mvolo *
Natural Resources Canada, Canadian Forest Service, Edmonton, AB T6H 3S5, Canada
Email: cyriac.mvolo@nrcan-rncan.gc.ca

Mike G. Cruickshank
Natural Resources Canada, Canadian Forest Service, Victoria, BC V8Z 1M5, Canada
Email: mike.cruickshank@nrcan-rncan.gc.ca

James D. Stewart
Natural Resources Canada, Canadian Forest Service, Edmonton, AB T6H 3S5, Canada
Email: jimstewart956@gmail.com

(Received 4 July 2025)

Abstract: Heartwood formation influences timber quality and utilization, yet the factors driving its variation remain poorly understood. Understanding these variations can guide management strategies to influence heartwood development and enhance timber value through adapted silvicultural practices. This study examined the relationships between heartwood area and various tree characteristics in Douglas-fir plantations aged 25–34 years, across four sites within their native range in the southern interior of British Columbia, Canada. Stem analysis was used to quantify heartwood area and its relationships with tree-level variables, including sapwood area, tree height, root infection, and competition. To account for vertical variation along the stem, discs were categorized into three height classes based on relative stem height: lower (0–30%), middle (31%–60%), and upper (61%–100%). Heartwood area was primarily influenced by sapwood area, with the strongest effect at the middle stem, followed by the upper and lower positions. Tree height showed a position-dependent effect: positive in the lower stem and negative in the middle and upper sections. Root infection significantly increased heartwood area in the lower stem, with its effect weakening at higher positions. Competition had statistically significant but minimal effects, ranging from slightly negative in the lower stem to slightly positive in the upper stem. Our findings suggest that promoting sapwood development, particularly in the mid-stem, can enhance heartwood formation. While practices like thinning may contribute to this, the positive association between competition and heartwood in the middle stem indicates that maintaining moderate stand density may be more beneficial than aggressive spacing. Although root infection may locally stimulate heartwood near the base, its longer-term effects can disrupt the sapwood-heartwood balance and reduce tree vigor. Therefore, silvicultural strategies should aim to promote heartwood primarily through stand density management while limiting reliance on root stressors, integrating disease control measures to sustain overall tree health.

Keywords: Tree structure; Douglas-fir; Heartwood; Sapwood; Root disease; Competition

Introduction

Douglas-fir (*Pseudotsuga menziesii* [Mirb.] Franco) is native to western North America, from southern British Columbia in Canada to central California in the United States (Hermann and Lavender 1990). In British Columbia (B.C.), it exists in two varieties: the coastal variety (var. *menziesii*), found along the southern mainland coast and Vancouver Island, and the interior variety (var. *glauca*), which occurs in the southern part of the province and extends north (Government of British Columbia 2024). Douglas-fir produces valuable commercial timber that has been introduced beyond its native range into European countries (Spiecker et al. 2019). It exhibits moderate hardness, stiffness, stability, and resistance to fungal and insect attacks (Nicolescu et al. 2023). The desirable wood properties have led to its continued high demand internationally (Spiecker et al. 2019). The wood's versatility extends to various applications, including building materials, furniture, lumber, veneer products, interior and exterior finishing, and pulp, suiting multiple industries (Nicolescu et al. 2023; Natural Resources Canada 2024).

* Corresponding author

Wood consists of sapwood and heartwood, which are distinguished by their appearance, anatomical structure, and functions. In coniferous trees such as Douglas-fir, sapwood is the portion of the xylem located between the cambium and heartwood. While most cells in the xylem are dead at maturity, the sapwood contains parenchyma cells, which remain alive and play a role in storage and metabolic functions (Wiedenhoeft and Miller 2005). The contents of sapwood flow across connections with adjacent tracheids through pairs of intertracheary bordered pits (Kozlowski and Pallardy 1996; Gartner and Meinzer 2005). These connections facilitate the transfer of water from the soil to the leaves (Gartner and Meinzer 2005).

In contrast, heartwood constitutes the inner, physiologically inactive portion of wood that does not conduct sap. As the xylem ages, parenchymal cells produce secondary metabolites before they die, which are released to the surrounding cells, resulting in the formation of more colored (compared to sapwood) xylem tissues (Zink-Sharp 2004). This alteration in color is attributed to chemical extractives such as tannins, dyestuffs, oils, gums, resins, and salts of organic acids that accumulate in cell lumens and walls, along with the disappearance of living nuclei and a reduction in nitrogen, starch, and sugar content (Kozlowski and Pallardy 1996; Zink-Sharp 2004; Wiedenhoeft and Miller 2005; Luo et al. 2018).

Heartwood formation and its development are influenced by various factors, including growth rate, tree biometric traits, stand characteristics, and environmental conditions (Larson 1969; Larson et al. 2001; Taylor et al. 2002). For example, in coastal Douglas-fir trees in plantations in Portugal, heartwood forms around 8–9 years of cambial age and progresses at a rate of 0.7–0.9 rings per year, with heartwood comprising about half of the lower stem's cross-sectional area, tapering upwards (Cardoso and Pereira 2017). While sapwood has an average radial width of 75 mm at the stem base and tapers upwards, it is denser (595 kg/m^3) and mechanically stronger than heartwood (544 kg/m^3), although heartwood's durability and decay resistance are vital for the tree's long-term integrity and industrial value (Duriot et al. 2021). This variation in heartwood formation is largely determined by growth conditions, including silvicultural treatments such as planting density and thinning methods (Pollet et al. 2017; Boakye et al. 2023). For instance, in uneven-age Douglas-fir stands in interior B.C., thinning was found to increase basal area increment (Acquah et al. 2024).

Silvicultural practices can influence wood properties such as juvenile wood percentage and ring density, with lower stand densities correlating with decreased juvenile wood content and ring density (Kantavichai et al. 2020). In addition, factors like disease and insect presence can affect wood quality, as evidenced by the susceptibility of sapwood to decay compared to heartwood in the central Cascades of Oregon (Gartner et al. 1999). In coastal plantations, such as those studied by Cardoso and Pereira (2017), the general variation in heartwood properties, including its proportion and decay resistance, depends on tree characteristics, growth conditions, and management practices (Bamber and Fukazawa 1985; Hillis 1987; Taylor et al. 2002). For example, while wood strength loss due to fungi is linked to the degradation of lignin and cellulose in heartwood (Schmidt 2006), changes in tree density or thinning treatments do not always affect heartwood proportion but can impact other wood properties, such as decay resistance (Gartner et al. 1999).

Armillaria ostoyae occurs circumpolar in the northern hemisphere (Watling et al. 1991) and is the primary causal fungus responsible for Armillaria root disease causing white rot decay. All woody species in Canada are hosts, but Douglas-fir is rated as highly susceptible to Armillaria root disease in the interior of British Columbia (Cleary et al. 2008). This disease infects roots and can lead to tree death or the non-lethal infections that are associated with significant reduced productivity (Cruickshank et al. 2011). Root infection in stands of interior Douglas-fir from stump inoculum leads to mortality of individual trees, typically starting about 5–7 years after stand establishment, with tree deaths peaking at around age 13–15, and then increasing again at about age 55 (Cruickshank and Filipescu 2012; Cruickshank 2017). Although aboveground symptoms are initially minimal, mortality can persist throughout the rotation (Cleary et al. 2008). Lumber from diseased trees often has fewer boards compared to healthy trees of similar breast height diameter, suggesting potential effects on stem taper or form. Warp is the most common issue affecting lumber and quality from diseased trees, while knots are the predominant defect in lumber from healthy trees (Cleary et al. 2008; Cruickshank et al. 2006; 2009).

Building on this context, our study aims to evaluate the factors influencing the formation of heartwood within planted interior Douglas-fir stands in B.C., focusing on how diseases, competition, and other tree characteristics influence this process. Heartwood and sapwood are complementary parts of the wood structure, with their proportions changing as trees grow. Therefore, understanding heartwood formation is critical for linking growth conditions and wood quality. We hypothesize that (1) greater sapwood area and belowground root infection will increase heartwood formation and (2) increased competi-

tion will reduce heartwood formation. The hypothesis assumes that greater sapwood area provides more material to transition into heartwood as trees grow. Root infections, while depriving sapwood of resources for growth, accelerate the transition to heartwood by causing sapwood to lose its function or die. In contrast, competition-induced resource scarcity limits overall sapwood development, ultimately reducing heartwood formation. While previous studies have focused on plantations with specific tree origins in regions outside of British Columbia, their findings may not be directly applicable to all populations or environments. Our study, conducted in the interior of B.C., therefore, takes into account local ecological and environmental factors that may differ significantly from those in other regions.

Material and Methods

Study area

The study area comprised Douglas-fir plantations within the Interior Cedar Hemlock (ICH) biogeoclimatic zone in southern British Columbia of Canada. The ICH is sheltered from maritime influence by coastal mountains, creating a continental climate with moist summers, cold wet winters, and a snowpack that mitigates summer moisture deficits (Lloyd et al. 1990). The ICH zone ranks second in productivity after the Coastal Western Hemlock zone and boasts the highest tree species diversity in British Columbia. Douglas-fir commonly dominates mature seral stands and is a preferred species for regeneration on harvested sites. The ICH zone harbors approximately 71,000 ha of Douglas-fir plantations. *Armillaria ostoyae* (Romagn.) Herink is prevalent in the Interior Douglas-Fir, Montane Spruce, Engelmann Spruce, Subalpine Fir, and Cedar Hemlock zones, with its incidence and damage most pronounced in the ICH (Morrison et al. 1991).

Study sites and measurements

Douglas-fir plantations were selected for sampling in four sites at Chuck Creek (CC), East Barriere (EB), Kingfisher (KF), and Kuskanax (KX) near Nakusp (Table 1). The selection criteria included accessibility by roads capable of accommodating a lowbed trailer with a 20-ton excavator and sufficient space for the excavator to travel on-site. In addition to these logistical factors, sites were chosen to represent a range of ecological conditions relevant to the study, such as differences in elevation, precipitation, and temperature. Kingfisher, for example, has about 1.86 times the precipitation of Chuck Creek and 1.67 times that of East Barriere, about 59% of Chuck Creek's and 64% of East Barriere's summer heat index, and an elevation about 270 m lower than Chuck Creek. The Kuskanax site was specifically chosen because it was planted after a wildfire, adding variability to the study. All sites, except Kuskanax, had previously undergone clearcutting and were planted with Douglas-fir at a density of 1600 stems/ha. These sites represent the oldest plantations that could be accessed with an excavator, which was a limiting factor in site selection.

Once areas for safe extractor travel and work were identified, a grid was overlayed on each area, and coordinates were selected from each grid until the required number of plots was

Table 1. Descriptive statistics of Douglas-fir site details and average stem data.

Attribute	Chuck Creek	East Barriere	Kingfisher	Kuskanax	Overall sites
Lat. / Long.	51.6N / 119.7W	51.3N / 119.8W	50.7N / 118.8W	50.2N / 117.8W	NA / NA
Elevation (m)	690	700	420	480	NA
Mean summer heat-moisture index	70	64	41	55	NA
Mean annual summer precipitation (mm)	224	249	416	320	NA
Mean tree age	34	25	30	32	34
Mean heartwood area (cm^2)	67.15 ± 79.24	38.49 ± 51.56	52.37 ± 54.70	67.63 ± 78.57	57.62 ± 69.23
Mean heartwood area prop. (%)	36.78 ± 20.14	24.42 ± 15.17	33.25 ± 16.47	32.52 ± 15.92	32.05 ± 17.53
Mean sapwood area (cm^2)	148.42 ± 116.97	173.16 ± 108.97	150.66 ± 99.27	203.36 ± 129.14	83.96 ± 75.37
Mean sapwood area prop.	63.21 ± 20.14	75.57 ± 15.17	66.74 ± 16.47	67.47 ± 15.92	67.94 ± 17.53
Mean diameter (cm)	15.64 ± 5.34	13.67 ± 3.93	15.40 ± 4.52	17.53 ± 5.15	15.56 ± 4.95
Mean tree height (m)	12.35 ± 2.57	9.97 ± 1.46	13.39 ± 2.57	15.76 ± 2.16	12.86 ± 3.05
Mean crown length (cm)	893 ± 291	928 ± 149	948 ± 262	963 ± 262	934 ± 252
Mean crown volume (cm^3)	39.04 ± 33.40	104.43 ± 59.39	37.20 ± 29.23	35.57 ± 22.20	54.06 ± 48.35
Number of infected and healthy trees per site (12 trees each for 24 trees per site)	24	24	24	24	NA
Mean proportion of infected roots	26	25	26	27	NA

Lat.: latitude, Long.: longitude, Min: minimum, Max: maximum, Prop: proportion, mean and standard deviation (denoted as mean ± standard deviation).

established. At each site, 6 plots (10-m radius) were randomly located. In each plot, 4 trees were randomly sampled, resulting in a total of 24 trees per site and 96 trees across all sites. Tree coordinates were measured using a traditional survey transit mounted on a tripod at the plot center. The angle from north to each tree and the distance from the tree to the plot center were recorded. From these measurements, the x and y coordinates for each tree were calculated.

The diameter of each tree was measured at breast height (1.3 m, DBH) and crown width measured at cardinal points. Trees were extracted in the fall using a 20-ton Link Belt excavator equipped with a clamshell bucket attachment to minimize root, stem, and branch breakage. Soil was manually removed from the roots of all trees in the plots after the soil thawed in the following spring. Infection was determined by the presence of mycelial fans in the bark or cambium. Tree height (m), crown length (m), and height to live crown (m) were recorded for each tree after pulling. Crown length ratio was calculated as the ratio of crown length to total tree height. The basal area of individual trees was calculated and used for further analysis, with DBH measured in centimeters. A non-spatial competition index was calculated for each sampled tree using the sum of the plot's basal area of trees that were larger than the target tree (basal area of larger trees or BAL, cm^2).

Cross-sectional stem disks were cut at intervals of 0, 0.3, 1.3, and 2 m from the base of the stem, and then at every 2-m interval thereafter until the diameter of the stem was reduced to 2 cm. The sapwood-heartwood boundary was distinct in Douglas-fir, especially after wetting with water, if need be, and was assessed visually and marked before digitization for on-screen area measurements of heartwood area (HWA, cm^2) and total wood area (cm^2). Sapwood area (SWA, cm^2) was calculated from the difference between total wood area and HWA.

Distance from the apex (DFA; m) was calculated by subtracting the disc sampling height relative the soil line from the total tree height to evaluate heartwood area consistently along the stem. The position of the sample disc relative to the base of the live crown (distance to crown base, DCR, m) was calculated as the difference between disc height and live crown height. Positive values indicate that the disc is located within the crown, while negative values indicate that the disc is below the crown.

Statistical analyses

We first conducted exploratory analyses in R software (R Core Team 2024) to examine relationships among predictor variables at the disc, tree, and plot levels (see Appendix Figure A1 for a full list of variables). At the disc level, we included sapwood area (SWA), disc height (m), distance from the apex (DFA), and disc crown radius (DCR, m). Tree-level variables included tree age (years), total height (m), crown length (CL, cm), height to the live crown (m), and the basal area of larger trees (BAL, cm^2). The binary variable for belowground root infection (BGRI; 0 = healthy, 1 = diseased) was excluded from correlation analysis because the Pearson correlation assumes continuous data.

To select candidate predictors for modeling, we evaluated multicollinearity using variance inflation factors (VIF). Variables with VIF < 5 and biological relevance, namely SWA, tree height, BAL, and BGRI were retained in the final model set.

To investigate the relationship between HWA and predictor variables, we fitted separate linear mixed-effects models (LME) for each relative stem height category using the *nlme* package in R (Pinheiro et al. 2024). Discs were grouped into three height classes based on their relative position along the stem: lower (0–30%), middle (31%–60%), and upper stem inside the crown (61%–100%). Preliminary analyses revealed height-specific variation in the effect of predictors on HWA, and interaction terms involving height were not readily interpretable in a unified model. Therefore, a stratified modeling approach was used to assess the relative importance of predictors within each stem position category.

The final model structure, applied separately to each stem height group, was:

$$\log(HWA_{ij} + 1) = \beta_0 + \beta_1 (SWA_{ij})^{0.1} + \beta_2 \, Height_j + \beta_3 \, BGRI_j + \beta_4 \, BAL_k + b_{0j} + \varepsilon_{ij} \quad [1]$$

Where:

- HWA_{ij} is the heartwood area of disc i within tree j; the response variable was log-transformed as $\log(HWA_{ij} + 1)$.
- $(SWA_{ij})^{0.1}$ is the 0.1-power-transformed sapwood area measured at the same disc level.
- $Height_j$ is the total height of tree j.
- $BGRI_j$ is a binary indicator of belowground root infection for tree j.
- BAL_k is the basal area of larger trees, calculated at the plot level k, where tree j is located.
- $b0_j$ is a random intercept for tree j, accounting for the clustering of disc samples within trees.
- ε_{ij} is the residual error term.

To account for repeated measurements at different disc heights within trees, the model included an exponential spatial correlation structure with a nugget effect (corExp), based on

vertical distance from the apex (DFA). Site and plot effects were tested, but did not significantly improve model fit and were therefore excluded.

Model diagnostics confirmed that residuals were normally distributed and exhibited no systematic patterns when plotted against model fixed effects (Appendix Figure A2). Because HWA was log-transformed, we applied a bias correction factor (Snowdon 1991) to back-transform model predictions for visualization on the original scale (cm^2).

Results and discussion

Stem position effects on heartwood area variability and model fit

Our results (Table 2) showed that the lower stem had negligible random effect variation (0.0001), the upper stem exhibited moderate variability (0.30), and the middle stem showed higher variability (0.49), indicating that unmodeled tree-level differences were most pronounced at mid-height. Given the financial and operational constraints, the sample size used in this study was considered appropriate for the scope of the research. However, larger sample sizes and a greater number of study sites would certainly provide more robust results and reduce the potential for bias due to limited sampling. Further research with expanded sample sizes and more diverse site conditions would improve the precision of the model, particularly in capturing between-tree variability in the middle stem. The residual variation ranged from 0.28 to 0.47, with the middle stem showing the lowest residual variance, suggesting better model precision at that position. Despite these considerations, overall model fit, as indicated by AIC, was best for the upper and lower stem sections (222.46 and 222.93, respectively), and poorest for the middle stem (279.81), likely due to greater between-tree variability that was not fully accounted for by the fixed effects. These results suggest that heartwood area was more consistently predictable across trees in the upper and lower stem sections, possibly due to more uniform structural traits and environmental exposure in those positions. Further studies with larger sample sizes would provide more insights into these dynamics.

Main Effects on heartwood formation

The effects of predictor variables on heartwood area varied by stem position (Table 2, Figure 1A), with SWA emerging as the strongest and most consistent driver of heartwood formation. Its influence was greatest in the middle stem (β_1 = 13.52), followed by the upper (β_1 = 8.63) and lower sections (β_1 = 4.74). The middle stem likely shows the strongest effect because it serves as a transitional zone for water transport and tree metabolism. Positioned near the crown, it sustains active water and nutrient flow, yet is old enough for inner sapwood layers to begin converting into heartwood. In contrast, the lower stem contains older, more stabilized heartwood, while the upper stem consists of younger tissue where this transition is not yet prominent. This intermediate position in the stem balances sapwood maintenance and heartwood formation, driving dynamic changes in wood structure. This pattern aligns with the role of sapwood as the active xylem responsible for water and nutrient transport (Kozlowski and Pallardy 1996). As trees age, older sapwood loses conductivity and transforms into heartwood through the accumulation of extractives and polyphenolic compounds that enhance decay resistance (Zink-Sharp 2004; Wiedenhoeft and Miller 2005; Luo et al. 2018). The strong SWA–heartwood relationship in the mid-stem reflects this transitional physiology, where expanding crowns demand sustained conductive capacity, while inner sapwood layers convert to heartwood to maintain functional sapwood volume (Bamber 1976; Zink-Sharp 2004).

Tree height exhibited a position-dependent influence on heartwood area (Table 2, Figure 1B), showing a positive association

Table 2. Summary of the linear mixed-effects model coefficients for predicting heartwood area based on Equation [1].

Effect Type	Parameter	Lower (0–30%)	Middle (31%–60%)	Upper (61%–100%)
Fixed	Intercept	-4.3901*	-16.7305*	-10.1728*
	SWA	4.7402*	13.5231*	8.6335*
	Height	0.0750*	-0.0754*	-0.0419*
	BGRI	0.3618*	0.1936	0.0819
	BAL	-0.0000	0.0001*	0.0000
Random	Intercept (SD)	0.0001	0.4916	0.3029
	Residual (SD)	0.4717	0.2779	0.3739
AIC		222.9330	279.8137	222.4609

Definition of abbreviations: sapwood area (SWA), basal area of larger trees (competition index, BAL), belowground root infection (BGRI), SD (standard deviation).
* Significant at $p \leq 0.05$

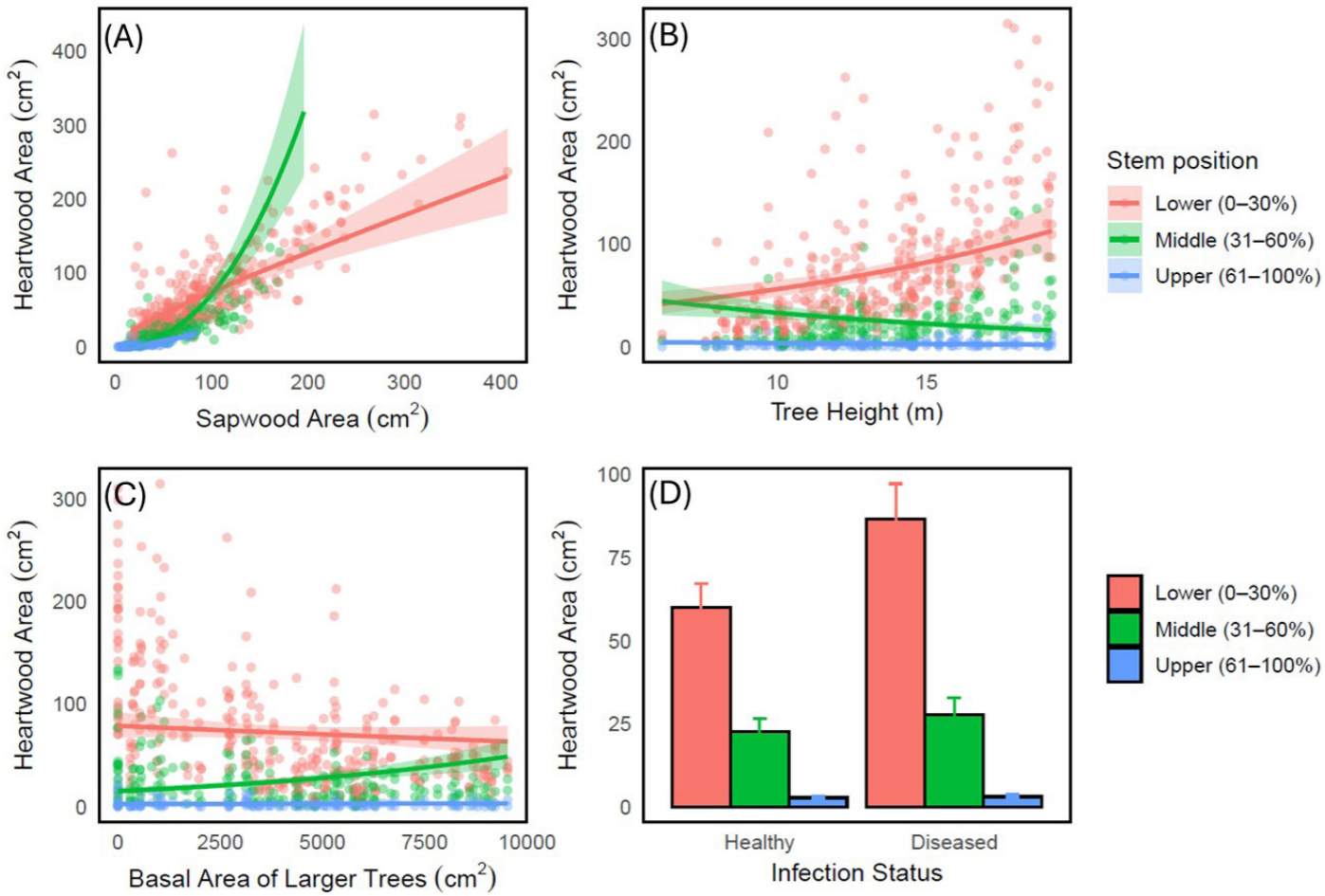

Figure 1. Effects of key predictors on heartwood area by stem position.
Relationships between heartwood area and (A) sapwood area, (B) tree height, (C) basal area of larger trees, and (D) infection status. All relationships are grouped by stem position (lower, middle, upper). Lines represent model predictions, shaded areas indicate 95% confidence intervals, and points show observed data.

at the lower stem ($\beta_2 = 0.08$), but negative associations in the middle ($\beta_2 = -0.08$) and upper ($\beta_2 = -0.04$) sections. However, we did not measure the age (i.e., ring number) at different stem heights in this study, and future studies should consider this as a critical factor in understanding heartwood development. While the age of the wood may play a significant role in heartwood formation, it is important to note that the transition from sapwood to heartwood does not occur uniformly at a given height. This variability could introduce a confounding effect when interpreting the results, as the timing and extent of the transition may differ between stem positions. At the base, taller trees may accumulate more heartwood because the older basal wood has had more time to undergo the sapwood-to-heartwood transition and may contribute to mechanical support (Cardoso and Pereira 2017). In contrast, the negative associations observed higher up the stem may reflect the prioritization of sapwood retention to sustain water transport to the crown. Additionally, upper stem sections generally exhibit slower basal growth than the base, particularly in mature trees, due to resource allocation toward height growth and crown development (Kozlowski and Pallardy 1996). This reduced secondary growth may limit the accumulation of heartwood in those sections.

This vertical trend aligns with the pipe model theory (Shinozaki et al. 1964), which suggests that the amount of sapwood in a stem segment is proportional to the foliage it supports, ensuring adequate water and nutrient transport from roots to canopy (Grier and Waring 1974; Waring et al. 1982). In the younger, upper sections of the tree, sapwood is actively produced and retained to meet these transport and storage demands. As xylem tissue ages, it loses conductivity and is transformed into heartwood, leading to greater heartwood accumulation in the lower stem where structural support becomes increasingly important (Rennolls 1994; Millers 2013). Similar verti-

cal patterns in heartwood distribution have been observed in Douglas-fir in Portugal (Cardoso and Pereira 2017) and western redcedar (*Thuja plicata*) in North America (DeBell and Lachenbruch 2009).

BGRI had a significant positive effect on heartwood area in the lower stem ($\beta_3 = 0.36$), but its influence weakened and became non-significant in the middle and upper sections, indicating a localized response near the tree base (Table 2, Figure 1D). This pattern suggests that the physiological and structural response to root infection is concentrated in the stem region closest to the infection source. The increased heartwood area in the lower stem likely reflects a defense mechanism, whereby trees deposit extractives and polyphenolic compounds to form reaction zones that limit the upward spread of root pathogens (Shigo 1984).

Root infections impair water and nutrient transport, reduce leader growth, and increase the shedding of lower foliage, diverting energy toward defense at the expense of overall growth (Cruickshank et al. 2011; Cruickshank and Filipescu 2012). In our study, the enhanced heartwood formation in the lower stem corresponds to reduced functionality of root vascular tissues and the tree's attempt to compartmentalize the infection. While we did not directly observe compartmentalization, this may reflect the tree's response to stressors, including both fungal and insect damage. This aligns with the progression of fungal lesions, which disrupt vascular transport over time (Cruickshank and Sattler 2020), forcing resource reallocation toward defense. For example, in conifers like Norway spruce infected with *Heterobasidion annosum*, trees form reaction zones to isolate pathogens, initially increasing heartwood in affected areas (Shigo 1979; Oliva et al. 2012; Mageroy et al. 2023).

This defensive strategy, while limiting pathogen spread, incurs significant costs. As root and lower stem vascular tissues become less functional, the tree's capacity to sustain growth diminishes, leading to reduced sapwood and heartwood volume and, in severe cases, mortality (Cruickshank et al. 2011; Westwood et al. 2012). Over time, the proportion of functional sapwood decreases, constraining the tree's ability to continue forming new heartwood (Oliva et al. 2012). Our results highlight that the most intense effects of root infection and the tree's defensive responses are concentrated near the stem base, where vascular disruption is greatest.

BAL had a negligible effect on heartwood area overall but exhibited a weak positive relationship at the middle stem section ($\beta_4 = 0.0001$; Table 2, Figure 1C). In this region, heartwood area tended to increase slightly with BAL, suggesting that trees may accelerate sapwood-to-heartwood conversion under resource-limited conditions such as reduced water or light availability (Sellin 1994). Because heartwood requires fewer metabolic resources to maintain than sapwood, this shift may provide a physiological advantage when competition restricts resource uptake (Moraes et al. 2023). In contrast, BAL had little influence at the lower and upper stem sections. At the base, heartwood is typically well-developed and less sensitive to competitive pressures. In the upper stem, the necessity of maintaining conductive sapwood for hydraulic function likely constrains heartwood formation, even under competition.

Conclusion

Heartwood formation in Douglas-fir plantations is strongly influenced by sapwood area, with the relationship being most pronounced in the middle stem section. Tree height increased heartwood area in the lower stem but reduced it in the middle and upper sections, likely due to structural needs, although these patterns may also be influenced by tree age, especially in younger stands. Root infection exhibited position-dependent effects, primarily increasing heartwood near the base as a defensive response. Competition had a positive effect on heartwood area in the middle stem section, suggesting that stand density influences heartwood development in a stem-position-specific manner. Forest managers aiming to enhance heartwood development and timber value may benefit from practices that promote sapwood expansion in the mid-stem region, where heartwood formation potential is highest. While wider spacing or selective thinning can encourage sapwood growth, stand density may also stimulate heartwood formation, suggesting that one or both factors might play a role in this process. Management strategies should therefore aim to strike a balance, avoiding both excessive crowding and over-thinning. Although root infection may initially stimulate heartwood formation near the base, it ultimately reduces overall growth and long-term heartwood potential if unmanaged. Reducing root disease inoculum prior to planting remains essential, or alternatively, heartwood should not be a management target on infected sites.

Acknowledgment

The authors express gratitude to the Pacific Forestry Centre of Natural Resources Canada for providing the database used in this study. The Canadian Wood Fibre Centre within Natural Resources Canada provided financial support. We acknowledge the valuable comments provided by colleagues at the Natural Resources Canada on the submitted manuscript.

References

Acquah SB, Marshall PL, Eskelson BNI, Moss I, Barbeito I (2024) Growth responses to thinning from below in uneven-aged interior Douglas-fir dominated stands. Can J For Res 54(5). https://doi.org/10.1139/cjfr-2023-0154

Bamber RK (1976) Heartwood, its function and formation. Wood Sci Technol 10(1):1–8. https://doi.org/10.1007/BF00376379

Bamber RK, Fukazawa K (1985) Sapwood and heartwood: A review. CAB International. Retrieved from https://cabidigitallibrary.org

Boakye EA, Mvolo CS, Stewart J (2023) Systematic review: Climate and non-climate factors influencing wood density in the boreal zone. BioResources 18(4):8757–8770. https://doi.org/10.15376/biores.18.4.Boakye

Cardoso S, Pereira H (2017) Characterization of Douglas-fir grown in Portugal: heartwood, sapwood, bark, ring width and taper. Eur J For Res 136:597–607. https://doi.org/10.1007/s10342-017-1058-z

Cleary M, van der Kamp B, Morrison D (2008) British Columbia's southern interior forests: Armillaria root disease stand establishment decision aid. BC J Ecosyst Manag 9(2):60–65. https://doi.org/10.22230/jem.2008v9n2a397

Cruickshank MG (2017) Climate and site factors affecting survival and yield of Douglas-fir in the Cedar-Hemlock ecosystem of the southern interior of British Columbia. For 90:219–233. https://doi.org/10.1093/forestry/cpw040

Cruickshank MG, Filipescu CN (2012) Allometries of coarse tree, stem, and crown measures in Douglas-fir are altered by Armillaria root disease. Botany 90(8):711–721. https://doi.org/10.1139/b2012-040

Cruickshank MG, Lejour D, Morrison DJ (2006) Traumatic resin canals as markers of infection events in Douglas-fir roots infected with Armillaria root disease. For Pathol 36(5):372–384. https://doi.org/10.1111/j.1439-0329.2006.00469.x

Cruickshank MG, Morrison DJ, Lalumière A (2011) Site, plot, and individual tree yield reduction of interior Douglas-fir associated with non-lethal infection by Armillaria root disease in southern British Columbia. For Ecol Manag 261(2):297–307. https://doi.org/10.1016/j.foreco.2010.10.023

Cruickshank MG, Morrison DJ, Lalumière A (2009) The interaction between competition in interior Douglas-fir plantations and disease caused by *Armillaria ostoyae* in British Columbia. For Ecol Manag 257(2):443–452. https://doi.org/10.1016/j.foreco.2008.09.013

Cruickshank MG, Sattler DF (2020) Fungal lesion length and expansion rate for the root pathogen *Armillaria ostoyae* in Douglas-fir affecting root colonization and damage. For Pathol 50(3):e12598. https://doi.org/10.1111/efp.12598

DeBell JD, Lachenbruch B (2009) Heartwood/sapwood variation of western redcedar as influenced by cultural treatments and position in tree. For Ecol Manag 258(9):2026–2032. https://doi.org/10.1016/j.foreco.2009.07.054

Duriot R, Rescalvo FJ, Pot G, Denaud L, Girardon S, Frayssinhes R (2021) An insight into mechanical properties of heartwood and sapwood of large French Douglas-fir LVL. Constr Build Mater 299:123859. https://doi.org/10.1016/j.conbuildmat.2021.123859

Farquharson KL (2008) Probing the role of auxin in wood formation. Plant Cell 20(4):822. https://doi.org/10.1105/tpc.108.200412

Gartner BL, Meinzer FC (2005) Structure-function relationships in sapwood water transport and storage. In Vascular Transport in Plants: Physiological Ecology, ed. N Holbrook, MA Zwieniecki, Academic Press, pp. 307–331. https://doi.org/10.1016/B978-012088457-5/50017-4

Gartner BL, Morrell JJ, Freitag CM, Spicer R (1999) Heartwood decay resistance by vertical and radial position in Douglas-fir trees from a young stand. Can J For Res 29(12):1993–1996. https://doi.org/10.1139/x99-166

Government of British Columbia (2024, January 25). Douglas-fir (*Pseudotsuga menziesii*). Retrieved from https://www2.gov.bc.ca/gov/content/industry/forestry/managing-our-forest-resources/silviculture/tree-species-selection/tree-species-compendium-index/douglas-fir

Grier CC, Waring RH (1974) Conifer foliage mass related to sapwood area. For Sci 20(3):205-206. https://doi.org/10.1093/forestscience/20.3.205

Hermann RK, Lavender DP (1990) *Pseudotsuga menziesii* (Mirb.) Franco Douglas-fir. In Silvics of North America, Vol 1, RM Burns and BH Honkala (tech coord), Agri Handbook 654, USDA For Serv, Washington, DC, pp. 527–540.

Hillis WE (1987) Heartwood and Tree Exudates, Springer Series in Wood Science (SSWOO), Vol. 4; reprint, 2012. Springer, New York. https://doi.org/10.1007/978-3-642-72534-0

Kantavichai R, Turnblom EC, Lowell EC (2020) Effects of density control and fertilization on log wood quality from a Douglas-fir stand in western Oregon, USA. For Sci 66(2):191–201. https://doi.org/10.1093/forsci/fxz069

Kozlowski TT, Pallardy SG (1996) Physiology of woody plants. Elsevier.

Larson PR (1969) Wood formation and the concept of wood quality. Yale Sch For Bull 74: 1–54. https://elischolar.library.yale.edu/yale_fes_bulletin/69

Larson PR, Kretschmann DE, Clark A III, Isebrands JG (2001) Formation and properties of juvenile wood in southern pines: A synopsis. Gen. Tech. Rep. FPL-GTR-129. US DA For Serv Forest Prod Lab, Madison, WI.

Lloyd D, Angrove K, Hope G, Thompson C (1990) A guide to site identification and interpretation for the Kamloops forests region. Research Branch, BC Ministry of Forests, Land Management Handbook no. 23, Victoria, BC. www.for.gov.bc.ca/hfd/pubs/docs/Lmh/Lmh23.pdf

Luo B, He R, Yang Y (2018) A review of physiological function of sapwood and formation mechanism of heartwood. J Beijing For Univ 40(1):120–129. https://doi.org/10.5555/20183131615

Mageroy MH, Nagy NE, Steffenrem A, Krokene P, Hietala AM (2023) Conifer defences against pathogens and pests—mechanisms, breeding, and management. Curr For Rep 9(6):429–443. https://doi.org/10.1007/s40725-023-00201-5

Millers M (2013) The proportion of heartwood in conifer (*Pinus sylvestris* L., *Picea abies* [L.] H. Karst.) trunks and its influence on trunk wood moisture. J For Sci 59(8):295–300.

Moraes LG, Lima MDR, Assis-Pereira G, de Almeida Gonçalves D, Vidaurre GB, Bufalino L, de Paula Protásio T (2023) Forking and planting spacing impacts on wood density, X-ray density, and heartwood proportion of *Tachigali vulgaris*. Trees 37(5):1567–1581.

Morrison DJ, Merler H, Norris D (1991) Detection, recognition, and management of Armillaria and Phellinus root diseases in the southern interior of British Columbia. In Canada – British Columbia Partnership Agreement on Forest Resource Development: FRDA II (FRDA Rep. 179). British Columbia Ministry of Forests.

Natural Resources Canada (2024) Natural resistance in Douglas firs. Retrieved from https://natural-resources.canada.ca/our-natural-resources/forests/industry-and-trade/forest-industry-tools-research/natural-resistance-douglas-firs/13339

Nicolescu VN, Mason WL, Bastien JC, Vor T, Petkova K, Podrázský V, Mihăilescu G (2023) Douglas-fir (*Pseudotsuga menziesii* (Mirb.) Franco) in Europe: An overview of management practices. J For Res 34(4):871–888. https://doi.org/10.1007/s11676-023-01607-4

Oliva J, Camarero JJ, Stenlid J (2012) Understanding the role of sapwood loss and reaction zone formation on radial growth of Norway spruce (*Picea abies*) trees decayed by *Heterobasidion annosum* sl. For Ecol Manag 274:201–209. https://doi.org/10.1016/j.foreco.2012.02.026

Pinheiro J, Bates D, R Core Team (2024) nlme: Linear and Nonlinear Mixed Effects Models. R package version 3.1-166, https://CRAN.R-project.org/package=nlme.

Pinheiro JC, Bates DM (2000) Mixed-Effects Models in S and S-PLUS. Springer, New York. https://doi.org/10.1007/b98882 https://doi.org/10.1007/b98882.

Pollet C, Henin JM, Hébert J, Jourez B (2017) Effect of growth rate on the physical and mechanical properties of Douglas-fir in western Europe. Can J For Res 47(8):1056–1065. https://doi.org/10.1139/cjfr-2016-0290

R Core Team (2024) R: A language and environment for statistical computing. R Foundation for Statistical Computing, Vienna, Austria. https://www.R-project.org/.

Rennolls K (1994) Pipe-model theory of stem-profile development. For Ecol Manag 69(1–3):41–55. https://doi.org/10.1016/0378-1127(94)90218-6

Schmidt O (2006) Wood Rot. In Wood and Tree Fungi, Springer, Berlin, Heidelberg, pp. 151–167. https://doi.org/10.1007/3-540-32139-X_7

Sellin A (1994) Sapwood–heartwood proportion related to tree diameter, age, and growth rate in *Picea abies*. Can J For Res 24(5):1022–1028. https://doi.org/10.1139/x94-133

Shigo AL (1979) Compartmentalization of decay associated with *Heterobasidion annosum* in roots of *Pinus resinosa*. Eur J For Pathol 9(6):341–347.

Shigo AL (1984) Compartmentalization: A conceptual framework for understanding how trees grow and defend themselves. Annu Rev Phytopathol 22(1):189–214. https://doi.org/10.1146/annurev.py.22.090184.001201

Shinozaki K, Yoda K, Hozumi K, Kira T (1964) A quantitative analysis of plant form—the pipe model theory: I. Basic analyses. Jpn J Ecol 14(3):97–105. https://doi.org/10.18960/seitai.14.3_97

Snowdon P (1991) A ratio estimator for bias correction in logarithmic regressions. Can J For Res 21(5):720–724.

Spiecker H, Lindner M, Schuler J (eds.) (2019) Douglas-fir – an option for Europe. EFI What Science Can Tell Us 9, European Forest Institute. Retrieved from https://efi.int/sites/default/files/files/publication-bank/2019/efi_wsctu9_2019.pdf

Taylor AM, Gartner BL, Morrell JJ (2002) Heartwood formation and natural durability—a review. Wood Fiber Sci 34(4):261–271.

Waring RH, Schroeder PE, Oren R (1982) Application of the pipe model theory to predict canopy leaf area. Can J For Res 12(3):556–560. https://doi.org/10.1139/x82-08

Watling R, Kile GA, Burdsall HH Jr (1991) Nomenclature, taxonomy, and identification. In Armillaria root disease, ed. CG Shaw & GA Kile, Agricultural Handbook No. 691, USDA Forest Service, Washington, DC, pp. 1–9.

Westwood, AR, Conciatori F, Tardif JC, Knowles K (2012) Effects of Armillaria root disease on the growth of *Picea mariana* trees in the boreal plains of central Canada. For Ecol Manag 266:1–10. https://doi.org/10.1016/j.foreco.2011.11.005

Wiedenhoeft AC, Miller RB (2005) Structure and function of wood. In Handbook of Wood Chemistry and Wood Composites, ed. RM Rowell. CRC Press, Boca Raton, pp. 9–33.

Zink-Sharp A (2004) Wood formation and properties. In Encyclopedia of Forest Sciences, ed. J Burley, J Evans, J Youngquist. Elsevier, Oxford, pp. 1806–1815.

Appendix – Figures

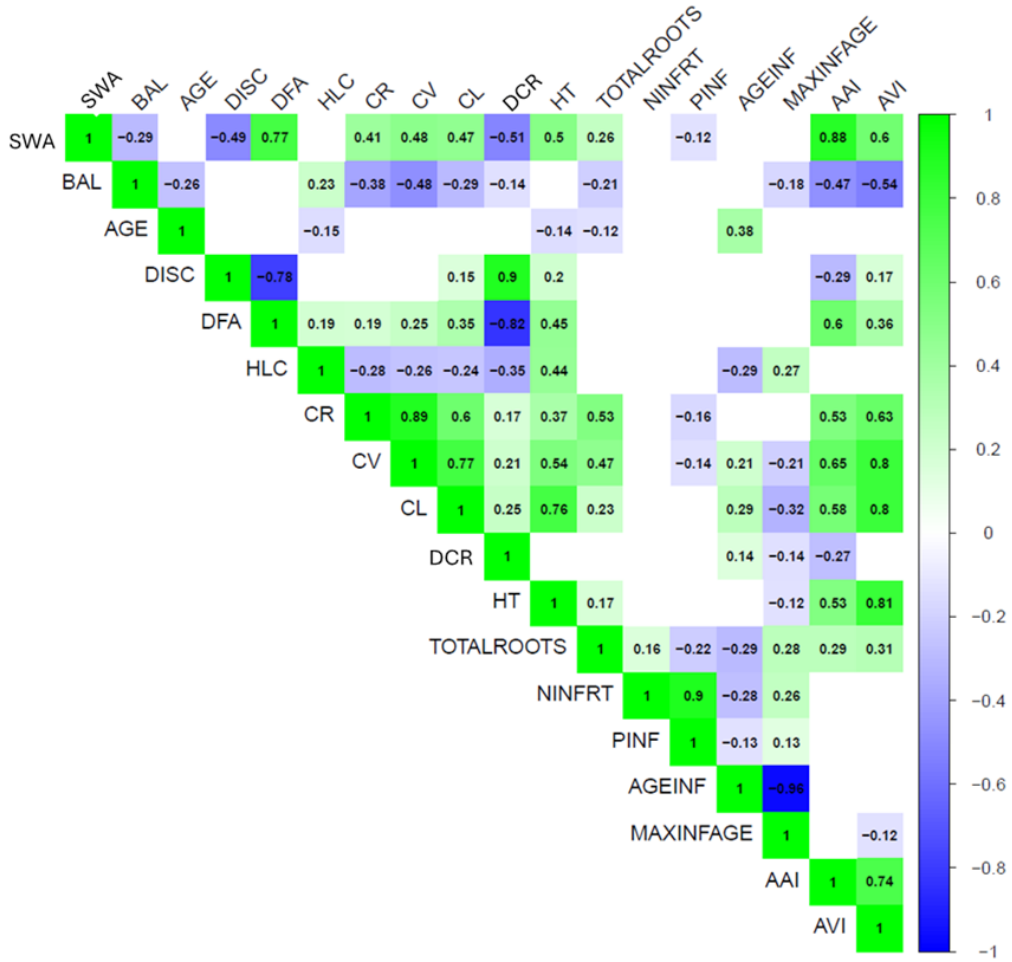

Figure A1. Pairwise correlation matrix between continuous tree variables. Only significant correlations ($P<0.05$) are shown. The blanks are not significant. **SWA** – Sapwood Area (cm²), **CL** – Crown Length (cm), **BAL** – Basal Area of Larger Trees (cm²), **MAXINFAGE** – Time Since Infection (years), **DFA** – Distance From Apex (m), **DISC** – Disc Height (m), **AGE** – Age of Tree (years), **HT** – Tree Height (m), **NINFRT** – Total number of infected primary roots at final age, **TOTALROOTS** – Total number of primary roots at final age, **PINF** – Percentage of primary roots infected at final age, **AGEINF** – Tree age at first infection, **HLC** – Height to Live Crown (cm), **CR** – Crown Radius (cm), **CV** – Crown Volume (m³), **AAI** – Average Yearly Area Increment for Last Years (cm²), **AVI** – Average Yearly Tree Volume Increment for Last Years (m³), **DCR** – Distance to Crown Base (m).

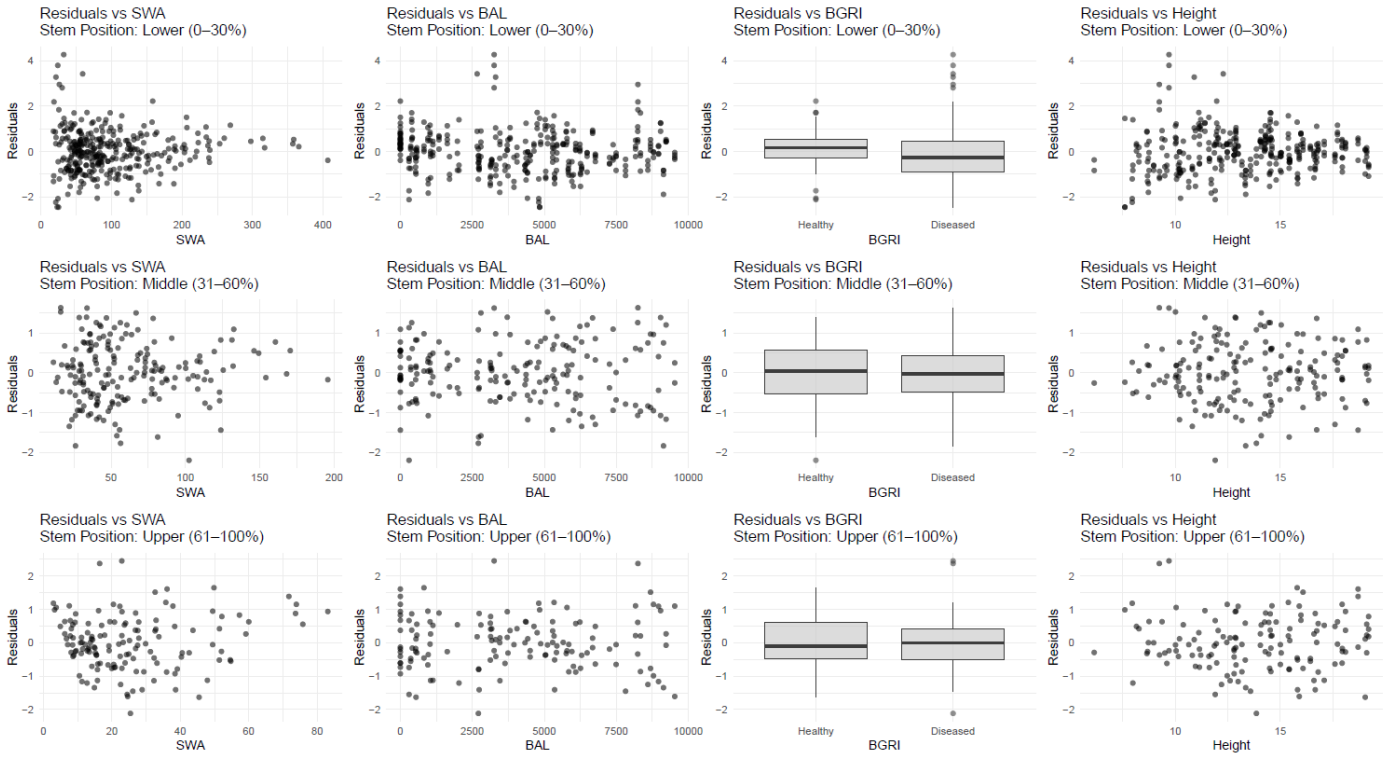

Figure A2. Residuals vs. Individual Predictors from the Linear Mixed-Effects Model. The model (Eq. 1) effectively predicts heartwood area in Douglas-fir, as evidenced by residual plots showing residuals centered around zero for all predictors, including sapwood area (SWA), basal area of larger trees (BAL), belowground root infection (BGRI), and tree height.

Estimation of Hankinson's formula coefficient for elastic wave transmission velocity of red pine by the indirect method

HyeongJun Han†
Timber Engineering Laboratory
Department of Forest Products Engineering
Chungbuk National University
Cheongju, Republic of Korea
E-mail: 2024247003@chungbuk.ac.kr

KyoungHyun Ryu†
Timber Engineering Laboratory
Department of Forest Products Engineering
Chungbuk National University
Cheongju, Republic of Korea
E-mail: wokohyun@chungbuk.ac.kr

KugBo Shim†*
Professor of Forest Products Engineering
Timber Engineering Laboratory
Department of Forest Products Engineering
Chungbuk National University
Cheongju, Republic of Korea
E-mail: kbshim@chungbuk.ac.kr

(Received 10 August 2025)

Abstract: This study determined the Hankinson's formula coefficient *n* for red pine (*Pinus densiflora*) using the indirect elastic wave transmission test under varying moisture contents (12%, 15%, and 18%). Hankinson's formula is a mathematical relationship used to predict the mechanical properties of wood at any angle relative to the grain. With information on the elastic wave transmission speed parallel (P, 0°) and perpendicular (Q, 90°) to the fiber direction, the wave transmission speed at intermediate angles can be predicted using Hankinson's formula. A visually defect-free 81- to 90-year red pine board (400 × 400 × 50 mm) was selected as the test specimen. The moisture content of specimens was adjusted to 12%, 15%, and 18%. Coefficient *n* of Hankinson's formula, was calculated by taking measurements were taken at grain angles of 0°, 15°, 30°, 45°, 60°, 75°, and 90° using both ultrasonic and stress waves by the indirect transmission method.
The coefficients (*n*) obtained from ultrasonic wave measurements were 2.0, 1.9, and 1.9 at 12%, 15%, and 18% moisture contents, respectively. The values determined from stress wave measurements were 1.7, 1.7, and 1.6 at the same moisture contents, respectively. These results indicate that the transmission path of elastic waves in red pine can be effectively modeled using the coefficient *n* from Hankinson's formula, which varies with moisture content. This suggests the potential applicability of the formula in evaluating internal defects or decay in wood through quantitative wave-based analysis.

Keywords: Nondestructive test; Ultrasonic wave; Stress wave; Indirect method; Hankinson's formula; *Pinus densiflora*

Introduction

Wood is an organic material that varies in moisture content based on the surrounding environment. High moisture wood contents favor insect and fungal attack. Insect activity within the wood causes structural damage that is often hidden from view and may not be detected until significant destruction has occurred (Verbist et al. 2019). This reduces the strength of wooden structural members, leading to overall damage in wooden buildings (Ghaly and Edwards 2011; Wang et al. 2018). Damage caused by termites is increasing due to climate change (Buczkowski and Bertelsmeier 2017; Lee et al. 2021).

The carbon emission reduction benefits of wooden structures for carbon neutrality increase with long-term use of wood (Churkina et al. 2020; Starzyk et al. 2024). To ensure the long-term use of wooden structures, it is essential to evaluate the

* Corresponding author
† Society of Wood Science & Technology member

strength of structural members. Strength evaluation methods are divided into destructive and nondestructive techniques. Destructive testing damages the material and can render it unsuitable for prolonging building life (Shabani et al. 2020). In contrast, nondestructive methods can predict strength without damaging the material, making them ideal for preserving wooden structures, cultural heritage sites, or for safety evaluations of existing buildings (Riggio et al. 2014).

Therefore, to extend the lifespan of wooden structures, nondestructive evaluation methods should be applied. Additionally, safety assessment protocols based on the degree of deterioration need to be established.

Various nondestructive testing methods for wooden structures have relied on experience, such as craftsmen's intuitive judgment, visual inspection, and tapping tests that diagnose through the sound produced by tapping wood (Azzi et al. 2025). Such empirical diagnoses lack accuracy and consistency, and thus lack a scientific basis for safety assessment of wooden structures (Kim et al. 2003). Therefore, a quantitative evaluation method using nondestructive testing is needed.

Currently, the most commonly used nondestructive testing methods include drilling resistance tests, X-rays, and elastic wave nondestructive tests (Ondrejka et al. 2020). Among these, nondestructive tests using elastic waves are advantageous for field application because the test process is fast and simple (Zielińska and Rucka 2021). This method measures the time of flight (ToF) for elastic waves to penetrate the interior of a member and calculates the transmission speed to detect decay and defects. The transmission speed of elastic waves is affected by the moisture content in the wood. As wood moisture content increases, the stiffness decreases (Kretschmann 2010), and the transmission speed of elastic waves slows (Montero et al. 2015; Yang et al. 2015).

Many studies have been conducted to detect internal decay using elastic nondestructive testing (Niederleithinger and Vössing 2018). However, most studies have been conducted using the direct measurement method, where transducers are placed face to face and measured. Since this direct measurement method is difficult to apply when the opposite side of the wood used in a wooden structure is not exposed, research on the indirect method, where the transducers are placed side by side and measured, is necessary.

The propagation of elastic waves through wood follows the fastest path between the transmitter and receiver (Figure 1, Path A). When decay or defects are present, the elastic waves detour around the cavity and travel along the fastest available path (Figure 1, Path B). As the waves travel around the cavity perimeter, the transmission distance becomes longer than in intact wood, resulting in a relatively lower measured velocity (Du et al. 2018; Pahnabi et al. 2024). During this detour, the elastic waves travel at various angles relative to the fiber direction. If the transmission velocity at different angles of fiber direction is known, the wave propagation path can be predicted.

Hankinson's formula (Eq. 1) provides a mathematical relationship to predict compressive strength when a load is applied at an angle between the parallel direction and the perpendicular-to-the-fiber direction in wood. The formula can predict both the strength and the elastic wave velocity according to the fiber orientation angle (Afoutou et al. 2024; Kabir 2001). In this equation, the coefficient *n* represents the degree of anisotropy. For isotropic materials, *n* equals 1, and it increases as anisotropy increases. For wood, *n* must be determined experimentally and typically ranges between 1.5 and 2.5, depending on the tree species (Bachtiar et al. 2017; Mascia et al. 2011; Senalik and Farber 2021).

$$N = \frac{P \times Q}{P \times \sin^n(\theta) + Q \times \cos^n(\theta)} \quad [1]$$

where, N is the predicted elastic wave propagation velocity, P is the wave velocity along the fiber direction (0°), Q is the wave velocity perpendicular to the fiber direction (90°), and θ is the angle of fiber direction.

Red pine (*Pinus densiflora*) has traditionally been used as beams and roof structures in Korean cultural heritage buildings, highlighting its historical and structural relevance. There is currently no established Hankinson's formula coefficient for red pine. To enhance measurement accuracy under varying field moisture conditions, coefficients were determined for moisture levels of 12%, 15%, and 18%.

Materials and methods

Materials

Specimen preparation

Test specimens were prepared by selecting defect-free sections from 81- to 90-year-old pine boards grown in Bonghwa, Gyeongbuk. A total of 15 specimens of 400 × 50 × 400 mm (longitudinal × radial × tangential) were produced. The specific gravity of the specimens was 0.50 ± 0.01.

Moisture content control

A thermo-hygrostat (Daihan Labtech, LTH-2250C, Namyangju-si, Korea) was used to control the moisture content of the test specimens. To achieve the target moisture contents of 12%,

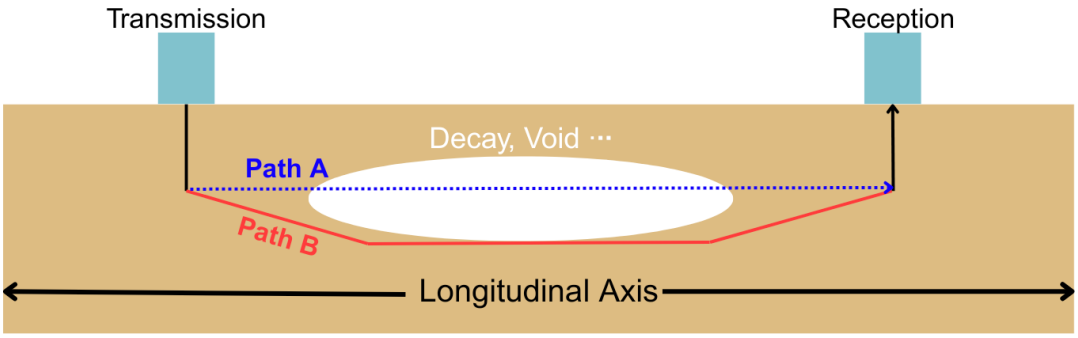

Figure 1. Changes in the path of acoustic wave transmission due to defects.

15%, and 18%, the temperature and relative humidity were set according to the values shown in Table 1 (Kang et al. 2008). The same 15 specimens were used to measure response at each moisture content. The specimens were stored under these controlled conditions until their masses stabilized.

Methods

Measurement angles of fiber direction

To determine the coefficient for Hankinson's formula, measurements were taken on the wide face at seven angles spaced at 15° intervals from 0° to 90°. The measurement paths, each 300 mm in length, were marked as shown in Figure 2. Here, the fiber direction was defined as 0°, and the direction perpendicular to the fibers was defined as 90°. Prior to testing, all specimens were visually inspected to ensure that the 0° direction was fully aligned with the fiber direction.

Indirect elastic wave measurement method

Elastic wave transmission velocity is calculated by dividing the distance by the time of flight between the transmitter and receiver (Huan et al. 2018; Liang et al. 2010; Wang et al. 2001). Ultrasonic and stress wave measurements were conducted by the indirect method, in which the transmitter and receiver were placed side by side on the surface, as shown in Figure 2 (Nowak et al. 2019). Transmission velocity was measured 30 times for each angle, yielding a total of 210 data sets per specimen. The origin was set at the point where all the angles converge, with the transmitter fixed at this origin and the receiver positioned at the endpoint corresponding to each angle. The transmitter remained stationary when changing angles, and only the receiver was moved.

Ultrasonic measurement method.

The ultrasonic transmission speed was measured using Pundit Lab equipment (Proceq, Pundit Lab, Switzerland) (Figure 3). The frequency of the ultrasonic transmission speed measurement was fixed at 54 kHz (Bucur and Feeney 1992; Espinosa et al. 2019; Tanasoiu et al. 2002).

Table 1. Temperature and relative humidity conditions used to achieve target moisture contents.

		Temperature	Relative Humidity
Target Moisture Content	12%	20°C	65%
	15%	20°C	77%
	18%	20°C	85%

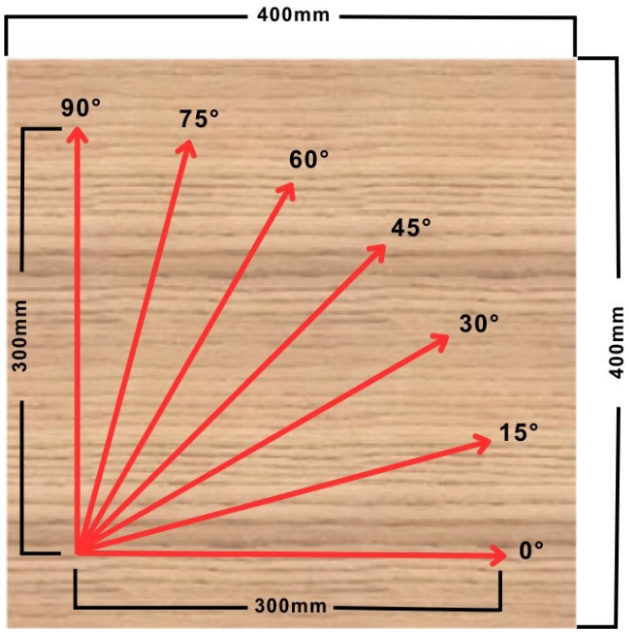

Figure 2. A schematic diagram of a specimen.

The contact surfaces of the measuring terminals were circular with a diameter of 50 mm, and the measurement distance was taken between the centers of the transmitter and receiver. To ensure accurate measurements, ultrasonic couplant (SLTECH, ULTRASONIC COUPLANT, Korea) was applied to the terminals before testing (Fang et al. 2017).

Stress wave measurement method

The stress wave transmission speed was measured using a Micro Hammer device (iML, Micro Hammer, Germany)

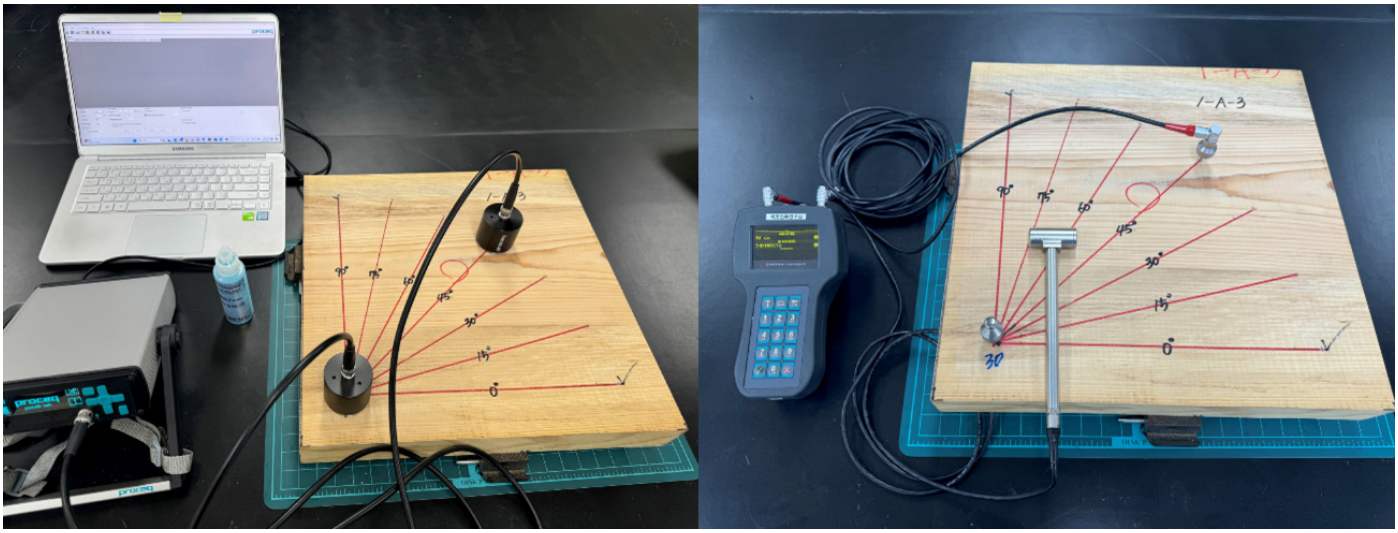

Figure 3. Examples of the ultrasonic wave (left) and stress wave (right) measuring devices on a test sample.

(Figure 3). The measurement involves striking the transmitter with a hammer connected to the device, generating a stress wave that is detected by the receiver. To account for variations in force and angle of striking, three measurements are taken and averaged.

Stress wave transmission velocity was measured by inserting the transmitter and receiver screws into the specimen. The insertion depth was set to 40 mm to ensure the screws were securely fixed and stable during the impact (Wang 1999).

Data processing

A total of 450 data sets per angle were collected from 15 red pine specimens with 30 repetitions each. Since the calculation of coefficient n using the Root Mean Square Error (RMSE) method is highly sensitive to outliers, the data were statistically analyzed to identify and remove outliers, as illustrated in Figure 4 (Shcherbakov et al. 2013).

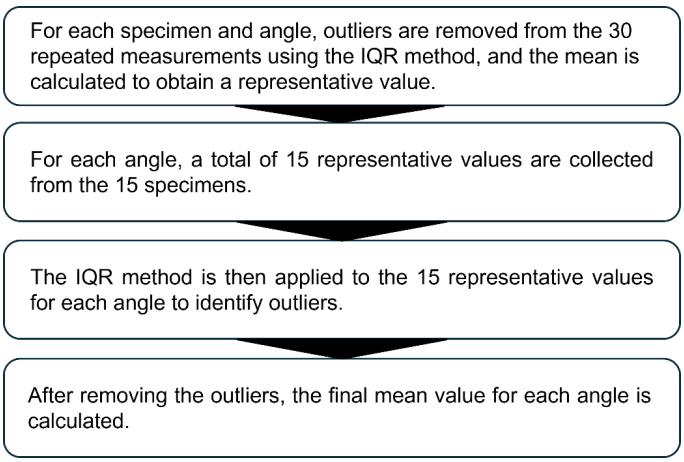

Figure 4. Data handling steps.

Outlier removal using IQR method

The interquartile range (IQR) method identifies outliers based on the central 50% range of the data. The IQR is calculated by subtracting the lower 25th percentile (first quartile, Q1) from the upper 75th percentile (third quartile, Q3), representing the range of the middle 50% of the data. Values lying beyond 1.5 times the IQR below Q1 or above Q3 are considered outliers, and in this study, it was chosen to remove them for increased reliability of the statistical analysis (Danasingh and Leavline 2016). This outlier removal was applied to each set of 30 repetitions, after which the average was calculated. In the case of ultrasonic wave measurements, 0 to 6 outliers were removed per set, whereas for stress wave measurements, 0 to 14 outliers were removed. These 15 mean values, each representing one specimen at a given angle, were then collectively subjected to a second round of IQR-based outlier detection. After removing outliers from this group, the final representative mean for each angle was calculated.

Calculating coefficient n using RMSE

The predicted values were calculated by substituting the actual measured transmission velocities at 0° and 90°, with outliers removed, into Hankinson's formula, where variables P and Q represent the velocities at 0° and 90°, respectively. The angle θ was set at 15° intervals and converted to radians based on the fiber orientation. The coefficient n was varied from 1.5 to 2.5 in increments of 0.1, and the predicted transmission velocities for ultrasonic and stress waves were calculated accordingly.

To select the most appropriate coefficient n, the accuracy of each prediction model was evaluated against the actual measurements using the RMSE. RMSE is a useful statistical measure for assessing the precision of prediction models. The

RMSE formula is provided in Equation 2. The n value with the smallest RMSE was selected as the optimal coefficient.

$$RMSE = \sqrt{\frac{1}{n}\sum_{i=1}^{n}(y_i - \hat{y}_i)^2} \quad [2]$$

where, n is the number of data points, y_i is the measured value, and $\hat{y}_i$ is the predicted value.

Evaluating prediction model accuracy using R^2 and NRMSE

The coefficient of determination (R^2, Eq 3) measures how well a prediction model explains the actual observed data by comparing the residual sum of squares (SSE) to the total sum of squares (SST). Values closer to 1 indicate a higher explanatory power of the model, while values closer to 0 indicate lower explanatory power.

$$R^2 = 1 - \frac{\sum_{I=1}^{n}(y_i - \hat{y}_i)^2}{\sum_{I=1}^{n}(y_i - \bar{y}_i)^2} \quad [3]$$

where, y_i is the measured value, $\hat{y}_i$ is the predicted value, and $\bar{y}_i$ is the average of the measured values.

Normalized RMSE (NRMSE; Eq 4) is a metric that evaluates the relative accuracy of a model's predictions by normalizing the RMSE value (Shcherbakov et al. 2013). The closer the NRMSE value is to 0, the more closely the predicted values match the actual values, indicating higher prediction accuracy.

$$NRMSE = \frac{RMSE}{X_{max} - X_{min}} \quad [4]$$

where, X_{max} is the maximum value of the data, X_{min} is the minimum value of the data.

Results and discussion

Average velocity of elastic waves under the moisture content variations

Both ultrasonic and stress wave tests exhibited a consistent trend of decreasing average transmission velocity as the angle increased from 0° to 90° (Figures 5–7). The repeated observation of similar trends under various specimens and moisture conditions provides important evidence supporting the applicability of the indirect measurement method for elastic wave nondestructive testing.

Calculating representative values by grain angle

Table 2 presents the averages and standard deviations of the 15 specimens for each angle after outlier removal, under moisture contents of 12%, 15%, and 18%.

Table 3 shows the elastic wave transmission velocities of ultrasonic and stress waves according to changes in moisture

Table 2. Effect of grain angle on ultrasonic wave and stress wave velocity of red pine at 12% to 18% moisture content.

		Velocity(m/s)						
MC	Wave Type	0°	15°	30°	45°	60°	75°	90°
12%	UW	5293	4530	2898	1947	1579	1331	1258
		[194]	[374]	[427]	[454]	[316]	[309]	[273]
	SW	2477	2072	1564	1249	1110	1018	993
		[135]	[183]	[164]	[145]	[159]	[115]	[69]
15%	UW	5123	4229	2597	1845	1544	1289	1233
		[191]	[400]	[468]	[457]	[289]	[309]	[238]
	SW	2414	2037	1489	1201	1071	976	960
		[135]	[165]	[146]	[147]	[138]	[105]	[64]
18%	UW	5070	4183	2761	1784	1443	1228	1222
		[272]	[388]	[255]	[411]	[307]	[273]	[223]
	SW	2374	1935	1435	1158	1023	941	933
		[76]	[191]	[150]	[142]	[147]	[97]	[79]

Values represent the mean of samples, while tables in brackets represent the standard deviation.

Table 3. Average change in acoustic wave transfer velocity after outlier removal due to change in moisture content.

Average	MC	0°	15°	30°	45°	60°	75°	90°
UW	12%	5293	4530	2898	1947	1579	1331	1258
	15%	5123	4229	2597	1845	1544	1289	1233
	18%	5070	4183	2761	1784	1443	1228	1222
SW	12%	2477	2072	1564	1249	1110	1018	993
	15%	2414	2037	1489	1201	1071	976	960
	18%	2374	1935	1435	1158	1023	941	933

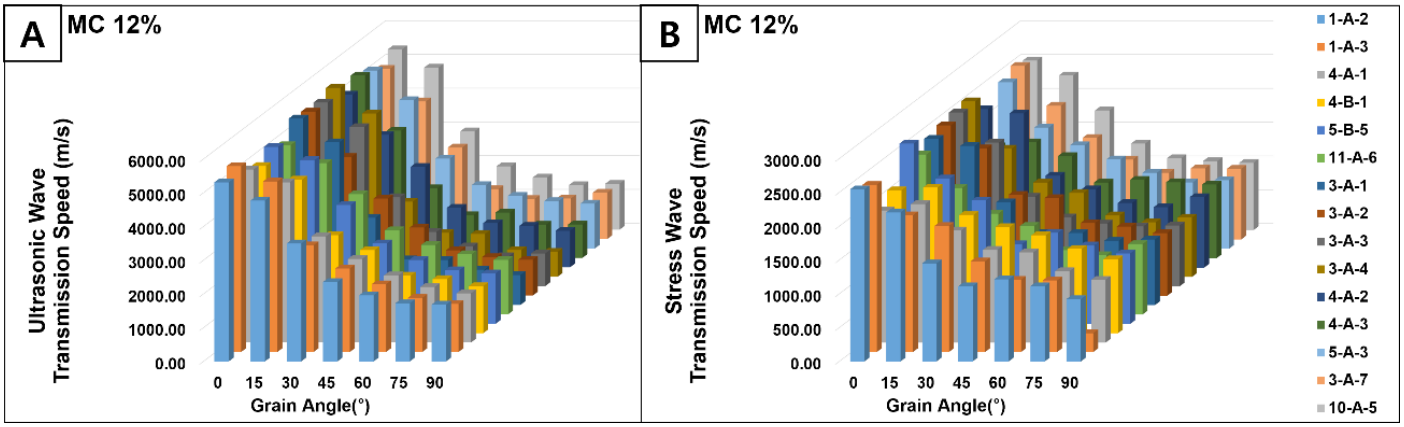

Figure 5. Effect of grain angle on transmission speed of ultrasonic waves (A) and stress waves (B) at 12% moisture content.

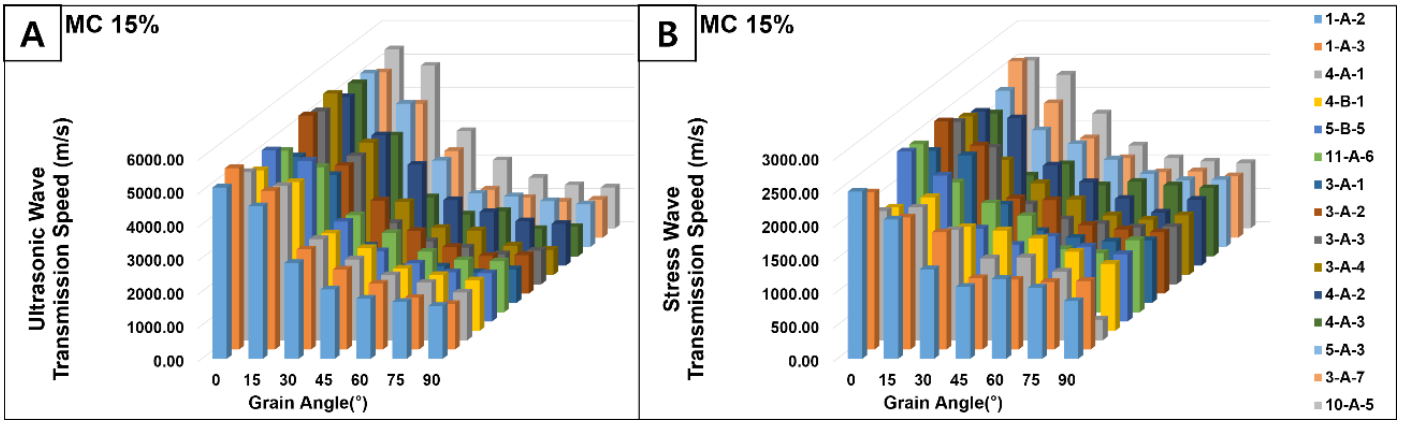

Figure 6. Effect of grain angle on transmission speed of ultrasonic waves (A) and stress waves (B) at 15% moisture content.

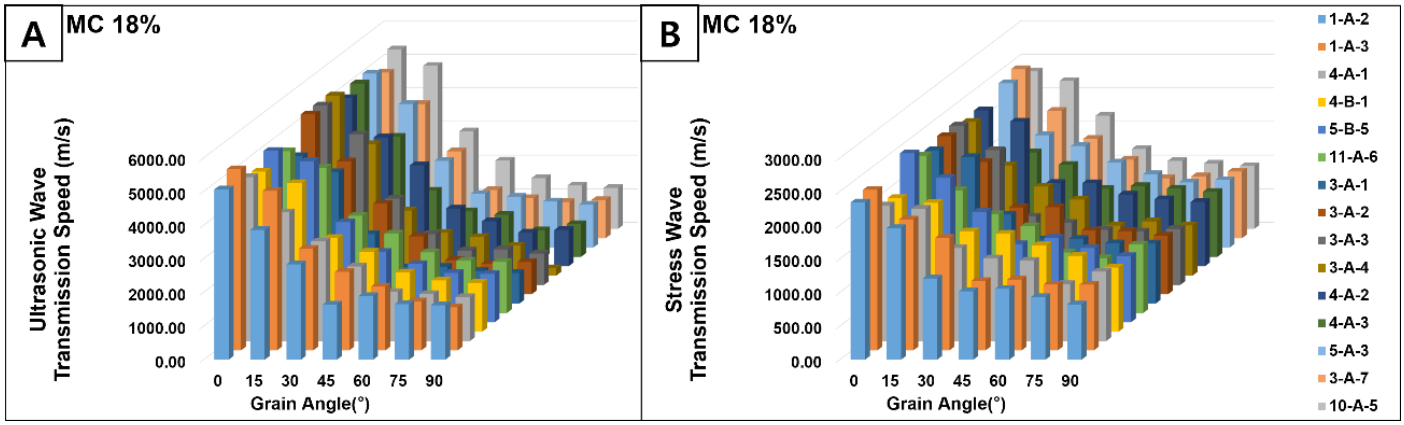

Figure 7. Effect of grain angle on transmission speed of ultrasonic waves (A) and stress waves (B) at 18% moisture content.

content and fiber orientation angle. Average transmission speed decreased as the angle increased from 0° to 90°. This behavior is attributed to the anisotropic nature of wood, where elastic waves propagate through cell walls. At 0°, fibers are long and most aligned, resulting in a relatively shorter transmission path. At 90°, the cell walls are densely arranged nearly perpendicular to the wave path, creating a longer transmission path, increased transmission time, and thus lower speed (Espinosa et al. 2019; Li et al. 2021).

Comparison of predicted and measured values according to changes in coefficients of Hankinson's formula

The results comparing the predicted and measured values for different values of n are presented in Figures 8 to 10.

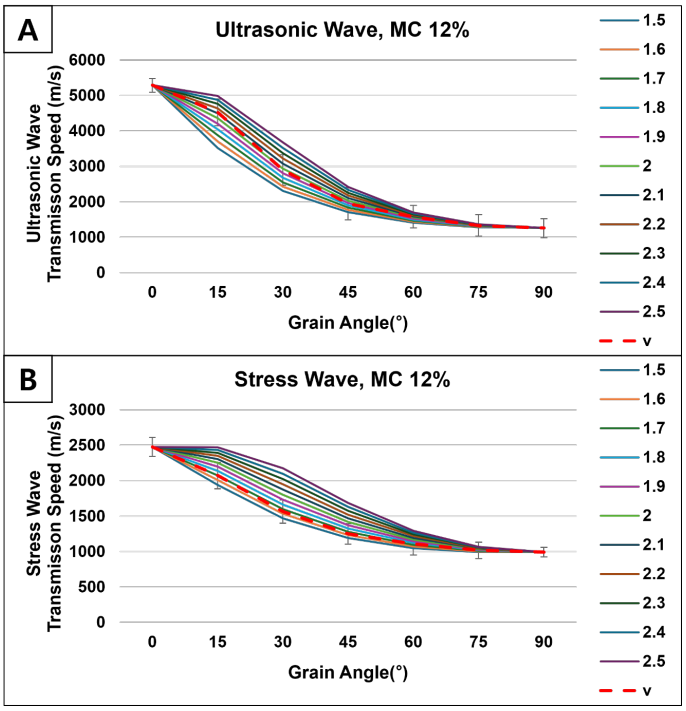

Figure 8. Effect of coefficient *n* on transmission speed of ultrasonic waves (A) and stress waves (B) in wood at 12% moisture content.

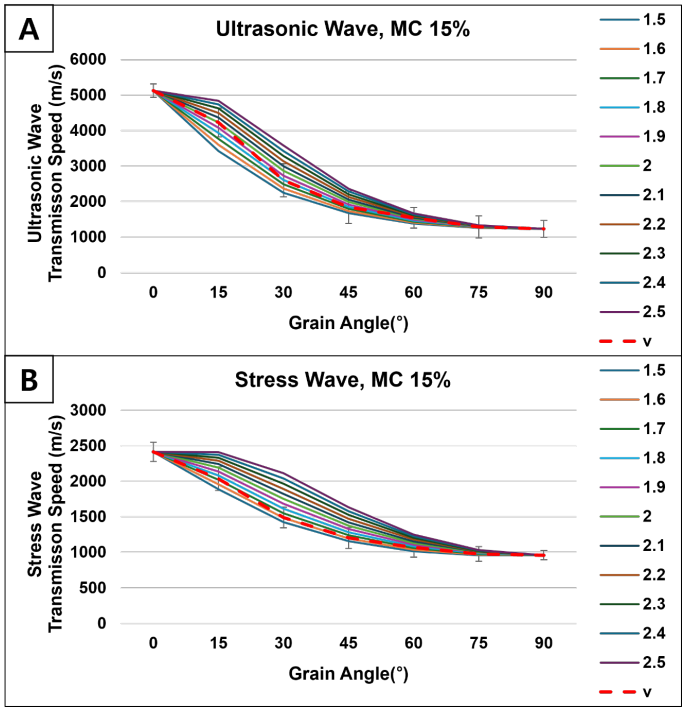

Figure 9. Effect of coefficient *n* on transmission speed of ultrasonic waves (A) and stress waves (B) in wood at 15% moisture content.

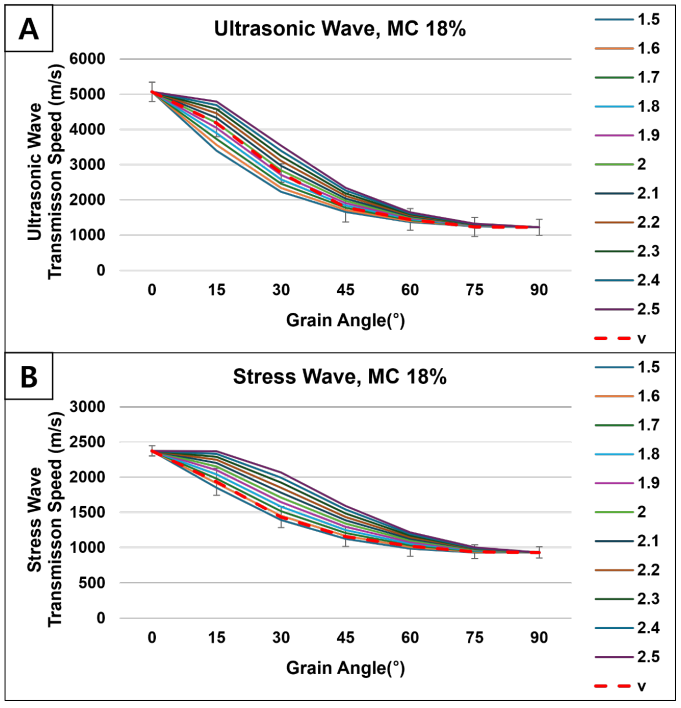

Figure 10. Effect of coefficient *n* on transmission speed of ultrasonic waves (A) and stress waves (B) in wood at 18% moisture content.

The measured ultrasonic and stress wave transmission velocities at moisture contents of 12%, 15%, and 18% are represented by v, while the predicted values corresponding to coefficient *n* varying from 1.5 to 2.5 are shown as thin solid lines.

Results of adopting coefficient n using RMSE

Based on the predicted and measured values shown in Figures 8 to 10, the RMSE was calculated to compare the errors of each prediction model as the coefficient *n* varied. The results are summarized in Table 4, and the coefficient *n* with the lowest RMSE was selected as the optimal value for each moisture content, ultrasonic wave, and stress wave.

Table 4. Effect of varying the coefficient n on RMSE in ultrasonic and stress wave analysis of red pine under different moisture content conditions.

	MC 12%		MC 15%		MC 18%	
n	UW	SW	UW	SW	UW	SW
1.5	455.60	70.60	343.44	68.39	364.81	40.84
1.6	370.72	31.55	262.91	33.93	284.51	*11.39
1.7	287.10	*17.65	185.75	*28.29	206.22	40.06
1.8	205.81	53.41	117.76	59.56	132.71	77.57
1.9	129.99	92.48	*82.91	96.60	*76.56	115.34
2.0	*75.12	131.79	114.54	134.56	82.98	153.04
2.1	90.43	171.13	179.45	172.79	142.44	190.66
2.2	155.27	210.49	252.49	211.15	213.82	228.25
2.3	230.48	249.94	327.83	249.64	287.92	265.89
2.4	308.20	289.55	403.95	288.32	362.81	303.65
2.5	386.78	329.40	480.40	327.23	438.01	341.61

* The smallest value as a result of RMSE calculation. Adopt the corresponding coefficient *n*.

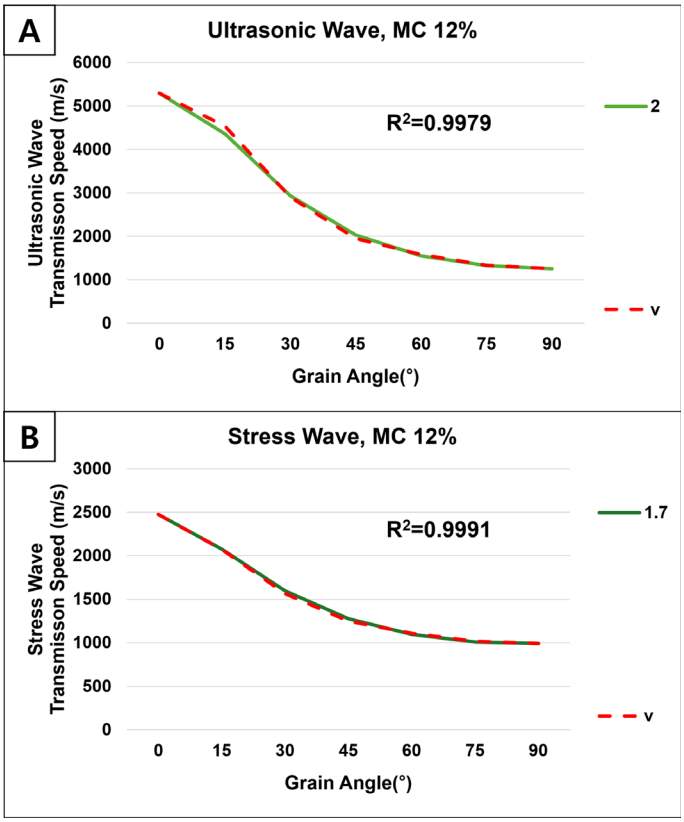

Figure 11. Effect of grain angle on stress wave and ultrasonic wave transmission speed when the coefficient calculation uses RMSE for wood at 12% moisture content.

The values marked with * in Table 4 indicate the cases where the RMSE between the predicted and measured values was the smallest. The corresponding coefficient *n* was adopted as the optimal value for each condition. For moisture contents of 12%, 15%, and 18%, the optimal *n* values were 2.0, 1.9, and 1.9 for ultrasonic waves, and 1.7, 1.7, and 1.6 for stress waves, respectively.

Results of evaluating the accuracy of the prediction model using R^2 and NRMSE

As moisture content increased, both wave types showed decreasing transmission velocities and lower *n* values, indicating a reduction in anisotropy within the wood.

By substituting the optimal coefficient *n*, Hankinson's formula for red pine was established for each moisture content condition (12%, 15%, and 18%). The predicted and measured values for each angle based on this formula are presented in Figures 11 to 13.

The coefficients of determination (R^2) were all very close to 1, indicating that the prediction model based on the adopted coefficient *n* explains the actual values very well. Additionally, the NRMSE results for ultrasonic and stress waves under the same conditions are presented in Table 5. In all cases, the

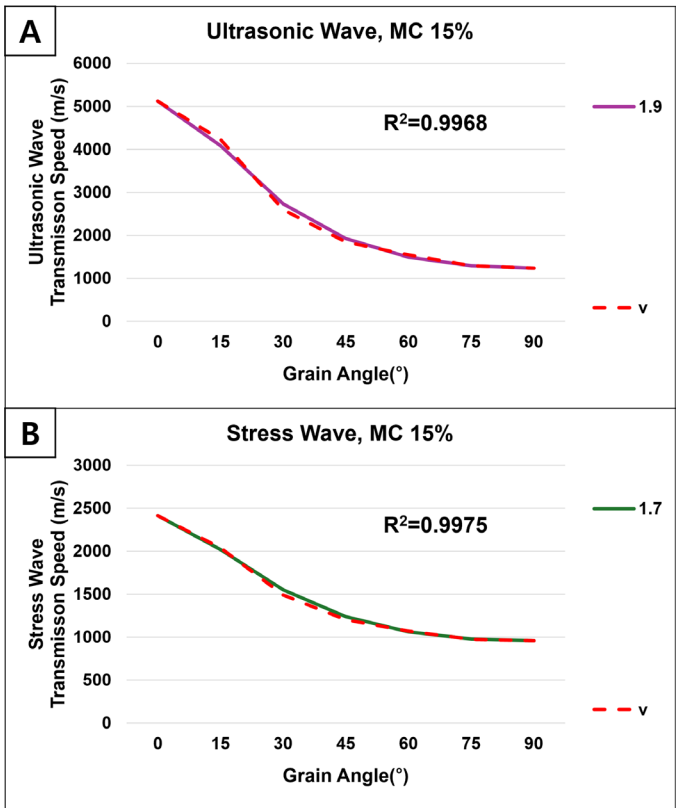

Figure 12. Effect of grain angle on stress wave and ultrasonic wave transmission speed when the coefficient calculation uses RMSE for wood at 15% moisture content.

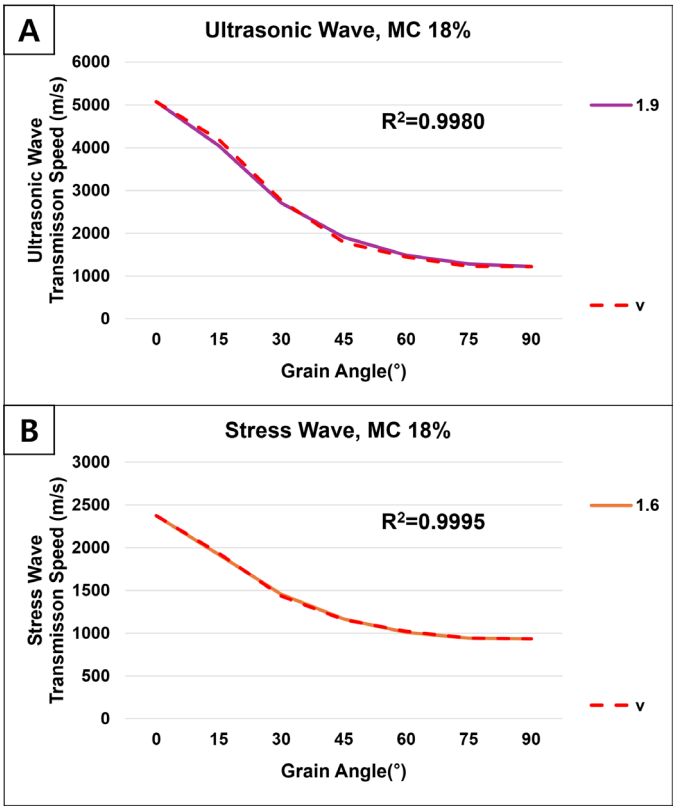

Figure 13. Effect of grain angle on stress wave and ultrasonic wave transmission speed when the coefficient calculation uses RMSE for wood at 18% moisture content.

Table 5. Predictive model accuracy evaluation results using NRMSE.

MC		*n*	NRMSE
12%	UW	2.0	0.0186
	SW	1.7	0.0120
15%	UW	1.9	0.0213
	SW	1.7	0.0199
18%	UW	1.9	0.0199
	SW	1.6	0.0081

NRMSE values ranged between 0 and 0.1, confirming that the completed Hankinson's formula had high prediction accuracy.

As shown in Table 5, the coefficient *n* gradually decreases with increasing moisture content. This occurs because higher moisture content enhances the viscoelastic effects within the wood, leading to a more uniform mechanical stiffness as moisture penetrates the cell structure (Eitelberger et al. 2012).

These changes reduce the anisotropy of the wood, which consequently lessens the variation in elastic wave propagation velocity with angle. This effect is reflected as a flatter slope in the angle-velocity graphs shown in Figures 14 and 15. Therefore, this reduction in anisotropy caused the coefficient *n* in Hankinson's formula to decrease.

Determining the effect of function ratio on elastic wave propagation speed

Ultrasonic waves consistently exhibited higher transmission velocities than stress waves, which is consistent with the findings of Chuang and Wang (2001). This trend was observed across most moisture content conditions and specimens, providing experimental support for the applicability of Hankinson's formula.

Figure 14 shows the change in transmission speed according to varying moisture content for ultrasonic waves, while Figure 15 illustrates the change in transmission speed for stress waves under different moisture content levels.

As the moisture content of the specimen increased from 12% to 18%, the elastic wave propagation velocity showed an overall decreasing trend, with a reduction of approximately 3% to 10% at each angle, as shown in Figure 16.

Generally, the propagation velocity of elastic waves increases when the increase in elastic modulus outweighs the increase in density. However, below the fiber saturation point, as the moisture content increases, density increases while the elastic modulus decreases, resulting in a decrease in elastic wave velocity (Liu et al. 2014; Montero et al. 2015).

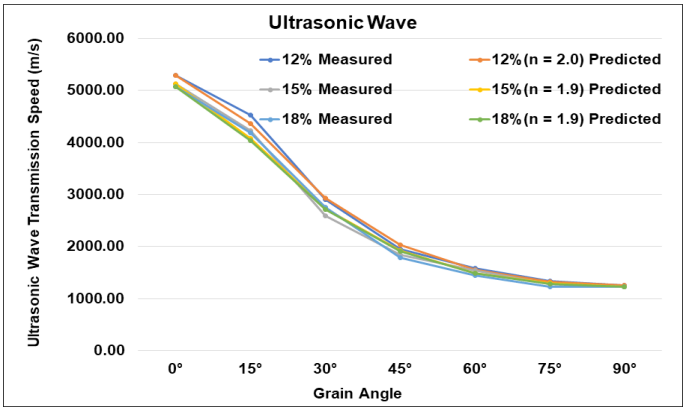

Figure 14. Effect of wood moisture content on ultrasonic wave transmission speed measured at different grain angles, including comparison between measured and predicted values.

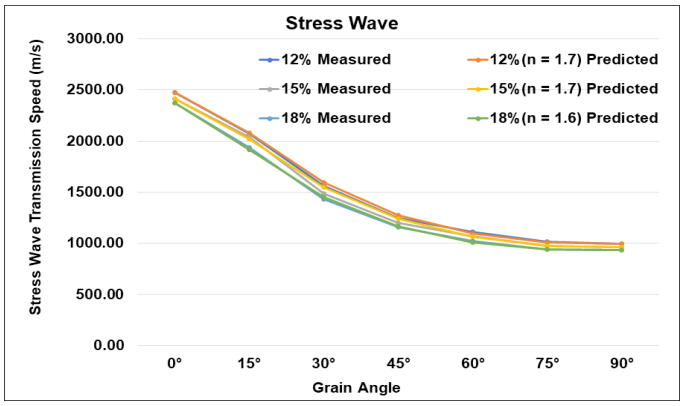

Figure 15. Effect of wood moisture content on stress wave transmission speed measured at different grain angles, including comparison between measured and predicted values.

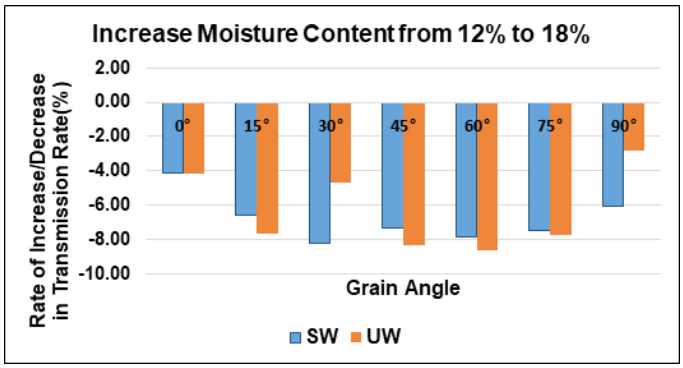

Figure 16. Effect of grain angle and wood moisture content on the velocities of ultrasonic and stress waves in red pine.

Conclusions

As moisture content increased, elastic wave velocity decreased, with ultrasonic waves consistently exhibiting higher velocities than stress waves. The optimal coefficient *n* in Hankinson's formula was identified for each moisture level, allowing for the development of a predictive model specific to red pine.

While stress wave velocities were much lower than ultrasonic wave velocities, Hankinson's formula effectively predicted both types of velocities across a range of grain angles and varying moisture conditions. These findings support the applicability of the formula in nondestructive testing (NDT) for evaluating wave propagation in moisture-affected wood. The methodology presented in this study may be repeatable with other wood species, suggesting broader applicability of Hankinson's formula in the field of NDT.

Acknowledgments

This research was supported by the Korea Heritage Service through the R&D project, "Development and verification of technology for aged wood recovery from architectural cultural heritage in response to climate damage" (Project No. RS-2024-000403459).

References

Afoutou JS, Zhang X, Dubois F (2024) Full elastic properties characterization of wood by ultrasound using a single sample. Wood Sci Technol 58:403–422. https://doi.org/10.1007/s00226-023-01525-y

Azzi Z, Al Sayegh H, Metwally O, Eissa M (2025) Review of nondestructive testing (NDT) techniques for timber structures. Infrastructures 10(2):28. https://doi.org/10.3390/infrastructures10020028

Bachtiar EV, Rüggeberg M, Hering S, Kaliske M, Niemz P (2017) Estimating shear properties of walnut wood: A combined experimental and theoretical approach. Mater Struct 50:248. https://doi.org/10.1617/s11527-017-1119-2

Bucur V, Feeney FE (1992) Attenuation of ultrasound in solid wood. Ultrasonics 30:76–81. https://api.semanticscholar.org/CorpusID:122875380

Buczkowski G, Bertelsmeier C (2017) Invasive termites in a changing climate: A global perspective. Ecol Evol 7:974–985. https://doi.org/10.1002/ece3.2674

Chuang ST, Wang SY (2001) Evaluation of standing tree quality of Japanese cedar grown with different spacing using stress-wave and ultrasonic-wave methods. J Wood Sci 47:245–253. https://doi.org/10.1007/BF00766709

Churkina G, Organschi A, Reyer CPO, Ruff A, Vinke K, Liu Z, Reck BK, Graedel TE, Schellnhuber HJ (2020) Buildings as a global carbon sink. Nat Sustain 3(4):269–276. https://doi.org/10.1038/s41893-019-0462-4

Danasingh AA, Leavline JE (2016) Model-based outlier detection system with statistical preprocessing. J Mod Appl Stat Methods 15(1):789–801. https://doi.org/10.22237/jmasm/1462077480

Du X, Li J, Feng H, Chen S (2018) Image reconstruction of internal defects in wood based on segmented propagation rays of stress waves. Appl Sci 8(10):1778. https://doi.org/10.3390/app8101778

Eitelberger J, Bader T, De BorstK, Jäger A (2012) Multiscale prediction of viscoelastic properties of softwood under constant climatic conditions. Comput Mater Sci 55:303–312. https://doi.org/10.1016/j.commatsci.2011.11.033

Espinosa L, Prieto F, Brancheriau L, Lasaygues P (2019) Effect of wood anisotropy in ultrasonic wave propagation: A ray-tracing approach. Ultrasonics 91:242–251. https://doi.org/10.1016/j.ultras.2018.07.015

Fang Y, Lin L, Feng H, Emms GW, Lu Z (2017) Review of the use of air-coupled ultrasonic technologies for nondestructive testing of wood and wood products. Comput Electron Agric 137:79–87. https://doi.org/10.1016/j.compag.2017.03.015

Ghaly A, Edwards S (2011) Termite damage to buildings: Nature of attacks and preventive construction methods. Am J Eng Appl Sci 4(2):187–200. https://doi.org/10.3844/ajeassp.2011.187.200

Huan Z, Jiao Z, Li G, Wu X (2018) Velocity error correction based tomographic imaging for stress wave nondestructive evaluation of wood. BioResources 13(2):2530–2545. https://doi.org/10.15376/biores.13.2.2530-2545

Kabir MF (2001) Prediction of ultrasonic properties from grain angle. J Inst Wood Sci 15(5):235–246.

Kang C, Kim N, Kim B, Kim Y, Byun H, So W, Yeo H, Oh S, Lee W, Lee H (2008) Introduction to Wood Physics and Mechanics. Hyangmunsa, Seoul. 338 p.

Kim GC, Bae MS, Lee JJ (2003) Difference of deterioration according to exposed condition of column in wooden traditional building. J Korean Wood Sci Technol 31(2):58–68.

Kretschmann DE (2010) Mechanical properties of wood. Chapter 5 in Wood handbook: Wood as an engineering material, Centennial ed., General Technical Report FPL-GTR-190. USDA Forest Service Forest Prod Lab, Madison, WI. https://www.fpl.fs.usda.gov/documnts/fplgtr/fplgtr190/chapter_05.pdf

Lee S-B, Tong RL, Kim S-H, Im I-G, Su N-Y (2021). Potential pest status of the Formosan subterranean termite, *Coptotermes formosanus* Shiraki (Blattodea: Isoptera: Rhinotermitidae), in response to climate change in the Korean Peninsula. Fla Entomol 103(4):431–437. https://doi.org/10.1653/024.103.00403

Li M, Wang M, Ding R, Deng T, Fang S, Lai F, Luoi R (2021) Study of acoustic emission propagation characteristics and energy attenuation of surface transverse wave and internal longitudinal wave of wood. Wood Sci Technol 55(6):1619–1637. https://doi.org/10.1007/s00226-021-01329-y

Liang S, Fu F, Lin L, Hu N (2010) Various factors and propagation trends of stress waves in cross sections of Euphrates poplar. For Prod J 60(5):440–446. https://meridian.allenpress.com/fpj/article-pdf/60/5/440/1698790/0015-7473-60_5_440.pdf

Liu H, Gao J, Chen Y, Liu Y (2014) Effects of moisture content and fiber proportion on stress wave velocity in Cathay poplar (*Populus cathayana*) wood. BioResources 9(2):2214–2226. https://bioresources.cnr.ncsu.edu/resources/effects-of-moisture-content-and-fiber-proportion-on-stress-wave-velocity-in-cathay-poplar-populus-cathayana-wood/

Mascia N, Nicolas EA, Todeschini R (2011) Comparison between Tsai-Wu failure criterion and Hankinson's formula for tension in wood. Wood Res 56(4):499-510.

Montero MJ, de La Mata J, Esteban M, Hermoso E (2015) Influence of moisture content on the wave velocity to estimate mechanical properties of large cross-section Scots pine. Maderas. Ciencia y tecnología 17(2):407–420. https://www.scielo.cl/scielo.php?pid=S0718-221X2015005000038&script=sci_arttext&tlng=en

Niederleithinger E, Vössing KJ (2018) Nondestructive assessment and imaging methods for internal inspection of timber: A review. Holzforschung 72(6):467–476. https://doi.org/10.1515/hf-2017-0122

Nowak T, Karolak A, Sobótka M, Wyjadłowski M (2019) Assessment of the condition of wharf timber sheet wall material by means of selected non-destructive methods. Materials 12(9):1532. https://doi.org/10.3390/ma12091532

Ondrejka V, Gergeľ T, Bucha T, Pástor M (2020) Innovative methods of non-destructive evaluation of log quality. Cent Eur For J 66, 1–11. https://doi.org/10.2478/forj-2020-0021

Pahnabi N, Schumacher T, Sinha A (2024) Imaging of structural timber based on in situ radar and ultrasonic wave measurements: A review of the state-of-the-art. Sensors 24(9):2901. https://doi.org/10.3390/s24092901

Riggio M, Anthony RW, Augelli F, Kasal B, Lechner T, Muller W, Tannert T (2014) In situ assessment of structural timber using non-destructive techniques. Mater Struct 47:749–766. https://doi.org/10.1617/s11527-013-0093-6

Senalik CA, Farber B (2021). Mechanical properties of wood. Chapter 5 in Wood handbook: Wood as an engineering material, General Technical

Report FPL-GTR-282. USDA Forest Service Forest Prod Lab, Madison, WI, 46 p. https://research.fs.usda.gov/treesearch/62244

Shabani A, Kioumarsi M, Plevris V, Stamatopoulos H (2020) Structural vulnerability assessment of heritage timber buildings: A methodological proposal. Forests 11(8):881. https://doi.org/10.3390/f11080881

Shcherbakov M, Brebels A, Shcherbakova NL, Tyukov A, Janovsky TA, Kamaev VA (2013) A survey of forecast error measures. World Appl Sci J 24(24):171–176. https://www.researchgate.net/publication/281718517_A_survey_of_forecast_error_measures

Starzyk A, Rybak-Niedziółka K, Nowysz A, Marchwiński J, Kozarzewska A, Koszewska J, Piętocha A, Vietrova P, Łacek P, Donderewicz M, Langie K, Walasek K, Zawada K, Voronkova I, Francke B, Podlasek A (2024) New zero-carbon wooden building concepts: A review of selected criteria. Energies 17(17):4502. https://doi.org/10.3390/en17174502

Tanasoiu V, Miclea C, Tanasoiu C (2002) Nondestructive testing techniques and piezoelectric ultrasonics transducers for wood and built-in wooden structures. JOAM 4(4):949–957.

Verbist M, Nunes L, Jones D, Branco JM (2019) Service life design of timber structures, in Long-term Performance and Durability of Masonry Structures: Degradation Mechanisms, Health Monitoring and Service Life Design, ed B Ghiassi, P B Lourenço. Woodhead Publishing, Duxford, UK, pp. 311–336. https://www.sciencedirect.com/science/article/pii/B978008102110100011X

Wang JY, Stirling R, Morris P, Taylor A, Lloyd J, Kirker G, Lebow S, Mankowski M, Barnes HM, Morrell JJ (2018) Durability of mass timber structures: A review of the biological risks. Wood Fiber Sci 50:110–127. https://doi.org/10.22382/wfs-2018-045

Wang X, Ross RJ, McClellan M, Barbour RJ, Erickson JR, Forsman JW, McGinnis GD (2001) Nondestructive evaluation of standing trees with a stress wave method. Wood Fiber Sci 33(4):522–533. http://wfs.swst.org/index.php/wfs/article/view/1014

Wang X (1999) Stress wave-based nondestructive evaluation (NDE) methods for wood quality of standing trees. ProQuest Diss Theses. https://search.proquest.com/openview/5c7470d4496f6503c6fd0c44cd8ddbc1/1?pq-origsite=gscholar&cbl=18750&diss=y

Yang H, Yu L, Wang L (2015) Effect of moisture content on the ultrasonic acoustic properties of wood. J For Res 26(3):753–757. https://doi.org/10.1007/s11676-015-0079-z

Zielińska M, Rucka M (2021) Non-destructive testing of wooden elements. IOP Conference Series: Materials Science and Engineering 1203:032058. https://doi.org/10.1088/1757-899X/1203/3/032058

Migration of polycyclic aromatic hydrocarbons from creosote-treated roundwood in soil under controlled laboratory conditions

Kaelin Quigley
Department of Wood Science and Engineering
Oregon State University
Email: kaelin.quigley@oregonstate.edu

Matthew Konkler
Senior Faculty Research Assistant II
Department of Wood Science and Engineering
Oregon State University
Email: matthew.konkler@oregonstate.edu

Skyler Foster
Department of Wood Science and Engineering
Oregon State University

Jed Cappellazzi
Senior Faculty Research Assistant II
Department of Wood Science and Engineering
Oregon State University
Email: jed.cappellazzi@oregonstate.edu

Nick Skoulis
Creosote Council
Email: nicholasskoulis@cox.net

Gerald Presley *†
Associate Professor
Department of Wood Science and Engineering
Oregon State University
Email: gerald.presley@oregonstate.edu

(Received 21 April 2025)

Abstract: Creosote is used as a wood preservative in a variety of terrestrial and aquatic environments, and some of its components can be detrimental to ecosystem function at high enough concentrations. Therefore, it is important to quantify chemical migration from creosote-treated commodities to better understand their impact. This work measures the migration of 16 polycyclic aromatic hydrocarbons (PAHs) from creosote-treated southern pine and Douglas-fir roundwood posts set in soil contact in barrels under controlled laboratory conditions. Experiments were carried out in soils with both low and high organic matter (OM) content. PAH content was measured in soil over a 32-month period at two distances from the post surface (76 and 152 mm) and at three different depths from the surface (0–15 cm, 15–30 cm, and 30–46 cm). PAH concentration varied widely among the 16 different compounds measured, but generally PAHs with four or fewer rings were more abundant and more frequently found than larger five-ringed PAHs across sample types. It was difficult to identify clear patterns in PAH migration by distance from wood and depth from soil surface because levels were generally low (below 0.4 PPM), and the data was highly variable, which eliminated the possibility of differentiating means statistically in most cases. In many cases, PAH levels found in controls that contained untreated wood were similar to levels found in control soil that contained treated wood, indicating some PAHs found could originate from the soil or surrounding environment. The clearest trend found was that high OM soils much more frequently contained measurable levels of the different PAHs, which is likely due to the known affinity PAHs have for OM. This work provides some methodological insight into studying PAH migration in soils that can help explain PAH migration patterns in soils with different proportions of OM. It also shows that without wetting with liquid water or other physical disturbances faced by wood in service, PAH migration from creosote-treated wood into soil is minimal.

Keywords: Wood preservative; Environmental impacts; Douglas-fir; Southern pine

* Corresponding author
† Society of Wood Science & Technology member

Introduction

Creosote is a widely used industrial wood preservative for protecting utility poles, marine pilings, railroad ties, and other infrastructure-related treated wood commodities for protection against fungi, insects, and marine borers. As a wood preservative, creosote has been in use since the 1830s (Webster 1992). A byproduct of the destructive distillation of high-temp carbonized bituminous coal, creosote is a complex and variable mixture of polycyclic aromatic hydrocarbons (85% of mass), phenolic compounds (10% of mass), and heterocyclic aromatic compounds (5% of mass) (Mueller et al. 1989).

Polycyclic aromatic hydrocarbons (PAHs) are formed as a result of incomplete combustion from both natural and anthropogenic processes. They are found as persistent environmental pollutants in aquatic and terrestrial environments and have an affinity for organic matter (OM) in soils (Wilson and Jones 1993). Some PAHs are regulated by the United States Environmental Protection Agency (US EPA), which includes at least 16 PAHs its priority pollutants list, all of which are found as constituents of coal tar creosote (US EPA 2014). These regulations have implications for the use and manufacture of creosote-treated commodities. Understanding the quantity and scope of PAH migration from creosote-treated wood is important both in a regulatory context and for the end user.

Much of the prior literature measuring PAH migration from creosote-treated commodities focuses on marine environments (Bestari et al. 1998; Morrell et al. 2011). However, the majority of creosote-treated commodities used today are deployed on land either in ground contact or supported on a railroad ballast. Railroad ballasts act as functional buffers between creosote-treated railroad ties and surrounding soils and likely mitigate their impact on surrounding soils and waterbodies (Brooks 2004). Relatively limited information is available on PAH migration from commodities in direct soil contact.

Soil is a complex and highly variable medium for chemical migration which can modulate chemical movement. Several factors determine the rate of migration through and the sorption of organic contaminants in soil, which ultimately determines how much chemical can accumulate in soil. Humic substances, which are part of the organic fraction in soils, have been shown to aid in the sorption of hydrophobic organic compounds in some cases (Pan et al. 2008). PAHs specifically are well known to have an affinity for OM in bulk in soil, which has implications for their rate of migration in different soil conditions (Kariyawasam et al. 2022; Ossai et al. 2020). However, different fractions of soil OM interact differently with PAHs. Humic substances of soils have a more complex relationship with PAHs, where some fractions have no affinity for PAHs and other fractions have condition-dependent affinity for PAHs (Ukalska-Jaruga et al. 2019). These prior findings suggest that the ultimate environmental impact of creosote-treated commodities on terrestrial systems depends in part on soil composition and the composition of soil OM.

In this study, the migration of PAHs from creosote-treated Douglas-fir and southern pine posts was quantified in controlled, indoor mesocosms over a 32-month period. Posts were set in high and low OM soil to measure the impact of soil composition on PAH accumulation in the soil medium. This work provides valuable methodological insights into studies on terrestrial migration of PAHs and can help better interpret future studies aimed at quantifying creosote's environmental impacts.

Methods and materials

Materials

Coastal Douglas-fir (*Pseudotsuga menziesii*) and southern pine posts 15–20 cm in diameter and 2.4 m long were treated with creosote according to the American Wood Protection Association (AWPA) Standard P1/P13-24, Standard for Creosote Preservative (AWPA 2024) at commercial facilities in the southeastern United States (southern pine) and Oregon (Douglas-fir) to Use class 4B retentions (160 kg/m^3) (AWPA 2025). Posts were stored under cover until they were halved to 1.2 m test pieces prior to inclusion in the study. When they were halved, the creosote retention levels of the posts were determined according to the AWPA A6-20 Standard, Method for the Determination of Retention of Oil-Type Preservatives from Small Samples (AWPA 2020) as an aggregate sample for all posts included in the test. The assay zones (0–25 mm) of creosote-treated Douglas-fir posts contained 52 kg/m^3 creosote and southern pine posts contained 143 kg/m^3 of creosote.

Two types of soil were acquired from a local garden supply center, a high OM soil and a low OM soil. The high OM soil blend consisted of half loam collected from near the Willamette River and half 3-in-1 compost of dairy manure and composted bark fines. The low OM soil was unamended loam from the same source as the high OM soil. Each soil was analyzed at the Oregon State University Soil Health Laboratory according to their advanced nutrient profile procedures. A summary of parameters measured for each soil type is shown in Table 1.

Experimental Design

Fourteen food-grade, high-density polyethylene (HDPE) 55-gallon barrels with lids were used in this laboratory PAH

Table 1. Soil nutrient profile and composition of high and low organic matter soils used in this study.

				PPM (mg nutrient/kg soil)				
Soil type	% C	% N	pH	PO_4	NO_3	NH_4		
High organic matter	6.6	0.16	6.95	0.6	4.3	2.1		
Low organic matter	0.1	0.01	7.36	BQL	1.5	0.3		
	PPM (mg nutrient/kg soil)							
Soil type	Ca	Mg	K	B	Cu	Fe	Mn	Zn
High organic matter	3079	923	813	1.1	3.1	115	59	3.7
Low organic matter	1952	654	97	0.2	1.1	24	2	0.6

BQL = below quantification limit.

migration study. A circular hole large enough to accommodate the posts was cut into each barrel lid to allow the top of the creosote-treated posts to stand upright. Tare weights were obtained for the barrels with lids prior to the addition of soil to account for the total mass of soil added. High OM soil to a depth of 15 cm was added to seven of the barrels and low OM soil was added to another seven barrels. Six halved creosote-treated posts 15–20 cm in diameter and 1.2 m long of each species were installed into these barrels. Three of the six creosote-treated Douglas-fir and three of the six creosote-treated southern pine posts were installed into high OM soil barrels, and the remaining three creosoted posts of each species were installed into low OM soil barrels. All posts were installed with the uncut (creosote penetrated) end-grain down into the soil column. One untreated Douglas-fir post was installed in a barrel containing each soil type to serve as low and high OM controls.

After installing posts, another 76 cm of soil was added into each barrel on top of the original 15 cm depth of soil to reach a depth of 91 cm. The total mass of soil added to each barrel was measured. The moisture-holding capacity of each type of soil was first determined using previously described methods (Bouyoucos 1935) in lab. Both soil types were wetted to a moisture content of 20%, which was the approximate moisture holding capacity of the low OM soil. The soils were then lightly tamped down to compact the soil to increase the ease of soil-core sampling. Lids were placed onto each of the barrels with a large plastic bag placed over the top of the posts and placed in between the lid and the barrel to minimize evaporation (Figure 1).

Barrels were incubated at ambient indoor conditions for 32 months. Background soil samples were taken before exposure to creosoted posts. Soil samples were taken at three points: 3, 12, and 32-months after installation. Soil samples were taken

Figure 1. Photo of post-in-barrel test showing southern pine and Douglas-fir posts set in soil within plastic drums. Posts were covered with plastic sheeting to prevent dust from accumulating on the surface, and one pine post is shown uncovered just before sampling.

using a 2.5 x 61 cm (1.0 x 24 in.) stainless steel soil sampler to obtain 46 cm (18 in.) soil cores. Soil cores were taken at two distances from the post, 76 mm (3 in.) and 152 mm (6 in.) with the center of the soil sampler centered at each sampling distance. For each sampling period, the soil cores were taken 60° clockwise from the previous sampling location to reduce disturbances between samplings. The 46 cm (18-in.) soil cores were divided into three sections of about 15 cm each (6-in.): an upper 0–15 cm, middle 15–30 cm, and lower 30–46 cm section. Each soil section (upper, middle, or lower) was homogenized and retained for PAH extraction. The soil corer was cleaned of all soil between each core taken by wiping off excess soil, rinsing the corer with water while cleaning with a brush, and finally spraying it down with ethanol and wiping it dry. All soil samples taken in this study were frozen until extracted for 16 PAHs, as described in the section below.

PAH soil extraction procedure

Triplicate 10 g subsamples of each soil sample were extracted via the following method. Each 10 g subsample was placed into a pre-weighed 50 mL Falcon tube; 20 mL of a 2:2:1 acetone: ethyl acetate: isooctane (v/v) mixture was added to each Falcon tube and weighed again. The samples were hand-shaken to remove any sediment stuck to the bottom of the tube then sonicated for 5 minutes. A modified QuEChERS (Quick, Easy, Cheap, Effective, Rugged, and Safe) (Agilent Technologies, Santa Clara, CA) technique was performed in this study. The procedure consisted of two steps, extraction and cleanup via dispersive solid-phase extraction (dSPE) (Anastassiades et al. 2003; Forsberg et al. 2011). The samples were then treated with a single QuEChERS packet consisting of a salt mixture containing 6 g of magnesium sulfate and 1.5 g of sodium acetate. After addition of the QuEChERS packet, the tubes were weighed (after drying the tubes after the initial sonication) and sonicated for another 5 minutes, followed by 5 minutes of centrifugation at 5,000 RPM.

All supernatants were transferred to a pre-weighed 20 mL amber glass scintillation vial and weighed to determine solvent recovery on a weight basis. Samples were then concentrated under a gentle stream of house air for approximately 15 minutes and weighed again. A 1.5 mL aliquot was then transferred to a 2 mL dispersive solid phase extraction (dSPE) microcentrifuge tube and sonicated for 5 minutes. The SPE tube was then centrifuged for 5 minutes at 5,000 RPM and a final 1 mL aliquot of supernatant was transferred to an amber autosampler vial and frozen until GC-MS analysis. The remaining supernatant in scintillation vials was retained and frozen, should future analysis be necessary.

GC-MS analysis

Sixteen PAHs listed as EPA priority pollutants were quantified using gas chromatography-mass spectrometry (GC-MS) according to modified previously published procedures (Martinez et al. 2004). All standards and samples were analyzed using a Shimadzu GCMS-QP2010S gas chromatograph mass spectrometer (Shimadzu, Kyoto, Japan) utilizing selective ion monitoring (SIM) and a Restek DB-5MS column 30.0 m long, 0.25 µmm thick, and 0.25 mm internal diameter (Restek Corp. Bellefonte, PA). Instrument injection was operated in spitless mode with a 3.5 mm glass liner with de-activated glass wool. A 1 µL injection was performed at 275°C. Chromatography of the 16 PAHs of interest was attained at a column flow rate of 2.50 mL/min using HP-5 grade ultra-high purity helium as the carrier gas. Column oven temperature was set to 70°C, held for 2 min, ramped to 265°C at a rate of 10.0°C/min and held for 18.5 minutes, for a total run time of 40 minutes. Mass spectrometer ion source and interface temperature were 225°C and 275°C, respectively, with a solvent cut time of 5 minutes. If no signal was detected using GC-MS, a value of zero was assigned to the PAH concentration in the extract and any non-detects were used to calculate average values shown below.

Calibration curves were generated by preparing standards from a 2000 µg/mL 16-PAH standard reference standard from Sigma Aldrich (St. Louis, Missouri) in dichloromethane. Concentrations of PAH standards prepared from the 2000 µg/mL stock solution were 0.005, 0.01, 0.1, 0.5, and 1.0 µg/mL.

Results and discussion

Concentrations of PAHs in soil were collected and summarized as mg PAH per kg of soil (PPM) for each PAH, and data for six PAHs that are known, or potential carcinogens, are shown below (Figures 2–6). Average PAH levels for all types were below 0.4 PPM. PAH concentrations were also highly variable at most sampling location/timepoint combinations, leading to high coefficients of variation for many of the average values. This made it very difficult to identify trends among the data because most of the averages could not be statistically differentiated from one another. In most cases, PAHs with four or fewer rings were found at higher concentrations in soil samples taken from barrels, and larger five-ringed PAHs were found less frequently. Control samples also had detectable levels of many PAHs that were like those found in barrels containing creosote-treated wood. This suggests that some of the PAH signal detected originated from the soil or the surroundings of the barrel mesocosms. The barrels were located in a shop space that had been used for wood preservation research for several decades. While the soil microcosms were covered with a lid and plastic sheeting to limit any cross contamination, incidental introduction of dust from the surrounding environment may have resulted in some contamination of the controls. In some cases, the 32-month sampling resulted in more positive detections of PAHs in the controls, as compared to earlier sampling points (Figure 3–6). This may be a result of greater exposure to the surrounding environment over the course of the experiment. Data summarizing migration patterns of the remaining 10 PAHs is available in the supplemental information (Table S1-3).

Average naphthalene concentrations in soils were low at all sampling points, and all averages were below 0.08 PPM (Figure 2). In addition, in most cases, naphthalene levels found in soil taken from untreated controls were similar to those found in

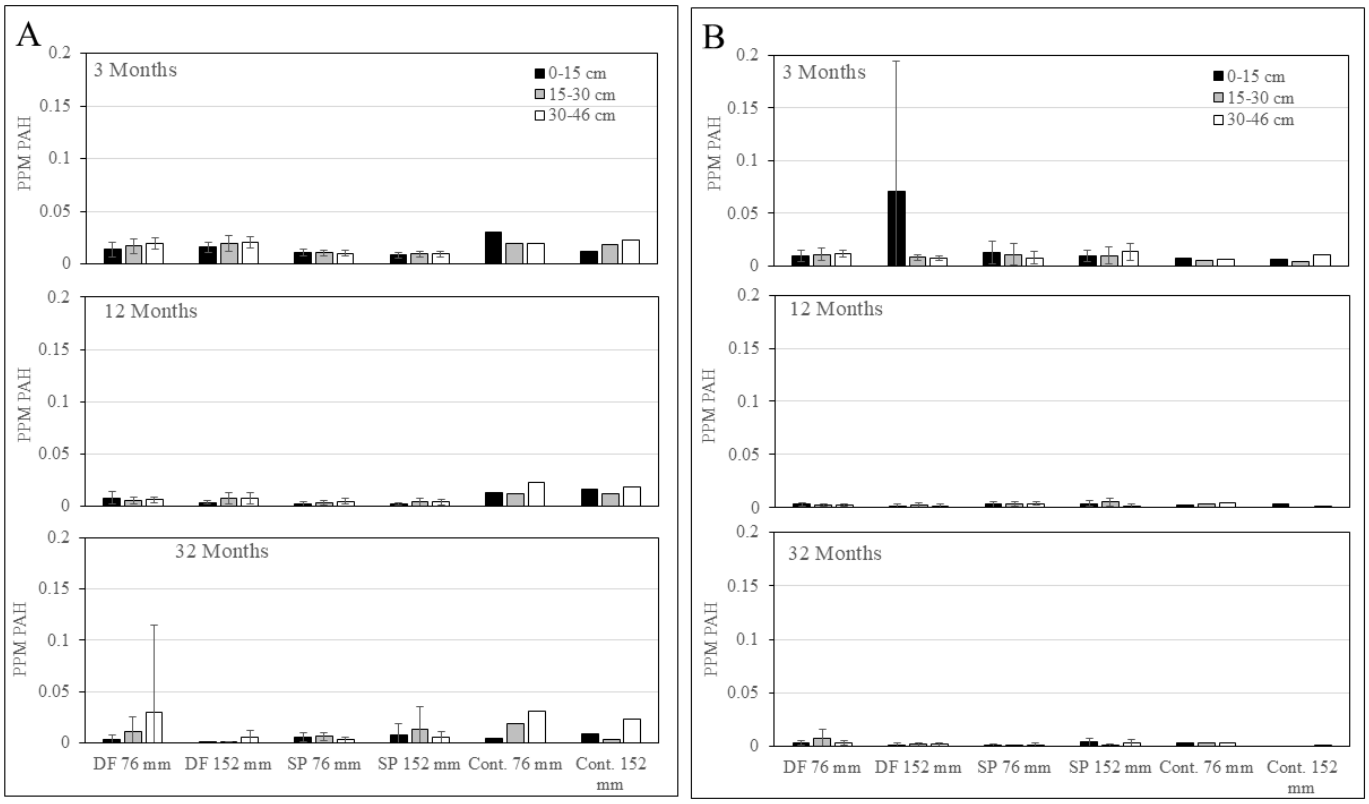

Figure 2. Average naphthalene concentration in high organic matter soil (A) or low organic matter soil (B) sampled at three depths, 0–15, 15–30, and 30–46 cm below the soil surface around southern pine (SP) or Douglas-fir (DF) posts either 76 or 152 mm from the post surface. The samples were taken 3 months, 12 months, and 32 months after installation.

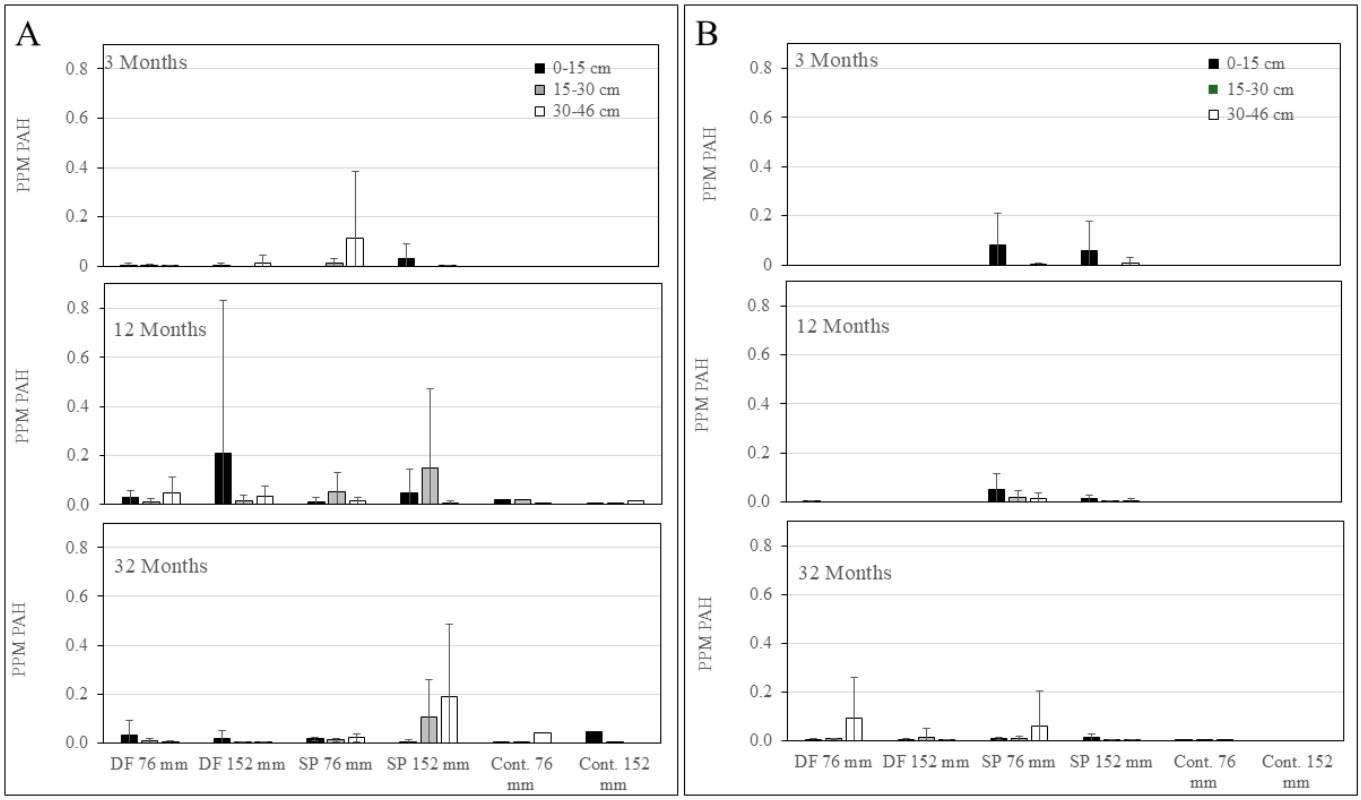

Figure 3. Average Benz[a]anthracene concentration in high organic matter soil (A) or low organic matter soil (B) sampled at three depths, 0–15, 15–30, and 30–46 cm below the soil surface around southern pine (SP) or Douglas-fir (DF) posts either 76 or 152 mm from the post surface. The samples were taken 3 months, 12 months, and 32 months after installation.

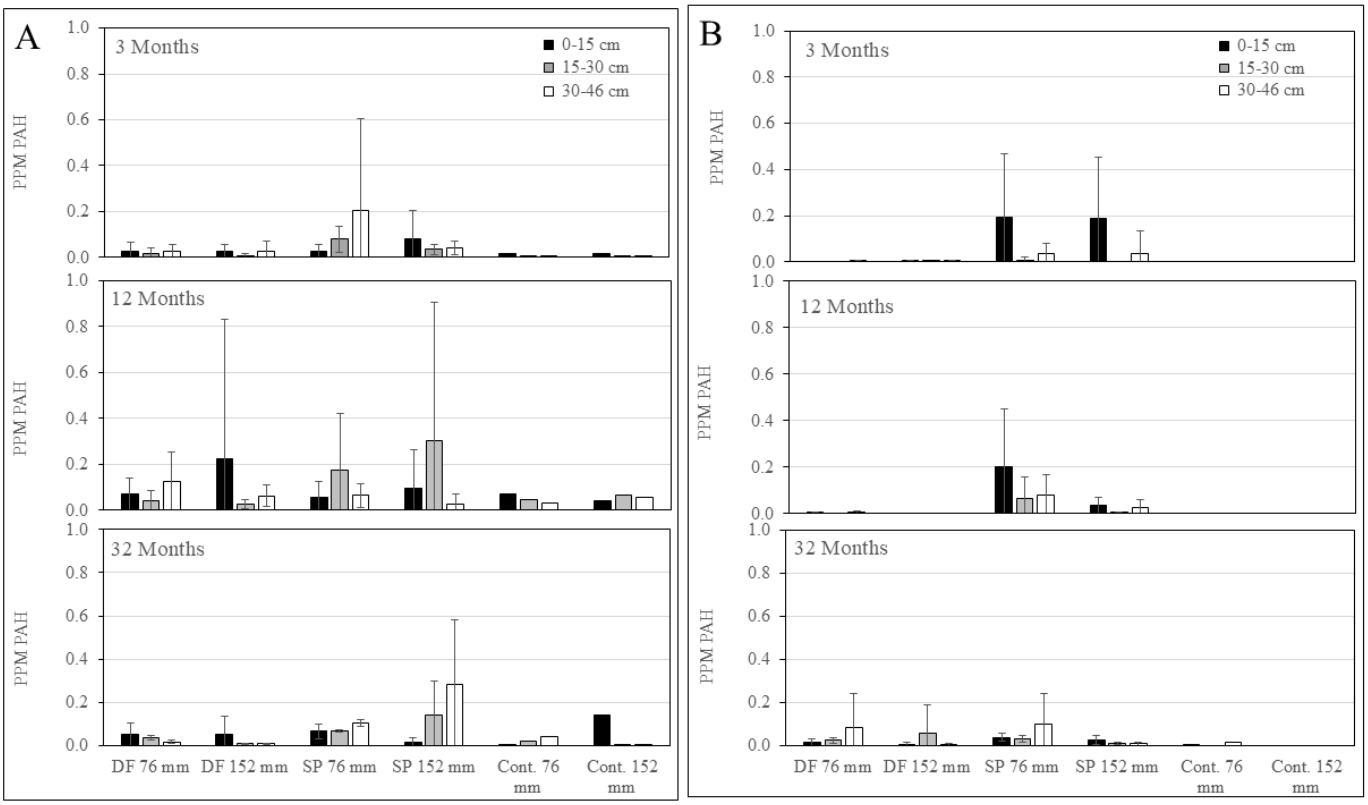

Figure 4. Average chrysene concentration in high organic matter soil (A) or low organic matter soil (B) sampled at three depths, 0–15, 15–30, and 30–46 cm below the soil surface around southern pine (SP) or Douglas-fir (DF) posts either 76 or 152 mm from the post surface. The samples were taken 3 months, 12 months, and 32 months after installation.

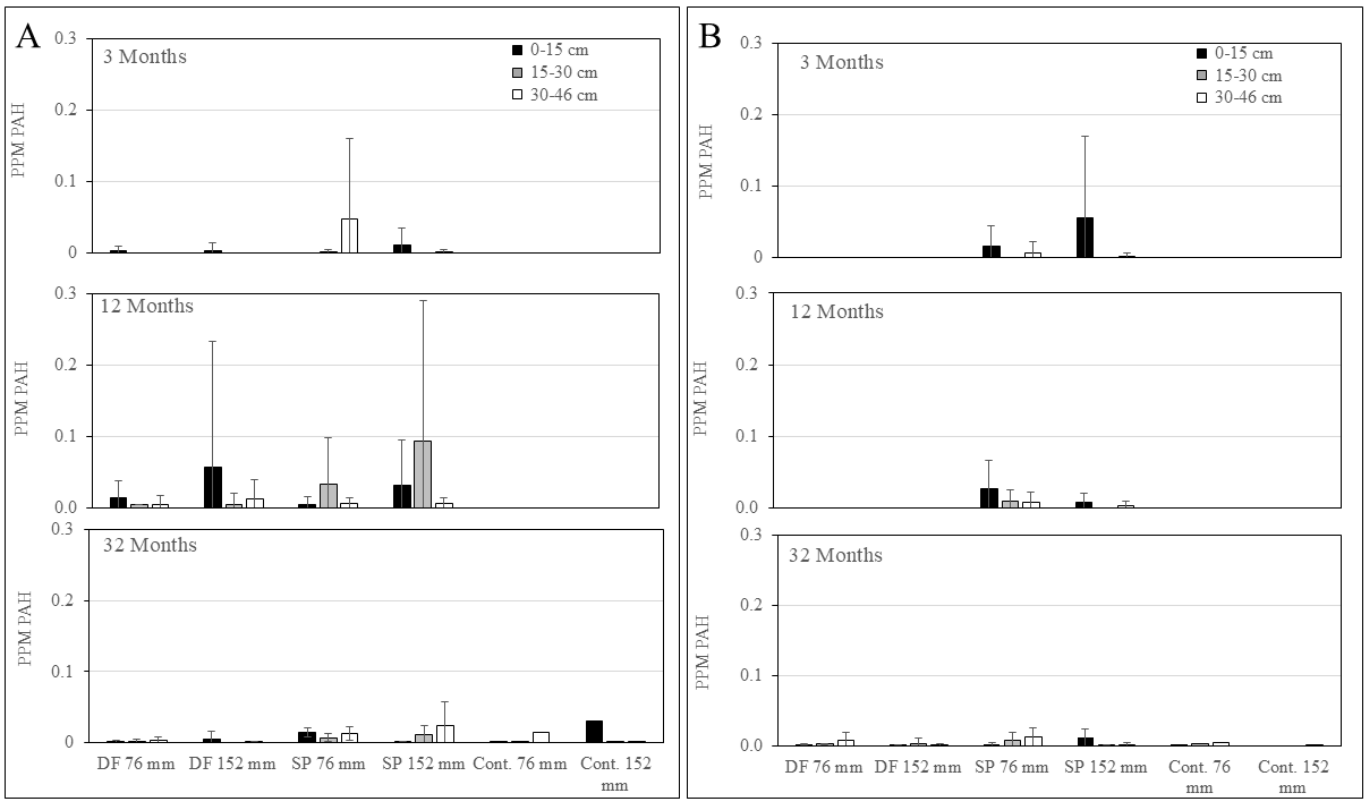

Figure 5. Average benzo[a]pyrene concentration in high organic matter soil (A) or low organic matter soil (B) sampled at three depths, 0–15, 15–30, and 30–46 cm below the soil surface around southern pine (SP) or Douglas-fir (DF) posts either 76 or 152 mm from the post surface. The samples were taken 3 months, 12 months, and 32 months after installation.

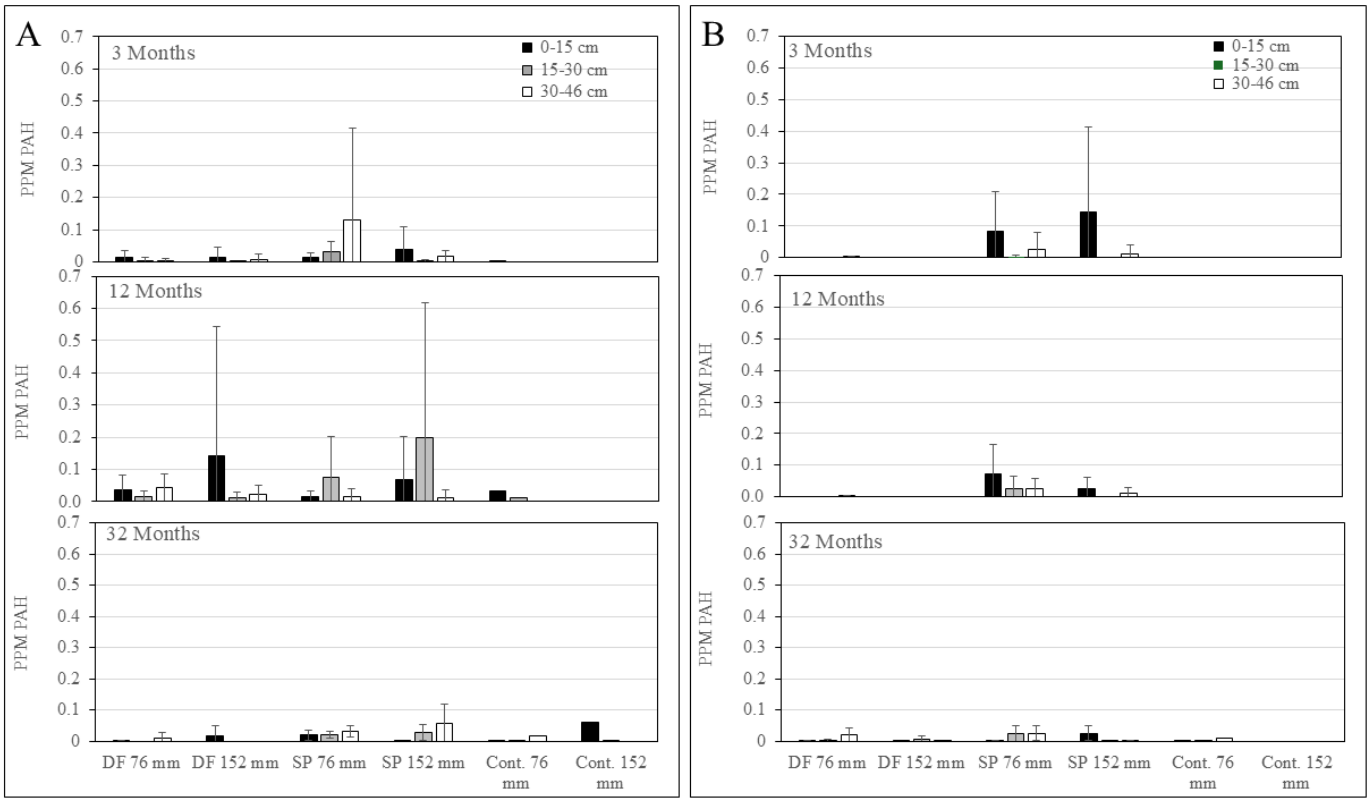

Figure 6. Average combined benzo[b] and [k] fluoranthene concentration in high organic matter soil (A) or low organic matter soil (B) sampled at three depths, 0–15, 15–30, and 30–46 cm below the soil surface around southern pine (SP) or Douglas-fir (DF) posts either 76 or 152 mm from the post surface. The samples were taken 3 months, 12 months, and 32 months after installation.

soil sourced from barrels containing creosote-treated wood. This suggests that the soil or the environment the experiment was run in was a source of naphthalene that could have accounted for most or all of the naphthalene measured here. No major trends among different sampling depths, distances from the posts, wood species, or time from experiment start were apparent. High organic matter soils had naphthalene levels that trended higher than those found in low organic matter soil in the 12- and 32-month sampling points, but levels were similar at the earliest, 3-month timepoint. This could be due to a higher affinity of naphthalene for soil organic matter, which allowed it to adsorb to high OM soil more effectively.

Average benz[a]anthracene concentrations in soil were all at or below 0.2 PPM, and for most of the extracts analyzed, levels found were near or below the detection limit of the method used here (Figure 3). Variation was too high to confidently resolve differences within each soil type at different sampling locations. However, for some sampling locations around treated Douglas-fir posts after 3 and 12 months set in low OM soil, no benz[a]anthracene was detected at all, and levels trended lower in the low OM soil as compared to high OM soil samples. Low average levels of benz[a]anthracene were detected in most of the high OM control soil samples (5.5–20 PPB), and in only three of the low OM soil controls (1–4 PPB). Interestingly, the highest average levels of benz[a]anthracene found were in samples taken 152 mm away from treated Douglas-fir or southern pine posts, opposite to a decreasing concentration trend from the post surface that would be expected.

Chrysene was found at somewhat higher average concentrations levels than the other PAHs discussed here, but all average chrysene concentrations were under 0.4 PPM (Figure 4). Chrysene was detected in most samples around creosote-treated wood, except those taken 12 months after installation at 152 mm away from treated Douglas-fir posts. Variation was too high to confidently resolve differences within each soil type at different sampling locations. Low average levels of chrysene were detected in all of the high OM control soil samples, ranging from 0.2 to 139 PPB. Chrysene was less frequently detected in low OM controls and was only at 0.003–0.013 PPM 32 months after installation. Soils taken around treated southern pine posts in many cases appeared to have more consistently higher chrysene levels, possibly due to the higher creosote loadings in these posts. However, statistical comparisons could not resolve differences due to the high level of variation in the data.

Benzo[a]pyrene was found in most soil samples taken around creosote-treated posts except for Douglas-fir posts in low OM soil after 12 months and the middle depth soil sample taken 76 mm (6 in.) away from the surface of treated Douglas-fir posts in high OM soil. Where it was found around creosote-treated posts, average benzo[a]pyrene levels ranged from 0.0002 to 0.093 PPM, and where it was found around control posts, average concentrations ranged from 0.0001 to 0.029 PPM. No benzo[a]pyrene was detected in any of the 12-month control samples. Variation was too high to confidently resolve differences within each soil type at different sampling locations. Soils taken around treated southern pine posts in some cases appeared to have more consistently higher benzo[a]pyrene levels, possibly due to the higher creosote loadings in these posts. However, statistical comparisons could not resolve differences, due to the high level of variation in the data.

Benzo[b] and [k] fluoranthene were considered together because chromatographic separation of the two compounds was insufficient to demarcate individual peaks. Where present around creosote-treated wood, average concentration of these compounds ranged from 0.05 to 199 PPB, and where present around control, concentrations ranged from 0.3-62 PPB. Detection in control soils was sporadic: only 8.3% of 3-month control samples, 16.7% of 12-month control soil samples, and 66.7% of 32-month control samples had detectable levels of benzo[b] and [k] fluoranthene. Average concentrations in control samples ranged from 0.3 to 61 PPB. Variation was too high to confidently resolve differences within each soil type at different sampling locations.

Soil samples were analyzed for a total of 16 PAHs in this study (Table S1-3). Trends varied slightly for each PAH, but migration was generally low, likely due to the absence of rainwater in this study. Despite their low solubility, rainwater can mobilize PAHs from creosote-treated wood surfaces (Konkler et al. 2020). The limited PAH migration measured from posts under controlled conditions not subjected to rainfall may suggest that rainfall is one of the primary drivers of PAH migration from creosote-treated commodities in ground contact.

For most PAHs measured here, averages soil concentrations trended higher in the high organic matter soil. This is due to the higher affinity PAHs have for soil organic matter than inorganic elements in soil (Kariyawasam et al. 2022; Ukalska-Jaruga et al. 2019). This trend suggests that soil characteristics can help modulate PAH accumulation around creosote-treated commodities. It would be beneficial to understand the soil characteristics in any study of PAH migration from creosote-treated wood to better explain migration patterns.

Conclusions

This work shows that in the absence of wetting and physical disturbances faced by creosote-treated wood when in service, very low levels of PAHs migrate from treated commodities. Chemical migration that was detected was sporadic and did not follow expected concentration gradients in relation to distance from wood surfaces. Background PAHs present in the soil or environment contributed to the overall PAH signal, and this should be a consideration in interpreting data in subsequent studies of the environmental impact of creosote-treated wood. The properties of the soil play a role in determining the efficiency of PAH capture in soil, with higher organic matter soils retaining more PAHs. Soil properties should be considered in any study of chemical migration from creosote-treated wood. This work will provide useful methodological insights for the future study of chemical migration from creosote-treated in service.

Acknowledgements

Funding for this research was provided by the Creosote Council and their contributor organizations.

References

Anastassiades M, Lehotay SJ, Stajnbaher D, Schenck FJ (2003) Fast and easy multiresidue method employing acetonitrile extraction/partitioning and “dispersive solid-phase extraction” for the determination of pesticide residues in produce. J AOAC Int 86(2):412–431. https://doi.org/10.1093/jaoac/86.2.412

AWPA (2025) Standard U1-25, Use Category System: User Specification for Treated Wood. American Wood Protection Association, Birmingham, AL.

AWPA (2024) Standard P1/P13-24, Standard for Creosote Preservative. American Wood Protection Association, Birmingham, AL.

AWPA (2020) Standard Method for the Determination of Retention of Oil-Type Preservatives from Small Samples. American Wood Protection Association, Birmingham, AL.

Bestari K, Robinson R, Solomon K, Steele T, Day K, Sibley P (1998) Distribution and composition of polycyclic aromatic hydrocarbons within experimental microcosms treated with creosote-impregnated Douglas-fir pilings. Environ Toxicol Chem 17(12):2369–2377. https://doi.org/10.1002/etc.5620171202

Bouyoucos GJ (1935) A comparison between the suction method and the centrifuge method for determining the moisture equivalent of soils. Soil Sci 40(2):165.

Brooks KM (2004) Polycyclic Aromatic Hydrocarbon Migration from Creosote-Treated Railway Ties into Ballast and Adjacent Wetlands. Res Pap FPL−RP−617. USDA For Serv, Forest Prod Lab, Madison, WI. 53 p. https://creosotecouncil.org/wp-content/uploads/2020/01/Polycyclic-Aromatic-Hydrocarbon-Migration-from-Creosote-Kenneth-Brooks.pdf

Forsberg ND, Wilson GR, Anderson KA (2011) Determination of parent and substituted polycyclic aromatic hydrocarbons in high-fat salmon using a modified QuEChERS extraction, dispersive SPE and GC-MS. J Agric Food Chem 59 (15):8108–8116. dx.doi.org/10.1021/jf201745a

Kariyawasam T, Doran GS, Howitt JA, Prenzler PD (2022) Polycyclic aromatic hydrocarbon contamination in soils and sediments: Sustainable approaches for extraction and remediation. Chemosphere 291(3). https://doi.org/10.1016/j.chemosphere.2021.132981

Konkler MJ, Cappellazzi J, Presley G, Morrell JJ (2020) Migration of creosote components from timbers treated with creosote and processed using Best Management Practices. J Environ Manage 276:111270. https://doi.org/10.1016/j.jenvman.2020.111270

Martinez E, Gros M, Lacorte S, Barcelo D (2004) Simplified procedures for the analysis of polycyclic aromatic hydrocarbons in water, sediments and mussels. J Chromatogr A 1047:181–188. https://doi.org/10.1016/j.chroma.2004.07.003

Morrell JJ, Brooks KM, Davis CM (Eds.) (2011) Managing Treated Wood in Aquatic Environments. Forest Products Society, Madison, WI.

Mueller J, Chapman P, Pritchard P (1989) Creosote-contaminated sites - Their potential for bioremediation. Environ Sci Technol 23(10):1197–1201. https://doi.org/10.1021/es00068a003

Ossai IC, Ahmed A, Hassan A, Hamid FS (2020) Remediation of soil and water contaminated with petroleum hydrocarbon: A review. Environ Technol Innov 17. https://doi.org/10.1016/j.eti.2019.100526

Pan B, Ning P, Xing B (2008) Part IV-sorption of hydrophobic organic contaminants. Environ Sci Pollut Res 15(7):554–564. https://doi.org/10.1007/s11356-008-0051-y

Ukalska-Jaruga A, Smreczak B, Klimkowicz-Pawlas A (2019) Soil organic matter composition as a factor affecting the accumulation of polycyclic aromatic hydrocarbons. J Soils Sediments 19:1890–1900. https://doi.org/10.1007/s11368-018-2214-x

US EPA 2014. https://www.epa.gov/sites/default/files/2015-09/documents/priority-pollutant-list-epa.pdf

Webster PD (1992) The wood crosstie: A 150-year success story (1st ed.). The Railway Tie Association.

Wilson S, Jones K (1993) Bioremediation of soil contaminated with polynuclear aromatic-hydrocarbons (PAHS)—A review. Environ Pollut 81(3):229–249. https://doi.org/10.1016/0269-7491(93)90206-4

Appendix: Supplemental Tables

Table S1. Concentration of PAHs found in soil around southern pine and Douglas-fir posts after 3 months in soil barrel mesocosms.

Naphthalene concentration (ppb)[a]

Species	Creosote	High organic matter soil						Low organic matter soil					
		76 mm away			150 mm away			76 mm away			150 mm away		
		0-15 mm	15-30 cm	30-45 cm	0-15 cm	15-30 cm	30-45 cm	0-15 cm	15-30 cm	30-45 cm	0-15 cm	15-30 cm	30-45 cm
Douglas-fir	+	13.7 (7.2)	17.0 (7.1)	19.8 (5.3)	16.1 (4.8)	19.6 (7.1)	21.0 (5.4)	9.3 (5.4)	11.0 (6.2)	11.5 (2.9)	71.2 (123.4)	7.8 (3.0)	7.2 (2.3)
	-	30.6	20.0	19.2	11.9	19.0	22.8	7.2	5.4	6.2	5.8	4.0	10.5
Southern pine	+	11.3 (3.2)	10.7 (2.5)	10.3 (2.8)	8.7 (2.6)	9.6 (2.6)	9.5 (2.5)	12.7 (10.6)	10.7 (10.2)	7.7 (5.5)	9.3 (5.6)	9.9 (7.7)	13.3 (8.5)
	-	30.6	20.0	19.2	11.9	19.0	22.8	7.2	5.4	6.2	5.8	4.0	10.5

Acenaphthylene concentration (ppb)[a]

Species	Creosote	High organic matter soil						Low organic matter soil					
		76 mm away			150 mm away			76 mm away			150 mm away		
		0-15 mm	15-30 cm	30-45 cm	0-15 cm	15-30 cm	30-45 cm	0-15 cm	15-30 cm	30-45 cm	0-15 cm	15-30 cm	30-45 cm
Douglas-fir	+	0 (0)	0.4 (1.1)	0 (0)	0 (0)	0 (0)	0 (0)	0 (0)	0 (0)	0 (0)	0 (0)	0 (0)	0 (0)
	-	0.8	0	0	0	0	0	0	0	0	0	0	0
Southern pine	+	0 (0)	0.1 (0.1)	1.9 (4.8)	0 (0)	0 (0)	0 (0)	0 (0)	0 (0)	0 (0)	9.9 (7.7)	0 (0)	0 (0)
	-	0.8	0	0	0	0	0	0	0	0	0	0	0

[a]Values are means of three replicate samples with one standard deviation in parentheses.

Acenaphthene concentration (ppb)[a]

Species	Creosote	High organic matter soil						Low organic matter soil					
		76 mm away			150 mm away			76 mm away			150 mm away		
		0-15 mm	15-30 cm	30-45 cm	0-15 cm	15-30 cm	30-45 cm	0-15 cm	15-30 cm	30-45 cm	0-15 cm	15-30 cm	30-45 cm
Douglas-fir	+	138.2 (147.7)	140.0 (86.5)	92.0 (32.2)	91.0 (33.8)	143.3 (87.6)	165.9 (83.8)	4.8 (7.6)	5.2 (7.8)	4.2 (6.6)	67.0 (119.2)	3.8 (5.8)	2.8 (4.6)
	-	239.9	107.0	91.9	80.3	255.6	315.6	0 (0)	0 (0)	0 (0)	200.0 (300.0)	0 (0)	0.5 (0.5)
Southern pine	+	63.1 (60.6)	78.7 (45.9)	77.4 (40.1)	62.3 (23.1)	69.0 (55.7)	75.0 (51.3)	4.9 (6.2)	600.0 (1.2)	0 (100.0)	6.3 (9.2)	100.0 (400.0)	700.0 (700.0)
	-	239.9	107.0	91.9	80.3	255.6	315.6	0 (0)	0 (0)	0 (0)	200.0 (300.0)	0 (0)	500.0 (500.0)

Table S1 (*continued*). Concentration of PAHs found in soil around southern pine and Douglas-fir posts after 3 months in soil barrel mesocosms.

Fluorene concentration (ppb)[a]

Species	Creosote	High organic matter soil						Low organic matter soil					
		76 mm away			150 mm away			76 mm away			150 mm away		
		0-15 mm	15-30 cm	30-45 cm	0-15 cm	15-30 cm	30-45 cm	0-15 cm	15-30 cm	30-45 cm	0-15 cm	15-30 cm	30-45 cm
Douglas-fir	+	37.7 (10.1)	92.3 (87.3)	99.7 (98.6)	52.6 (33.2)	45.5 (29.7)	107.8 (153.8)	10.2 (12.5)	12.3 (10.2)	23.0 (20.9)	16.3 (14.7)	10.1 (7.9)	8.9 (7.5)
	-	49.6 (9.0)	37.2 (11.1)	32.0 (3.7)	20.5 (20.8)	21.7 (4.4)	23.8 (4.3)	6.1 (1.6)	4.0 (1.6)	2.4 (900.0)	1.3 (1.2)	1.6 (400.0)	3.0 (2.1)
Southern pine	+	23.5 (18.9)	63.1 (82.2)	356.5 (797.0)	73.0 (104.3)	26.1 (12.7)	20.4 (8.4)	78.4 (93.7)	15.4 (14.2)	24.7 (39.0)	43.4 (57.7)	8.6 (8.3)	31.3 (32.3)
	-	49.6 (9.0)	37.2 (11.1)	32.0 (3.7)	20.5 (20.8)	21.7 (4.4)	23.8 (4.3)	6.1 (1.6)	4.0 (1.6)	2.4 (900.0)	1.3 (1.2)	1.6 (400.0)	3.0 (2.1)

[a]Values are means of three replicate samples with one standard deviation in parentheses.

Phenanthrene concentration (ppb)[a]

Species	Creosote	High organic matter soil						Low organic matter soil					
		76 mm away			150 mm away			76 mm away			150 mm away		
		0-15 mm	15-30 cm	30-45 cm	0-15 cm	15-30 cm	30-45 cm	0-15 cm	15-30 cm	30-45 cm	0-15 cm	15-30 cm	30-45 cm
Douglas-fir	+	22.2 (9.8)	21.3 (13.1)	19.7 (11.8)	23.3 (13.4)	28.3 (19.8)	35.3 (17.6)	0 (0)	1.7 (3.6)	6.2 (12.1)	9.2 (11.8)	2.6 (4.9)	1.3 (2.6)
	-	50.3 (6.4)	22.9 (7.1)	15.9 (5.7)	12.9 (6.0)	17.5 (7.2)	25.0 (2.5)	0 (0)	0 (0)	0 (0)	0 (0)	0 (0)	0 (0)
Southern pine	+	21.4 (22.0)	41.5 (28.4)	164.9 (340.1)	40.7 (50.7)	27.1 (6.8)	26.5 (4.7)	27.8 (39.1)	800.0 (1.6)	3.8 (7.1)	18.8 (29.9)	0 (0)	4.9 (9.2)
	-	50.3 (6.4)	22.9 (7.1)	15.9 (5.7)	12.9 (6.0)	17.5 (7.2)	25.0 (2.5)	0 (0)	0 (0)	0 (0)	0 (0)	0 (0)	0 (0)

Anthracene (ppb)[a]

Species	Creosote	High organic matter soil						Low organic matter soil					
		76 mm away			150 mm away			76 mm away			150 mm away		
		0-15 mm	15-30 cm	30-45 cm	0-15 cm	15-30 cm	30-45 cm	0-15 cm	15-30 cm	30-45 cm	0-15 cm	15-30 cm	30-45 cm
Douglas-fir	+	4.5 (5.7)	0 (0)	0 (0)	0 (0)	0 (0)	7.5 (22.5)	0 (0)	0 (0)	0 (0)	1.7 (5.2)	0 (0)	0 (0)
	-	0 (0)	0 (0)	0 (0)	0 (0)	0 (0)	0 (0)	0 (0)	0 (0)	0 (0)	0 (0)	0 (0)	0 (0)
Southern pine	+	1.0 (2.5)	40.0 (66.3)	60.0 (134.6)	15.2 (26.1)	300.0 (800.0)	2.4 (1.9)	28.7 (43.6)	0 (100.0)	600.0 (1.2)	20.5 (37.0)	0 (0)	3.8 (11.3)
	-	0 (0)	0 (0)	0 (0)	0 (0)	0 (0)	0 (0)	0 (0)	0 (0)	0 (0)	0 (0)	0 (0)	0 (0)

[a]Values are means of three replicate samples with one standard deviation in parentheses.

Fluoranthene concentration (ppb)[a]

Species	Creosote	High organic matter soil						Low organic matter soil					
		76 mm away			150 mm away			76 mm away			150 mm away		
		0-15 mm	15-30 cm	30-45 cm	0-15 cm	15-30 cm	30-45 cm	0-15 cm	15-30 cm	30-45 cm	0-15 cm	15-30 cm	30-45 cm
Douglas-fir	+	37.7 (10.1)	92.3 (87.3)	99.7 (98.6)	52.6 (33.2)	45.5 (29.7)	107.8 (153.8)	10.2 (12.5)	12.3 (10.2)	23.0 (20.9)	16.3 (14.7)	10.1 (7.9)	8.9 (7.5)
	-	49.6 (9.0)	37.2 (11.1)	32.0 (3.7)	20.5 (20.8)	21.7 (4.4)	23.8 (4.3)	6.1 (1.6)	4.0 (1.6)	2.4 (900.0)	1.3 (1.2)	1.6 (400.0)	3.0 (2.1)
Southern pine	+	23.5 (18.9)	63.1 (82.2)	356.5 (797.0)	73.0 (104.3)	26.1 (12.7)	20.4 (8.4)	78.4 (93.7)	15.4 (14.2)	24.7 (39.0)	43.4 (57.7)	8.6 (8.3)	31.3 (32.3)
	-	49.6 (9.0)	37.2 (11.1)	32.0 (3.7)	20.5 (20.8)	21.7 (4.4)	23.8 (4.3)	6.1 (1.6)	4.0 (1.6)	2.4 (900.0)	1.3 (1.2)	1.6 (400.0)	3.0 (2.1)

Pyrene (ppb)[a]

Species	Creosote	High organic matter soil						Low organic matter soil					
		76 mm away			150 mm away			76 mm away			150 mm away		
		0-15 mm	15-30 cm	30-45 cm	0-15 cm	15-30 cm	30-45 cm	0-15 cm	15-30 cm	30-45 cm	0-15 cm	15-30 cm	30-45 cm
Douglas-fir	+	26.0 (12.3)	52.0 (54.5)	57.0 (64.6)	28.9 (24.9)	19.8 (18.6)	61.9 (96.4)	0 (100.0)	100.0 (400.0)	5.8 (12.9)	7.1 (9.0)	1.2 (3.7)	500.0 (1.3)
	-	23.1 (6.8)	9.2 (4.9)	9.2 (2.0)	31.6 (21.1)	6.2 (2.5)	6.3 (6.4)	0 (0)	0 (0)	0 (0)	0 (0)	0 (0)	0 (0)
Southern pine	+	17.3 (16.4)	56.4 (70.5)	296.8 (666.6)	62.8 (99.8)	17.3 (11.8)	14.9 (11.1)	68.3 (92.6)	2.7 (6.1)	13.4 (25.8)	31.1 (46.8)	100.0 (200.0)	13.3 (18.2)
	-	23.1 (6.8)	9.2 (4.9)	9.2 (2.0)	31.6 (21.1)	6.2 (2.5)	6.3 (6.4)	0 (0)	0 (0)	0 (0)	0 (0)	0 (0)	0 (0)

[a]Values are means of three replicate samples with one standard deviation in parentheses.

Table S1 (*continued*). Concentration of PAHs found in soil around southern pine and Douglas-fir posts after 3 months in soil barrel mesocosms.

Benz [a] anthracene concentration (ppb)[a]

Species	Creosote	High organic matter soil						Low organic matter soil					
		76 mm away			150 mm away			76 mm away			150 mm away		
		0-15 mm	15-30 cm	30-45 cm	0-15 cm	15-30 cm	30-45 cm	0-15 cm	15-30 cm	30-45 cm	0-15 cm	15-30 cm	30-45 cm
Douglas-fir	+	2.8 (8.5)	2.8 (5.5)	1.7 (3.4)	3.9 (10.4)	0 (0)	13.9 (30.3)	0 (0)	0 (0)	0 (0)	0 (0)	0 (0)	0 (0)
	-	0	0	0	0	0	0	0	0	0	0	0	0
Southern pine	+	0 (0)	12.6 (19.2)	113.2 (269.8)	28.8 (61.3)	0 (0)	1.6 (2.7)	79.9 (128.3)	0 (0)	2.0 (6.0)	59.6 (119.0)	0 (0)	7.2 (21.6)
	-	0	0	0	0	0	0	0	0	0	0	0	0

Chrysene (ppb)[a]

Species	Creosote	High organic matter soil						Low organic matter soil					
		76 mm away			150 mm away			76 mm away			150 mm away		
		0-15 mm	15-30 cm	30-45 cm	0-15 cm	15-30 cm	30-45 cm	0-15 cm	15-30 cm	30-45 cm	0-15 cm	15-30 cm	30-45 cm
Douglas-fir	+	28.6 (39.3)	17.5 (23.2)	26.5 (28.8)	24.8 (32.8)	7.0 (9.4)	27.3 (44.6)	0 (0)	0 (0)	1.8 (5.3)	1.2 (3.7)	500.0 (1.6)	1.1 (3.3)
	-	17.4	1.5	2.0	15.6	700.0	3.3	0	0	0	0	0	0
Southern pine	+	27.5 (30.3)	78.7 (57.1)	205.6 (399.4)	80.8 (123.6)	35.5 (21.8)	43.4 (29.5)	194.8 (273.6)	7.7 (13.4)	36.1 (42.6)	188.9 (265.0)	0 (0)	37.7 (95.9)
	-	17.4	1.5	2.0	15.6	700.0	3.3	0	0	0	0	0	0

[a]Values are means of three replicate samples with one standard deviation in parentheses.

Benzo[b] and [k] fluoranthene concentration (ppb)[a]

Species	Creosote	High organic matter soil						Low organic matter soil					
		76 mm away			150 mm away			76 mm away			150 mm away		
		0-15 mm	15-30 cm	30-45 cm	0-15 cm	15-30 cm	30-45 cm	0-15 cm	15-30 cm	30-45 cm	0-15 cm	15-30 cm	30-45 cm
Douglas-fir	+	13.5 (22.2)	5.1 (9.0)	4.1 (5.8)	14.7 (29.6)	400.0 (800.0)	8.4 (15.8)	0 (0)	0 (0)	1.4 (4.1)	0 (0)	0 (0)	0 (0)
	-	5.2	0	0	0	0	0	0	0	0	0	0	0
Southern pine	+	14.6 (13.8)	30.3 (32.7)	129.4 (286.5)	37.5 (70.9)	2.7 (3.2)	19.0 (17.7)	83.0 (126.3)	2.5 (6.7)	24.5 (56.1)	145.0 (266.6)	0 (0)	10.2 (29.7)
	-	5.2	0	0	0	0	0	0	0	0	0	0	0

Benzo[a] pyrene (ppb)[a]

Species	Creosote	High organic matter soil						Low organic matter soil					
		76 mm away			150 mm away			76 mm away			150 mm away		
		0-15 mm	15-30 cm	30-45 cm	0-15 cm	15-30 cm	30-45 cm	0-15 cm	15-30 cm	30-45 cm	0-15 cm	15-30 cm	30-45 cm
Douglas-fir	+	2.2 (6.5)	0 (0)	0 (0)	3.4 (10.3)	0 (0)	0 (0)	0 (0)	0 (0)	0 (0)	0 (0)	0 (0)	0 (0)
	-	0 (0)	0 (0)	0 (0)	0 (0)	0 (0)	0 (0)	0 (0)	0 (0)	0 (0)	0 (0)	0 (0)	0 (0)
Southern pine	+	0 (0)	1.7 (2.7)	47.6 (111.8)	10.4 (24.1)	0 (0)	1.2 (2.9)	15.4 (29.5)	0 (0)	5.7 (17.1)	55.2 (114.1)	0 (0)	1.6 (4.7)
	-	0 (0)	0 (0)	0 (0)	0 (0)	0 (0)	0 (0)	0 (0)	0 (0)	0 (0)	0 (0)	0 (0)	0 (0)

[a]Values are means of three replicate samples with one standard deviation in parentheses.

Dibenz[a,h] anthracene concentration (ppb)[a]

Species	Creosote	High organic matter soil						Low organic matter soil					
		76 mm away			150 mm away			76 mm away			150 mm away		
		0-15 mm	15-30 cm	30-45 cm	0-15 cm	15-30 cm	30-45 cm	0-15 cm	15-30 cm	30-45 cm	0-15 cm	15-30 cm	30-45 cm
Douglas-fir	+	0 (0)	0 (0)	0 (0)	0 (0)	0 (0)	0 (0)	0 (0)	0 (0)	0 (0)	0 (0)	0 (0)	0 (0)
	-	0 (0)	0(0)	0 (0)	0 (0)	0 (0)	0 (0)	0 (0)	0 (0)	0 (0)	0 (0)	0 (0)	0 (0)
Southern pine	+	0 (0)	0 0)	3.4 (8.3)	6.0 (1.6)	0 (0)	0 (0)	5 (1.5)	0 (0)	8.0 (2.3)	7.4 (15.6)	0 (0)	0 (0)
	-	0 (0)	0 (0)	0 (0)	0 (0)	0 (0)	0 (0)	0 (0)	0 (0)	0 (0)	0 (0)	0 (0)	0 (0)

Table S1 (*continued*). Concentration of PAHs found in soil around southern pine and Douglas-fir posts after 3 months in soil barrel mesocosms.

Benzo[g,h,i] concentration (ppb)[a]

Species	Creosote	High organic matter soil						Low organic matter soil					
		76 mm away			150 mm away			76 mm away			150 mm away		
		0-15 mm	15-30 cm	30-45 cm	0-15 cm	15-30 cm	30-45 cm	0-15 cm	15-30 cm	30-45 cm	0-15 cm	15-30 cm	30-45 cm
Douglas-fir	+	0 (0)	0 (0)	0 (0)	0 (0)	0 (0)	0 (0)	0 (0)	0 (0)	0 (0)	0 (0)	0 (0)	0 (0)
	-	0 (0)	0 (0)	0 (0)	0 (0)	0 (0)	0 (0)	0 (0)	0 (0)	0 (0)	0 (0)	0 (0)	0 (0)
Southern pine	+	0 (0)	0 (0)	7.8 (19.0)	0 (0)	0 (0)	0 (0)	0 (0)	0 (0)	1.2 (3.6)	21.5 (49.1)	0 (0)	0 (0)
	-	0 (0)	0 (0)	0 (0)	0 (0)	0 (0)	0 (0)	0 (0)	0 (0)	0 (0)	0 (0)	0 (0)	0 (0)

[a]Values are means of three replicate samples with one standard deviation in parentheses.

Indeno[1,2,3-cd] pyrene concentration (ppb)[a]

Species	Creosote	High organic matter soil						Low organic matter soil					
		76 mm away			150 mm away			76 mm away			150 mm away		
		0-15 mm	15-30 cm	30-45 cm	0-15 cm	15-30 cm	30-45 cm	0-15 cm	15-30 cm	30-45 cm	0-15 cm	15-30 cm	30-45 cm
Douglas-fir	+	0 (0)	0 (0)	0 (0)	0.2 (0.5)	0 (0)	0 (0)	0 (0)	0 (0)	0 (0)	0 (0)	0 (0)	0 (0)
	-	0 (0)	0 (0)	0 (0)	0 (0)	0 (0)	0 (0)	0 (0)	0 (0)	0 (0)	0 (0)	0 (0)	0 (0)
Southern pine	+	0 (0)	0 (0)	11.5 (28.0)	0 (0)	0 (0)	0 (0)	0 (0)	0 (0)	2.4 (7.1)	26.2 (59.7)	0 (0)	0 (0)
	-	0 (0)	0 (0)	0 (0)	0 (0)	0 (0)	0 (0)	0 (0)	0 (0)	0 (0)	0 (0)	0 (0)	0 (0)

[a]Values are means of three replicate samples with one standard deviation in parentheses.

Table S2. Concentration of PAHs found in soil around southern pine and Douglas-fir posts after 12 months in soil barrel mesocosms.

Naphthalene concentration (ppb)[a]

Species	Creosote	High organic matter soil						Low organic matter soil					
		76 mm away			150 mm away			76 mm away			150 mm away		
		0-15 mm	15-30 cm	30-45 cm	0-15 cm	15-30 cm	30-45 cm	0-15 cm	15-30 cm	30-45 cm	0-15 cm	15-30 cm	30-45 cm
Douglas-fir	+	7.9 (5.9)	5.9 (3.2)	6.3 (2.9)	3.8 (1.9)	8.1 (5.6)	8.2 (5.4)	3.3 (1.7)	2.3 (1.3)	2.9 (1.1)	1.7 (1.4)	2.2 (2.1)	1.9 (1.7)
	-	13.0	12.0	22.7	16.4	12.3	18.5	2.8	3.9	4.2	4.1	0	1.2
Southern pine	+	2.4 (2.0)	3.6 (1.9)	4.8 (2.8)	2.6 (1.2)	4.3 (3.7)	4.1 (2.7)	3.2 (3.0)	3.3 (2.3)	3.9 (1.9)	3.8 (2.7)	5.4 (3.7)	1.9 (1.6)
	-	13.0	12.0	22.7	16.4	12.3	18.5	2.8	3.9	4.2	4.1	0	1.2

Acenaphthylene concentration (ppb)[a]

Species	Creosote	High organic matter soil						Low organic matter soil					
		76 mm away			150 mm away			76 mm away			150 mm away		
		0-15 mm	15-30 cm	30-45 cm	0-15 cm	15-30 cm	30-45 cm	0-15 cm	15-30 cm	30-45 cm	0-15 cm	15-30 cm	30-45 cm
Douglas-fir	+	3.0 (5.4)	0 (0)	500.0 (1.6)	1.0 (3.0)	0 (0)	400.0 (1.2)	0 (0)	0 (0)	0 (0)	0 (0)	0 (0)	0 (0)
	-	0	0	0	0	0	0	0	0	0	0	0	0
Southern pine	+	0 (0)	0 (0)	0 (0)	400.0 (1.2)	1.2 (3.8)	0 (0)	1.2 (3.5)	600.0 (1.7)	300.0 (1.0)	1.7 (2.6)	0 (0)	0 (0)
	-	0	0	0	0	0	0	0	0	0	0	0	0

[a]Values are means of three replicate samples with one standard deviation in parentheses.

Acenaphthene concentration (ppb)[s]

Species	Creosote	High organic matter soil						Low organic matter soil					
		76 mm away			150 mm away			76 mm away			150 mm away		
		0-15 mm	15-30 cm	30-45 cm	0-15 cm	15-30 cm	30-45 cm	0-15 cm	15-30 cm	30-45 cm	0-15 cm	15-30 cm	30-45 cm
Douglas-fir	+	45.1 (33.9)	16.7 (10.3)	14.9 (12.0)	15.8 (15.5)	33.4 (30.6)	36.1 (35.5)	300.0 (1.0)	0 (0)	0 (0)	0 (0)	0 (0)	0 (0)
	-	25.3	28.6	32.0	24.0	18.3	31.8	0	0	0	0	0	1.7
Southern pine	+	29.9 (18.6)	22.3 (12.9)	15.5 (8.1)	22.0 (36.5)	10.1 (8.1)	7.6 (4.4)	56.6 (76.2)	26.3 (42.4)	15.8 (20.0)	58.7 (63.6)	6.2 (4.5)	6.7 (6.1)
	-	25.3	28.6	32.0	24.0	18.3	31.8	0	0	0	0	0	1.7

Table S2 (*continued*). Concentration of PAHs found in soil around southern pine and Douglas-fir posts after 12 months in soil barrel mesocosms.

Fluorene concentration (ppb)[a]

Species	Creosote	High organic matter soil						Low organic matter soil					
		76 mm away			150 mm away			76 mm away			150 mm away		
		0-15 mm	15-30 cm	30-45 cm	0-15 cm	15-30 cm	30-45 cm	0-15 cm	15-30 cm	30-45 cm	0-15 cm	15-30 cm	30-45 cm
Douglas-fir	+	24.1 (19.2)	8.5 (5.8)	8.0 (7.5)	9.1 (12.9)	15.1 (12.8)	16.4 (13.6)	300.0 (1.0)	0 (0)	0 (0)	0 (0)	0 (0)	0 (0)
	-	12.7	18.5	14.1	13.9	9.6	17.1	0	0	0	0	0	0
Southern pine	+	17.4 (9.5)	13.5 (8.5)	7.6 (4.6)	6.1 (6.3)	16.1 (25.1)	3.9 (4.2)	20.9 (27.0)	7.3 (10.3)	6.6 (8.1)	21.8 (22.5)	3.4 (3.7)	3.1 (2.6)
	-	12.7	18.5	14.1	13.9	9.6	17.1	0	0	0	0	0	0

[a]Values are means of three replicate samples with one standard deviation in parentheses.

Phenanthrene concentration (ppb)[a]

Species	Creosote	High organic matter soil						Low organic matter soil					
		76 mm away			150 mm away			76 mm away			150 mm away		
		0-15 mm	15-30 cm	30-45 cm	0-15 cm	15-30 cm	30-45 cm	0-15 cm	15-30 cm	30-45 cm	0-15 cm	15-30 cm	30-45 cm
Douglas-fir	+	37.3 (29.9)	15.8 (12.7)	20.8 (17.3)	34.7 (61.9)	20.1 (8.0)	26.4 (10.5)	3.5 (6.9)	0 (0)	2.1 (2.7)	1.6 (3.3)	600.0 (2.0)	0 (0)
	-	26.8	32.7	33.0	36.2	30.1	35.6	0	0	0	0	0	0
Southern pine	+	23.2 (11.8)	45.2 (42.9)	19.3 (9.6)	16.6 (17.0)	53.0 (93.4)	7.9 (8.7)	78.5 (103.0)	28.2 (36.9)	23.8 (25.9)	68.6 (73.4)	9.1 (5.6)	17.8 (16.0)
	-	26.8	32.7	33.0	36.2	30.1	35.6	0	0	0	0	0	0

Anthracene (ppb)[a]

Species	Creosote	High organic matter soil						Low organic matter soil					
		76 mm away			150 mm away			76 mm away			150 mm away		
		0-15 mm	15-30 cm	30-45 cm	0-15 cm	15-30 cm	30-45 cm	0-15 cm	15-30 cm	30-45 cm	0-15 cm	15-30 cm	30-45 cm
Douglas-fir	+	11.9 (13.3)	3.3 (2.8)	10.0 (9.3)	22.1 (62.5)	1.5 (2.6)	6.9 (6.5)	0 (0)	0 (0)	1.6 (2.5)	0 (0)	0 (0)	0 (0)
	-	4.3	6.3	4.9	6.2	6.1	8.0	0	0	0	0	0	0
Southern pine	+	17.1 (19.2)	33.0 (42.8)	12.4 (8.5)	13.9 (19.6)	52.9 (105.5)	4.2 (6.8)	47.6 (60.6)	14.4 (23.1)	15.5 (17.5)	22.4 (17.6)	5.7 (8.5)	7.3 (9.6)
	-	4.3	6.3	4.9	6.2	6.1	8.0	0	0	0	0	0	0

[a]Values are means of three replicate samples with one standard deviation in parentheses.

Fluoranthene concentration (ppb)[a]

Species	Creosote	High organic matter soil						Low organic matter soil					
		76 mm away			150 mm away			76 mm away			150 mm away		
		0-15 mm	15-30 cm	30-45 cm	0-15 cm	15-30 cm	30-45 cm	0-15 cm	15-30 cm	30-45 cm	0-15 cm	15-30 cm	30-45 cm
Douglas-fir	+	24.1 (24.2)	10.9 (10.2)	31.7 (49.1)	41.2 (94.1)	10.3 (4.8)	23.7 (16.1)	6.9 (7.3)	0 (0)	2.6 (3.6)	4.4 (6.6)	1.3 (2.7)	0 (0)
	-	36.6	18.5	28.6	27.7	22.5	14.2	0	0	0	0	0	0
Southern pine	+	4.0 (4.2)	15.8 (11.6)	7.5 (4.2)	30.4 (51.3)	48.8 (103.5)	3.3 (5.4)	85.0 (88.3)	28.9 (37.9)	25.6 (23.6)	60.8 (51.2)	7.5 (5.2)	18.5 (14.8)
	-	36.6	18.5	28.6	27.7	22.5	14.2	0	0	0	0	0	0

Pyrene (ppb)[a]

Species	Creosote	High organic matter soil						Low organic matter soil					
		76 mm away			150 mm away			76 mm away			150 mm away		
		0-15 mm	15-30 cm	30-45 cm	0-15 cm	15-30 cm	30-45 cm	0-15 cm	15-30 cm	30-45 cm	0-15 cm	15-30 cm	30-45 cm
Douglas-fir	+	20.4 (21.0)	6.3 (5.7)	21.8 (35.8)	29.5 (58.5)	8.1 (5.4)	15.5 (16.1)	8.2 (8.3)	0 (0)	1.8 (3.0)	5.5 (8.4)	1.2 (2.4)	0 (0)
	-	31.0	12.3	17.5	18.7	19.7	8.6	0	0	0	0	0	0
Southern pine	+	7.4 (8.3)	22.3 (29.0)	7.5 (4.3)	108.4 (208.8)	113.2 (243.7)	6.3 (9.1)	84.4 (69.2)	24.3 (32.2)	20.8 (19.4)	56.1 (37.7)	6.6 (5.1)	14.1 (11.1)
	-	31.0	12.3	17.5	18.7	19.7	8.6	0	0	0	0	0	0

[a]Values are means of three replicate samples with one standard deviation in parentheses.

Table S2 (*continued*). Concentration of PAHs found in soil around southern pine and Douglas-fir posts after 12 months in soil barrel mesocosms.

Benz [a] anthracene concentration (ppb)[a]

Species	Creosote	High organic matter soil						Low organic matter soil					
		76 mm away			150 mm away			76 mm away			150 mm away		
		0-15 mm	15-30 cm	30-45 cm	0-15 cm	15-30 cm	30-45 cm	0-15 cm	15-30 cm	30-45 cm	0-15 cm	15-30 cm	30-45 cm
Douglas-fir	+	28.4 (28.3)	12.1 (11.4)	49.6 (63.7)	209.0 (622.4)	14.3 (22.6)	32.2 (43.1)	800.0 (2.5)	0 (0)	0 (0)	0 (0)	0 (0)	0 (0)
	-	19.9	17.8	5.9	5.5	5.9	16.1	0	0	0	0	0	0
Southern pine	+	11.9 (15.4)	50.0 (81.3)	16.0 (13.7)	49.1 (94.4)	149.2 (322.3)	6.7 (10.7)	51.7 (65.3)	17.0 (28.4)	14.3 (21.6)	12.1 (15.4)	1.5 (4.5)	5.4 (9.8)
	-	19.9	17.8	5.9	5.5	5.9	16.1	0	0	0	0	0	0

Chrysene (ppb)[a]

Species	Creosote	High organic matter soil						Low organic matter soil					
		76 mm away			150 mm away			76 mm away			150 mm away		
		0-15 mm	15-30 cm	30-45 cm	0-15 cm	15-30 cm	30-45 cm	0-15 cm	15-30 cm	30-45 cm	0-15 cm	15-30 cm	30-45 cm
Douglas-fir	+	69.6 (71.8)	42.9 (42.7)	126.8 (126.1)	222.0 (612.4)	24.6 (19.1)	62.1 (46.0)	1.8 (5.5)	0 (0)	3.7 (6.4)	0 (0)	0 (0)	0 (0)
	-	69.2	46.3	30.8	42.7	64.4	54.8	0	0	0	0	0	0
Southern pine	+	55.9 (67.2)	172.7 (250.2)	64.1 (52.7)	94.8 (170.6)	301.2 (604.3)	27.7 (45.3)	203.9 (248.5)	64.3 (96.1)	78.8 (87.7)	34.3 (33.8)	2.7 (5.6)	29.0 (32.4)
	-	69.2	46.3	30.8	42.7	64.4	54.8	0	0	0	0	0	0

[a]Values are means of three replicate samples with one standard deviation in parentheses.

Benzo[b] and [k] fluoranthene concentration (ppb)[a]

Species	Creosote	High organic matter soil						Low organic matter soil					
		76 mm away			150 mm away			76 mm away			150 mm away		
		0-15 mm	15-30 cm	30-45 cm	0-15 cm	15-30 cm	30-45 cm	0-15 cm	15-30 cm	30-45 cm	0-15 cm	15-30 cm	30-45 cm
Douglas-fir	+	37.6 (46.0)	15.7 (17.5)	43.3 (43.4)	140.9 (404.1)	10.9 (16.8)	22.3 (29.5)	0 (0)	0 (0)	800.0 (2.3)	0 (0)	0 (0)	0 (0)
	-	33.3	10.8	0	0	0	0	0	0	0	0	0	0
Southern pine	+	15.3 (17.4)	75.9 (124.9)	16.6 (21.4)	68.4 (134.4)	199.9 (416.1)	13.3 (21.6)	73.9 (90.4)	25.0 (41.2)	27.3 (30.6)	25.8 (34.2)	0 (0)	11.2 (16.5)
	-	33.3	10.8	0	0	0	0	0	0	0	0	0	0

Benzo[a] pyrene (ppb)[a]

Species	Creosote	High organic matter soil						Low organic matter soil					
		76 mm away			150 mm away			76 mm away			150 mm away		
		0-15 mm	15-30 cm	30-45 cm	0-15 cm	15-30 cm	30-45 cm	0-15 cm	15-30 cm	30-45 cm	0-15 cm	15-30 cm	30-45 cm
Douglas-fir	+	14.0 (23.3)	4.4 (0)	4.4 (13.2)	57.4 (176.1)	5.0 (15.0)	12.5 (27.5)	0 (0)	0 (0)	0 (0)	0 (0)	0 (0)	0 (0)
	-	0	0	0	0	0	0	0	0	0	0	0	0
Southern pine	+	5.0 (10.6)	33.3 (64.1)	5.5 (8.5)	31.5 (62.7)	93.1 (197.4)	5.4 (8.8)	27.5 (39.0)	9.3 (16.2)	7.8 (13.9)	7.9 (12.7)	0 (0)	3.2 (6.5)
	-	0	0	0	0	0	0	0	0	0	0	0	0

[a]Values are means of three replicate samples with one standard deviation in parentheses.

Dibenz[a,h] anthracene concentration (ppb)[a]

Species	Creosote	High organic matter soil						Low organic matter soil					
		76 mm away			150 mm away			76 mm away			150 mm away		
		0-15 mm	15-30 cm	30-45 cm	0-15 cm	15-30 cm	30-45 cm	0-15 cm	15-30 cm	30-45 cm	0-15 cm	15-30 cm	30-45 cm
Douglas-fir	+	0 (0)	0 (0)	0 (0)	0 (0)	0 (0)	0 (0)	0 (0)	0 (0)	0 (0)	0 (0)	0 (0)	0 (0)
	-	0	0	0	0	0	0	0	0	0	0	0	0
Southern pine	+	0 (0)	9.6 (29.5)	0 (0)	8.2 (25.1)	20.1 (45.2)	0 (0)	21.9 (36.0)	9.1 (15.3)	3.0 (6.3)	6.7 (10.5)	0 (0)	0 (0)
	-	0	0	0	0	0	0	0	0	0	0	0	0

Table S2 (*continued*). Concentration of PAHs found in soil around southern pine and Douglas-fir posts after 12 months in soil barrel mesocosms.

Benzo[g,h,i] concentration (ppb)[a]

Species	Creosote	High organic matter soil						Low organic matter soil					
		76 mm away			150 mm away			76 mm away			150 mm away		
		0-15 mm	15-30 cm	30-45 cm	0-15 cm	15-30 cm	30-45 cm	0-15 cm	15-30 cm	30-45 cm	0-15 cm	15-30 cm	30-45 cm
Douglas-fir	+	0 (0)	0 (0)	0 (0)	26.3 (80.7)	0 (0)	0 (0)	0 (0)	0 (0)	0 (0)	0 (0)	0 (0)	0 (0)
	-	0	0	0	0	0	0	0	0	0	0	0	0
Southern pine	+	0 (0)	15.3 (47.1)	0 (0)	13.8 (42.1)	45.9 (103.5)	0 (0)	8.0 (13.2)	2.0 (6.0)	0 (0)	0 (0)	0 (0)	0 (0)
	-	0	0	0	0	0	0	0	0	0	0	0	0

[a]Values are means of three replicate samples with one standard deviation in parentheses.

Indeno[1,2,3-cd] pyrene concentration (ppb)[a]

Species	Creosote	High organic matter soil						Low organic matter soil					
		76 mm away			150 mm away			76 mm away			150 mm away		
		0-15 mm	15-30 cm	30-45 cm	0-15 cm	15-30 cm	30-45 cm	0-15 cm	15-30 cm	30-45 cm	0-15 cm	15-30 cm	30-45 cm
Douglas-fir	+	0 (0)	0 (0)	4.4 (0)	26.3 (80.7)	0 (0)	0 (0)	0 (0)	0 (0)	0 (0)	0 (0)	0 (0)	0 (0)
	-	0	0	0	0	0	0	0	0	0	0	0	0
Southern pine	+	0 (0)	15.3 (47.1)	0 (0)	13.8 (42.1)	78.6 (178.4)	0 (0)	31.3 (46.0)	11.7 (19.9)	4.1 (8.5)	12.0 (15.0)	0 (0)	0 (0)
	-	0	0	0	0	0	0	0	0	0	0	0	0

[a]Values are means of three replicate samples with one standard deviation in parentheses.

Table S3. Concentration of PAHs found in soil around southern pine and Douglas-fir posts after 32 months in soil barrel mesocosms.

Naphthalene concentration (ppb)[s]

Species	Creosote	High organic matter soil						Low organic matter soil					
		76 mm away			150 mm away			76 mm away			150 mm away		
		0-15 mm	15-30 cm	30-45 cm	0-15 cm	15-30 cm	30-45 cm	0-15 cm	15-30 cm	30-45 cm	0-15 cm	15-30 cm	30-45 cm
Douglas-fir	+	3.6 (4.2)	10.6 (14.9)	30.2 (84.4)	0 (0)	0.2 (0.6)	5.8 (6.1)	3.3 (2)	7.3 (8.1)	2.9 (2.2)	1.3 (2)	1.5 (1.8)	1.5 (1.9)
	-	4.1	18.3	31.3	9.2	3.4	23.3	3.1	3	2.8	0	0	0.8
Southern pine	+	5.5 (4)	6.1 (3.9)	2.8 (2.7)	7.1 (11.2)	13.3 (22)	5.5 (5.2)	0.8 (1.3)	0 (0.1)	1.4 (2)	3.9 (3.8)	0.6 (1.2)	3.2 (3.1)
	-	4.1	18.3	31.3	9.2	3.4	23.3	3.1	3	2.8	0	0	0.8

Acenaphthylene concentration (ppb)[a]

Species	Creosote	High organic matter soil						Low organic matter soil					
		76 mm away			150 mm away			76 mm away			150 mm away		
		0-15 mm	15-30 cm	30-45 cm	0-15 cm	15-30 cm	30-45 cm	0-15 cm	15-30 cm	30-45 cm	0-15 cm	15-30 cm	30-45 cm
Douglas-fir	+	0 (0)	0.3 (0.8)	0 (0)	0 (0)	0 (0)	0 (0)	0.1 (0.3)	0.2 (0.6)	0 (0)	0 (0)	0 (0)	0 (0)
	-	0	6.3	4.1	0.7	0	1.9	0	0	0	0	0	0
Southern pine	+	0.6 (0.9)	0.2 (0.6)	0.1 (0.2)	0.4 (0.9)	1.9 (3)	0 (0)	0 (0)	0 (0.1)	0 (0)	2.1 (2.6)	0 (0)	0.1 (0.3)
	-	0	6.3	4.1	0.7	0	1.9	0	0	0	0	0	0

[a]Values are means of three replicate samples with one standard deviation in parentheses.

Table S3 (*continued*). Concentration of PAHs found in soil around southern pine and Douglas-fir posts after 32 months in soil barrel mesocosms.

Acenaphthene concentration (ppb)[a]

Species	Creosote	High organic matter soil						Low organic matter soil					
		76 mm away			150 mm away			76 mm away			150 mm away		
		0-15 mm	15-30 cm	30-45 cm	0-15 cm	15-30 cm	30-45 cm	0-15 cm	15-30 cm	30-45 cm	0-15 cm	15-30 cm	30-45 cm
Douglas-fir	+	197.8 (240.2)	109.7 (81)	41.3 (42.2)	20.3 (16.2)	16.2 (12.9)	17 (7.9)	43.8 (68.7)	31.8 (52.9)	5.5 (8)	0 (0)	0 (0)	18.9 (25.3)
	-	0	319.9	296.9	31.3	0	124.6	0	0	21.5	0	0	0
Southern pine	+	59.6 (83.9)	109.5 (135.3)	13.3 (12.8)	27.1 (57)	94.6 (144.3)	9.6 (7)	5.1 (6.9)	20.1 (16.2)	5.6 (14.4)	23.1 (32.7)	0 (0)	1.3 (2.5)
	-	0	319.9	296.9	31.3	0	124.6	0	0	21.5	0	0	0

Fluorene concentration (ppb)[a]

Species	Creosote	High organic matter soil						Low organic matter soil					
		76 mm away			150 mm away			76 mm away			150 mm away		
		0-15 mm	15-30 cm	30-45 cm	0-15 cm	15-30 cm	30-45 cm	0-15 cm	15-30 cm	30-45 cm	0-15 cm	15-30 cm	30-45 cm
Douglas-fir	+	8.9 (7.9)	8.4 (10)	12.3 (20.6)	119.3 (275.4)	1.2 (2.9)	0.1 (0.2)	33 (43.9)	24.1 (19.6)	48.4 (65.8)	8.5 (11.6)	11.7 (13)	34.3 (41.8)
	-	1.3	9.5	3.8	115.5	2.1	9.4	4.6	1.6	11.2	64.2	0	6.2
Southern pine	+	12.3 (5)	12.3 (5.5)	31.5 (20.8)	16.7 (21.5)	38.6 (45.5)	84.6 (127.7)	28.5 (17.3)	49 (38.3)	11.2 (14.7)	31.6 (36.3)	1 (2.2)	6.9 (7.2)
	-	1.3	9.5	3.8	115.5	2.1	9.4	4.6	1.6	11.2	64.2	0	6.2

[a]Values are means of three replicate samples with one standard deviation in parentheses.

Phenanthrene concentration (ppb)[a]

Species	Creosote	High organic matter soil						Low organic matter soil					
		76 mm away			150 mm away			76 mm away			150 mm away		
		0-15 mm	15-30 cm	30-45 cm	0-15 cm	15-30 cm	30-45 cm	0-15 cm	15-30 cm	30-45 cm	0-15 cm	15-30 cm	30-45 cm
Douglas-fir	+	36.7 (29.7)	20.7 (43.5)	122 (233.9)	24.4 (59.8)	0.2 (0.6)	9.8 (21.6)	237.1 (403.7)	108.2 (197.5)	97.7 (141.8)	1.4 (3.6)	16.4 (28.6)	0.3 (0.6)
	-	0.3	61.7	48.6	61.8	1.9	6.6	1.1	8.1	62.4	0	0	0
Southern pine	+	19.6 (15.8)	16.4 (5)	47.6 (56.4)	13 (10)	124.5 (178.4)	38.6 (53.3)	6.8 (4.4)	238.3 (329.6)	329.5 (377)	12.8 (9.4)	0.3 (0.6)	7.2 (8.2)
	-	0.3	61.7	48.6	61.8	1.9	6.6	1.1	8.1	62.4	0	0	0

Anthracene concentration (ppb)[a]

Species	Creosote	High organic matter soil						Low organic matter soil					
		76 mm away			150 mm away			76 mm away			150 mm away		
		0-15 mm	15-30 cm	30-45 cm	0-15 cm	15-30 cm	30-45 cm	0-15 cm	15-30 cm	30-45 cm	0-15 cm	15-30 cm	30-45 cm
Douglas-fir	+	16.8 (9.9)	17.7 (10)	48.5 (95.9)	24.4 (59.8)	0.2 (0.6)	9.8 (21.6)	13.8 (9.2)	18.3 (15.9)	11.9 (8.1)	1.4 (3.6)	16.4 (28.6)	0.3 (0.6)
	-	16.6	43.6	39.8	33.4	13.4	23.3	18.4	16.9	2.8	284.7	6.5	0.8
Southern pine	+	21 (13.5)	13.4 (10.1)	14 (9.4)	15 (9.4)	23 (22.1)	14.1 (11)	9.7 (5.6)	1.8 (3.1)	5.8 (7.9)	12.8 (9.9)	5.4 (4.1)	10.1 (7.6)
	-	16.6	43.6	39.8	33.4	13.4	23.3	18.4	16.9	2.8	284.7	6.5	0.8

[a]Values are means of three replicate samples with one standard deviation in parentheses.

Fluoranthene concentration (ppb)[a]

Species	Creosote	High organic matter soil						Low organic matter soil					
		76 mm away			150 mm away			76 mm away			150 mm away		
		0-15 mm	15-30 cm	30-45 cm	0-15 cm	15-30 cm	30-45 cm	0-15 cm	15-30 cm	30-45 cm	0-15 cm	15-30 cm	30-45 cm
Douglas-fir	+	8.9 (7.9)	8.4 (10)	12.3 (20.6)	119.3 (275.4)	1.2 (2.9)	0.1 (0.2)	33 (43.9)	24.1 (19.6)	48.4 (65.8)	8.5 (11.6)	11.7 (13)	34.3 (41.8)
	-	1.3	9.5	3.8	115.5	2.1	9.4	4.6	1.6	11.2	64.2	0	6.2
Southern pine	+	12.3 (5)	12.3 (5.5)	31.5 (20.8)	16.7 (21.5)	38.6 (45.5)	84.6 (127.7)	28.5 (17.3)	49 (38.3)	11.2 (14.7)	31.6 (36.3)	1 (2.2)	6.9 (7.2)
	-	1.3	9.5	3.8	115.5	2.1	9.4	4.6	1.6	11.2	64.2	0	6.2

Table S3 (*continued*). Concentration of PAHs found in soil around southern pine and Douglas-fir posts after 32 months in soil barrel mesocosms.

Pyrene concentration (ppb)[a]

Species	Creosote	High organic matter soil						Low organic matter soil					
		76 mm away			150 mm away			76 mm away			150 mm away		
		0-15 mm	15-30 cm	30-45 cm	0-15 cm	15-30 cm	30-45 cm	0-15 cm	15-30 cm	30-45 cm	0-15 cm	15-30 cm	30-45 cm
Douglas-fir	+	7.1 (6.1)	3.4 (3.2)	8.3 (13.6)	84.1 (191.9)	1.7 (3.4)	1.4 (3.8)	17.9 (15.3)	14.9 (10.7)	36.7 (55.6)	6.2 (8.2)	8.7 (10.6)	12.1 (13.8)
	-	0.2	4.5	3.2	97.2	0.6	1.7	2.6	0	6.4	0	0	0
Southern pine	+	11.7 (4.8)	7 (4.4)	22.3 (16)	14.8 (20.9)	24.8 (30)	63.9 (95.2)	41.6 (18.7)	41.1 (42.5)	10.9 (11.7)	45.8 (55.7)	0.6 (1.6)	4.8 (5.2)
	-	0.2	4.5	3.2	97.2	0.6	1.7	2.6	0	6.4	0	0	0

[a]Values are means of three replicate samples with one standard deviation in parentheses.

Benz [a] anthracene concentration (ppb)[a]

Species	Creosote	High organic matter soil						Low organic matter soil					
		76 mm away			150 mm away			76 mm away			150 mm away		
		0-15 mm	15-30 cm	30-45 cm	0-15 cm	15-30 cm	30-45 cm	0-15 cm	15-30 cm	30-45 cm	0-15 cm	15-30 cm	30-45 cm
Douglas-fir	+	33.5 (59.5)	6.2 (10.9)	3.9 (6.3)	17.3 (34.6)	0.8 (1.3)	1.2 (1.4)	4.5 (3.1)	7.1 (3)	92.9 (167.5)	3.6 (3.5)	14.4 (34.8)	1.6 (2)
	-	1.8	3.7	41.2	46.8	2.5	0	3.1	1.4	3.8	0	0	0
Southern pine	+	15.8 (6.6)	11.1 (6.5)	21.8 (16.2)	4.7 (6.2)	104.4 (155.7)	190.5 (297.7)	9.8 (3.2)	7.9 (10.4)	62.1 (142.3)	12.9 (12.9)	1.7 (2)	3.6 (2.5)
	-	1.8	3.7	41.2	46.8	2.5	0	3.1	1.4	3.8	0	0	0

Chrysene concentration (ppb)[a]

Species	Creosote	High organic matter soil						Low organic matter soil					
		76 mm away			150 mm away			76 mm away			150 mm away		
		0-15 mm	15-30 cm	30-45 cm	0-15 cm	15-30 cm	30-45 cm	0-15 cm	15-30 cm	30-45 cm	0-15 cm	15-30 cm	30-45 cm
Douglas-fir	+	50.9 (54.4)	36.4 (58.9)	16.1 (18)	51.4 (82.5)	6.7 (6.1)	6.5 (4.8)	12.5 (13.9)	21.5 (15.3)	83.6 (157.8)	5.3 (6.1)	53.6 (133.6)	3 (4.4)
	-	0.2	16.5	40.8	139.1	4.5	0.5	0.3	0	12.9	0	0	0
Southern pine	+	64.2 (33.8)	66.3 (44)	104.3 (71.9)	14.9 (19.9)	140.7 (159.8)	281.3 (386.9)	36.2 (20.1)	28 (14.6)	98.6 (139.1)	22.5 (22.5)	8.5 (7.4)	7.6 (7.5)
	-	0.2	16.5	40.8	139.1	4.5	0.5	0.3	0	12.9	0	0	0

[a]Values are means of three replicate samples with one standard deviation in parentheses.

Benzo[b] and [k] fluoranthene concentration (ppb)[a]

Species	Creosote	High organic matter soil						Low organic matter soil					
		76 mm away			150 mm away			76 mm away			150 mm away		
		0-15 mm	15-30 cm	30-45 cm	0-15 cm	15-30 cm	30-45 cm	0-15 cm	15-30 cm	30-45 cm	0-15 cm	15-30 cm	30-45 cm
Douglas-fir	+	0.9 (1.8)	0 (0)	9.8 (17.2)	18.1 (31.9)	0 (0)	0 (0)	2.2 (1.8)	3.1 (2.7)	19.3 (22.2)	0.1 (0.2)	5.7 (11.7)	0.2 (0.3)
	-	0.4	0.5	17.3	61.7	0.3	0	0.6	0.5	9.4	0	0	0
Southern pine	+	20.1 (16)	19.3 (11)	31.9 (17.6)	0.3 (0.2)	27.4 (24.5)	58.9 (61.3)	0.4 (0.7)	24.7 (26.2)	26 (23.5)	26 (24.7)	0 (0.1)	1.2 (1.3)
	-	0.4	0.5	17.3	61.7	0.3	0	0.6	0.5	9.4	0	0	0

Benzo[a] pyrene concentration (ppb)[a]

Species	Creosote	High organic matter soil						Low organic matter soil					
		76 mm away			150 mm away			76 mm away			150 mm away		
		0-15 mm	15-30 cm	30-45 cm	0-15 cm	15-30 cm	30-45 cm	0-15 cm	15-30 cm	30-45 cm	0-15 cm	15-30 cm	30-45 cm
Douglas-fir	+	1.3 (1.6)	1.6 (3.2)	3.5 (5.1)	4.7 (11.5)	0 (0)	0.4 (1)	1.4 (0.8)	2.3 (0.8)	8.1 (11.6)	0.4 (0.6)	3 (7.1)	0.9 (1.3)
	-	1.6	2.4	14.5	29.7	1.3	0.1	2.3	2	3.7	0	0	0.1
Southern pine	+	14.7 (6.7)	7.2 (5)	13.3 (9.8)	1.2 (0.7)	10.6 (13.1)	24 (33.3)	1.7 (2.7)	7.8 (11.2)	12.1 (13.4)	10.9 (12.5)	0.2 (0.5)	1.9 (2.3)
	-	1.6	2.4	14.5	29.7	1.3	0.1	2.3	2	3.7	0	0	0.1

[a]Values are means of three replicate samples with one standard deviation in parentheses.

Table S3 (*continued*). Concentration of PAHs found in soil around southern pine and Douglas-fir posts after 32 months in soil barrel mesocosms.

Dibenz[a,h] anthracene concentration (ppb)[a]

Species	Creosote	High organic matter soil						Low organic matter soil					
		76 mm away			150 mm away			76 mm away			150 mm away		
		0-15 mm	15-30 cm	30-45 cm	0-15 cm	15-30 cm	30-45 cm	0-15 cm	15-30 cm	30-45 cm	0-15 cm	15-30 cm	30-45 cm
Douglas-fir	+	36.4 (19.9)	48.1 (35)	38.9 (6.5)	34 (11.9)	35.3 (7.2)	36.5 (8.7)	34 (11.9)	35.3 (7.2)	36.5 (8.7)	34.7 (10.4)	37.5 (5.4)	41.3 (16.1)
	-	36.4	8.3	10.3	65.9	29.1	31.1	51.3	45.6	41	1178.7	33.8	32.9
Southern pine	+	43.2 (24.3)	34.2 (11.5)	41.2 (10.2)	42.8 (13.3)	34.3 (7.5)	31.7 (9.8)	40.2 (12.6)	32.1 (6)	36.6 (6.5)	37 (9.4)	30.7 (5.6)	30.3 (13.5)
	-	36.4	8.3	10.3	65.9	29.1	31.1	51.3	45.6	41	1178.7	33.8	32.9

Benzo[g,h,i] concentration (ppb)[a]

Species	Creosote	High organic matter soil						Low organic matter soil					
		76 mm away			150 mm away			76 mm away			150 mm away		
		0-15 mm	15-30 cm	30-45 cm	0-15 cm	15-30 cm	30-45 cm	0-15 cm	15-30 cm	30-45 cm	0-15 cm	15-30 cm	30-45 cm
Douglas-fir	+	2 (4)	1.5 (2.6)	2.9 (4.6)	9 (14.5)	0 (0)	0 (0)	7.1 (4.7)	6.9 (3.8)	9.8 (7.1)	2.4 (3.4)	2.1 (0.3)	5.7 (6.8)
	-	9.1	10	9.3	32.8	7.3	1.8	12.8	11.4	2.3	0	0	1.9
Southern pine	+	18.2 (7.5)	5 (3.4)	14.2 (10.9)	7.3 (3.3)	6.4 (8.7)	12.5 (12.9)	7 (5.6)	5.5 (7.2)	9.2 (7.9)	10.4 (7)	5.3 (7.5)	6 (4.4)
	-	9.1	10	9.3	32.8	7.3	1.8	12.8	11.4	2.3	0	0	1.9

[a]Values are means of three replicate samples with one standard deviation in parentheses.

Indeno[1,2,3-cd] pyrene concentration (ppb)[a]

Species	Creosote	High organic matter soil						Low organic matter soil					
		76 mm away			150 mm away			76 mm away			150 mm away		
		0-15 mm	15-30 cm	30-45 cm	0-15 cm	15-30 cm	30-45 cm	0-15 cm	15-30 cm	30-45 cm	0-15 cm	15-30 cm	30-45 cm
Douglas-fir	+	4.4 (3.2)	6.6 (7.8)	6.8 (5.7)	12.4 (17)	2.3 (0.6)	2.4 (0.5)	7.7 (3.2)	7.9 (2)	10.7 (5.5)	4 (2)	7.1 (1)	7.7 (5.3)
	-	8.5	9.4	12.4	27.7	6.8	5.9	12	10.7	7.8	82.5	2.4	6.2
Southern pine	+	18.7 (8.3)	8 (2.7)	14.6 (10.4)	9.3 (2.3)	9.7 (7.6)	14.8 (14.8)	6.2 (4)	9.9 (10.6)	10 (6.2)	12.3 (5.7)	7.6 (6.1)	6.8 (3.3)
	-	8.5	9.4	12.4	27.7	6.8	5.9	12	10.7	7.8	82.5	2.4	6.2

[a]Values are means of three replicate samples with one standard deviation in parentheses.

Horizontal flame spread of flame-retardant-treated Japanese cedar (*Cryptomeria japonica*) exterior siding material

Eun-Suk Jang
Ph.D., Research Institute of Human Ecology, College of Human Ecology
Jeonbuk National University, Jeonju 54896, South Korea
Department of Wood Science Technology, College of Agriculture & Life Sciences
Jeonbuk National University, Jeonju 54896, South Korea
Sambo Scientific Co. Ltd, R&D center, Seoul 07258, South Korea
Email: esjang@sambosc.com

Hee-Jun Park *
Professor, Department of Housing Environmental Design, College of Human Ecology
Jeonbuk National University, Jeonju 54896, South Korea
Email: phjun@jbnu.ac.kr

(Received 22 September 2025)

Abstract: The primary objective of this study was to determine whether in-house-developed flame-retardant-treated cedar could serve as an exterior material, not only by meeting the fire-resistance criteria of the cone calorimetry test, but also by demonstrating dependable performance under realistic fire conditions. The results of the cone calorimetry test indicated that the material met the established criteria for total heat release and peak heat release rate, validating its classification as a quasi-noncombustible material. Furthermore, the ASTM E84 Steiner tunnel test was conducted to evaluate the performance of the flame-retardant cedar siding under conditions that simulated real fire scenarios more closely. Flame propagation exhibited a delayed onset and progressed gradually from 2.5 ft to 5 ft over 10 min, indicating restrained flame spread. Concurrently, smoke development remained negligible throughout the test, which is critical for maintaining visibility and minimizing exposure to toxic combustion byproducts. Post-test examination revealed minimal structural degradation, with no evidence of cracking or penetration beyond superficial charring, suggesting that the material retained its physical integrity even under elevated thermal stress. Collectively, these findings confirm that the flame-retardant cedar siding meets the requirements for an ASTM E84 Class A rating and functions as a reliable exterior cladding material capable of enhancing occupant safety in fire scenarios.

Keywords: Flame retardant; quasi-noncombustible performance; siding material; cone calorimeter; Steiner tunnel test

Introduction

In recent years, the construction industry has increasingly emphasized eco-friendliness and sustainability, leading to a steady increase in the demand for wood as a building material (Mergel et al. 2024; Jang et al. 2025a). Wood has a natural texture, aesthetic appeal, and excellent insulation properties. Its carbon storage capacity renders it a sustainable building material (Emre Ilgin and Karjalainen 2022; Jang and Kang 2022; Leszczyszyn et al. 2022; Blanchet et al. 2024).

However, wood has a fatal flaw: its inherent flammability. In the event of a fire, wooden structures can spread flames more easily than concrete structures, causing damage to life and property (Lowden and Hull 2013; Hansen-Bruhn and Hull 2023). Therefore, flame-retardant treatment technology is essential to ensure the safety of wood materials in buildings (Liang et al. 2023; Gao et al. 2024). According to the Korean Ministry of Land, Infrastructure, and Transport (MOLIT) Notification No. 2020-1053 (MOLIT 2020), flame-retardant treatment is legally required for exterior materials used in high-rise buildings in Korea.

Flame retardants used in wood materials typically consist of phosphates, borates, and nitrogen-based compounds. These compounds react with heat to form a carbon layer on the wood surface or inhibit combustion (Chen et al. 2021; Wu et al. 2021).

Common flame-retardant treatment methods for wood include surface coating and vacuum-pressure impregnation. Vacuum-pressure impregnation allows flame retardants to deeply penetrate the porous structure of wood, providing more reliable fire-retardant than coatings (Jang et al. 2024a; Jang et al. 2024b; Jo et al. 2024; Holeček et al. 2025; Jang et al. 2025b).

* Corresponding author

The easiest method for evaluating the fire-retardant properties of wood after flame-retardant treatment is cone calorimetry. The cone calorimetry test is a laboratory test based on KS ISO 5660-1 (Korean Agency for Technology and Standards 2015), Reaction-to-fire tests—Heat release, smoke production and mass loss rate—Part 1: Heat release rate (cone calorimeter method) and smoke production rate (dynamic measurement). Small specimens (100 × 100 mm^2) are exposed to a constant radiant heat flux. The test measures quantitative indicators such as the heat release rate (HRR), total heat release (THR), mass loss rate (MLR), time to ignition (TTI), and smoke production rate (SPR).

Recently, research has been actively conducted on various chemical compositions and treatment technologies for enhancing the flame retardancy of wood. The performance of flame-retardant-treated timber is evaluated using a cone calorimeter.

Wu et al. (2021) conducted a cone calorimetry analysis to assess the combustion behavior of plywood treated with flame retardants. Their findings demonstrated substantial reductions in key fire-related metrics. The treated specimens exhibited reductions of 63.7%, 91.9%, and 53.7% in the average HRR, THR, and effective heat of combustion, respectively. Additionally, the smoke production and toxic gas emissions were significantly mitigated, with the total smoke output, carbon monoxide generation, and oxygen consumption reduced by 76.8%, 85.0%, and 91.9%, respectively. The flame-retardant plywood also exhibited improved fire-resistance indices, including a fire growth index of 3.454 $kW \cdot m^{-2} \cdot s^{-1}$ and a fire performance index of 0.136 $s \cdot m^2 \cdot kW^{-1}$.

Jo et al. (2024) conducted cone calorimetry experiments to examine how variations in the solid content of flame-retardant impregnation (SCFI) influenced THR in Korean larch and Japanese cedar. Through simple linear regression analysis, they determined that achieving the flame-retardancy threshold of 8 MJ/m^2 required SCFI levels of 93.9 kg/m^3 for larch and 144.6 kg/m^3 for cedar. These findings provide a quantitative basis for defining the optimal impregnation dosage necessary to meet the fire safety standards for both wood species.

Zhang et al. (2025) performed cone calorimetry experiments on pinewood samples treated with various flame-retardant additives to quantitatively analyze the combustion characteristics according to heat-flux variations. They found that complex flame retardants, such as DOPO, TPP, and $(NH_4)_2HPO_4$, promoted sample decomposition and reduced the surface temperature, thereby inducing ignition delay. Significantly enhanced flame-retardant performance was observed, particularly under radiant heat conditions of 25 and 30 kW/m^2. Treated samples exhibited ignition delay times at least 1.5 times longer than untreated samples, along with reductions in MLR, THR, oxygen consumption, and CO/CO_2 emissions.

These studies have demonstrated that the cone calorimetry test is useful for quantitatively assessing the fundamental combustion characteristics of wood, highlighting the importance of advancing flame-retardant treatment technologies to ensure the fire safety of buildings. However, the specimen size used in the cone calorimetry tests was limited, and complex variables such as the material installation method, structural connections, ventilation conditions, and material interactions were excluded.

In particular, measurement device errors and reproducibility issues in tests performed in high-temperature environments can lead to quantitative discrepancies with actual fire situations. These limitations suggest that although the cone calorimetry test is suitable for understanding the basic combustion characteristics of materials, it is insufficient for evaluating the fire safety of buildings (Bray et al. 2023; Jang et al. 2024a).

Meanwhile, the ASTM E84 Standard Test Method for Surface Burning Characteristics of Building Materials (ASTM International 2024)—a representative flame-retardancy test stipulated in the U.S. Building Code—evaluates the surface burning characteristics of materials in a 7.6-m-long tunnel-type device called the "Steiner tunnel." Test specimens are installed on the tunnel ceiling and exposed to a 79-kW gas burner at one end under forced ventilation for 10 min. The measurements include the Flame Spread Index (FSI) and Smoke Developed Index (SDI), which indicate the flame retardancy rating of a material (Class A, B, or C). The ASTM E84 test uses large specimens to reflect the actual installation conditions of building materials (ASTM International 2024). It comprehensively evaluates flame spread and smoke development, making a substantial contribution to ensuring building fire safety.

Therefore, the objective of this study was to evaluate the fire performance of flame-retardant-treated cedar siding using both the KS F ISO 5660-1 cone calorimeter test (Korean Agency for Technology and Standards 2015) and the ASTM E84 Steiner tunnel test (ASTM International 2024). This approach was not intended to diminish the value of cone calorimetry in flame-retardancy assessment, but rather to complement it with ASTM E84 testing, which provides additional insights under more realistic fire conditions.

Materials and methods

Sample preparation

We obtained heat-dried cedar (*Cryptomeria japonica*), used as exterior building siding, from Gaonwood, Co., Ltd. in Jeonju, Korea. The timber was standardized to be 21 mm thick, 151 mm wide, and 2,500 mm long. Our previous research indicated that grooved wood significantly increased chemical uptake and improved fire retardant performance by increasing the surface area (Jang et al. 2024a). Therefore, we grooved the surface of the cedar siding, as shown in Figure 1.

Flame retardant

The inorganic non-halogenated flame retardant employed in this study was independently developed and patented by our research team (Park 2013). The primary components of flame retardants are diammonium phosphate (DAP), ammonium polyphosphate (APP), anhydrous borax, and water. The solids content of the flame retardant was 27%.

This formulation leveraged the complementary effects of phosphorus- and boron-containing compounds, which, when exposed to heat, facilitated the development of both a protective char layer and an intumescent barrier. These layers functioned as physical shields, significantly limiting the penetration of oxygen and thermal energy.

Vacuum-pressure impregnation process

The cedar-siding samples underwent vacuum-pressure impregnation to ensure the deep penetration of the flame retardant. Initially, the samples were placed in an impregnation chamber, where they were subjected to a vacuum of -0.1 MPa using a vacuum pump for approximately 3 min. This process removed air from inside the chamber and on the wood surface, facilitating the penetration of the flame retardant.

Subsequently, the flame-retardant solution was introduced into the chamber for >10 min. The system was then pressurized to approximately 1.5–1.7 MPa and maintained under this condition for 60 min to ensure thorough diffusion of the flame retardant into the wood pore structure. Following the pressure phase, the flame retardant was extracted from the chamber within 10 min, and the specimen was again subjected to vacuum conditions (-0.1 MPa) for an additional 10 min to remove the residual surface solution and promote uniform distribution.

The final solids content of the flame retardant within the cedar siding was 162 ± 11 kg/m³. According to prior cone calorimetry testing conducted by our research group, cedar wood achieves the required flame-retardant performance threshold when impregnated with a minimum of 144.6 kg/m³ of flame retardant (Jo et al. 2024). Therefore, the authors predicted that the treated specimens would satisfy the necessary criteria for fire-retardant.

To stabilize the chemical treatment and moisture levels, the impregnated wood was air-dried under controlled laboratory conditions (20 ± 3°C, 60 ± 5% relative humidity) for approximately four weeks. After drying, the moisture content was approximately 12%, as determined using an electronic moisture meter (model: Testo 606-1, Testo SE & Co. KGaA, Germany), indicating its suitability for further thermal performance evaluation (Jo et al. 2024; Lardet et al. 2024).

Cone calorimetry test

The quasi-noncombustible performance of the cedar-siding samples was evaluated in accordance with the MOLIT notification criteria based on the KS F ISO 5660-1 (Korean Agency for Technology and Standards 2015) cone calorimetry test method (MOLIT 2020).

Three specimens with dimensions of 100 mm × 100 mm and a moisture content of 12% were prepared. Each specimen was exposed horizontally to an external heat flux of 50 kW/m² using a cone heater. Heat release rate (HRR), total heat release (THR), mass loss rate (MLR), time to ignition (TTI) were recorded continuously during the 10-min exposure. Post-test observations included an assessment of physical damage, such as cracking, melting, or penetration, in accordance with quasi-noncombustible material performance requirements.

To qualify as a flame retardant, materials must meet stringent criteria under thermal stress: the THR must remain below 8 MJ/m² during the initial 5 min of exposure, the peak HRR must not exceed 200 kW/m² for at least 10 continuous seconds, and the specimen must show no signs of structural compromise, such as cracking, perforation, or melting, after 5 min of heating.

In comparison, quasi-noncombustible materials are subject to slightly different standards. They must maintain a THR under 8 MJ/m² over a 10-min heating period, maintain a peak HRR below 200 kW/m² for a minimum of 10 s, and exhibit no critical damage, breach-like cracks, or melt-through after 10 min of thermal exposure.

These differences in the threshold values reflect stricter fire safety requirements for quasi-noncombustible materials. In this study, the cone calorimetry test was conducted by Korea Conformity Laboratories (KCL, 7, Nambusunhwan-ro 319-gil, Seocho-gu, Seoul).

Steiner tunnel test based on ASTM E84

The cone calorimetry test was performed by applying radiant heat to a small test specimen (100 mm × 100 mm). By contrast, the Steiner tunnel test involved a real fire test on actual wood (21 mm thick, 151 mm wide, and 2,500 mm long), allowing a more detailed investigation into the fire safety of the occupants.

Surface burning characteristics of the flame-retardant-treated cedar siding were assessed using the ASTM E84 standard test method (ASTM International 2024). This method evaluates the FSI and SDI of building materials under controlled fire-exposure conditions. The test lasted 10 min, during which the FSI was determined by calculating the area beneath the curve of the flame tip position over time. Cement board yielded an FSI of zero, whereas red oak served as a reference material with a normalized value close to 100.

The SDI was computed by multiplying the ratio of the area under the light absorption curve over time to that for a standard heptane pan fire by 100.

The ASTM E84 standard (ASTM International 2024) evaluates flame-retardant-treated materials according to their FSI and SDI values. The materials were classified into three classes: Class A, Class B, and Class C. Class A represents the highest flame retardancy, with an FSI between 0 and 25 and an SDI below 450. Class B represents an FSI between 26 and 75, whereas Class C corresponds to a higher flame spread potential, with an FSI between 76 and 200. The SDI must remain below 450 for all classes.

Figure 2 shows the Steiner tunnel. Nineteen observation windows were placed at 300 mm intervals in a 7.5 m-long tunnel, each of which recorded the position of the flame front over time. The FSI was then calculated using these data.

The Steiner tunnel furnace was preheated to a minimum brick temperature of 65.6°C and then cooled to 40.6 ± 2.8°C. The specimen was mounted horizontally on the ceiling, with the exposed surface facing downward toward the ignition source. A protective fiber cement board was placed behind the specimen to shield the tunnel cover. Airflow was maintained at 1.22 m/s through a tunnel. The specimens were preheated for 2 min prior to ignition. Two burners delivering a combined heat output of 89 kW were ignited and operated continuously for 10 min.

The flame propagation was tracked visually along the tunnel length by an observer. Smoke density was measured using a photometric system installed in the exhaust duct. The laboratory environment was maintained at a temperature of 22.2°C and a relative humidity of 40%. Specimen moisture content was 12%. In this study, the Steiner tunnel test was conducted by KCL.

Results and discussion

Cone calorimetry test

Cone calorimetry tests were conducted on three individual cedar-sided specimens to assess their fire-safety performance. Table 1 presents the THR per unit area for cedar sidings. All values were below the regulatory threshold of 8 MJ/m².

Our previous study (Jo et al. 2024) proposed a regression model that predicted the THR would remain below 8 MJ/m² when the SCFI exceeded 144.6 kg/m³, provided the flame retardant was impregnated into cedar. In this study, the SCFI was approximately 162 kg/m³, and the measured THR was <8 MJ/m². These results are consistent with the values predicted by the existing regression model and can be interpreted as an experimental confirmation of the model's reliability and applicability.

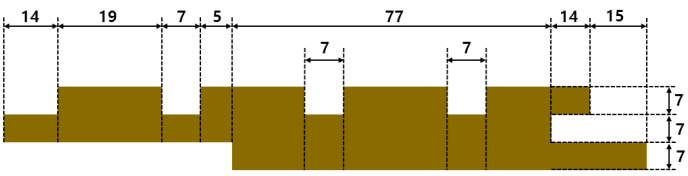

Figure 1. Schematic of the cedar siding material with grooves (unit: mm).

Figure 2. Steiner tunnel tester at KCL.

Table 1. Cone calorimetry test results for the cedar siding material.

Test item	Test results			MOLIT notification criteria
	Rep 1	Rep 2	Rep 3	
THR per unit area (8 MJ/m²)	7.7	1.6	5.1	≤8 MJ/m²
Time exceeding 200 kW/m² HRR continuously (s)	0	0	0	≤10 s
Presence of harmful fire-related factors in test specimen	None	None	None	Should be none

In addition, none of the samples exhibited a continuous HRR exceeding 200 kW/m² for >0 s, satisfying the criterion of ≤10 s. Furthermore, no harmful fire-related factors were detected in the specimens.

These consistent results across all three samples demonstrated that the cedar-siding material maintained stable thermal behavior under high-temperature conditions and met the required standard of quasi-noncombustible performance.

Results of Steiner tunnel test

Figure 3 illustrates the flame spread and smoke development behavior of flame-retardant-treated cedar siding under the ASTM E84 Steiner tunnel test (ASTM International 2024). The flame spread curve (black line with circular markers) indicated delayed ignition, initiating at approximately 4.5 min, followed by a gradual increase in flame propagation from 2.5° to 5° over the 10-min test duration. This slow and limited flame spread indicated effective thermal insulation and combustion resistance.

By contrast, the smoke-developed curve (blue line) remained nearly flat and close to 0% obscuration throughout the test period, suggesting minimal smoke generation. This is a critical safety feature because lower smoke production corresponds to better visibility and lower risk of inhaling toxins during fire events.

Figure 4 shows the cedar-sided specimens before (a) and after (b) the ASTM E84 Steiner tunnel test (ASTM International 2024). The untreated surface of the flame-retardant cedar siding (a) appeared clean and structurally intact, with uniform coloration and no visible damage. This baseline condition highlighted the initial integrity of the material before thermal exposure. Image (b) shows the post-test condition, where the specimens exhibited significant charring and surface blackening, indicative of exposure to elevated temperatures and combustion. Despite visible discoloration, the absence of deep cracks, perforations, or melt-throughs confirmed the structural resilience of the material under fire conditions.

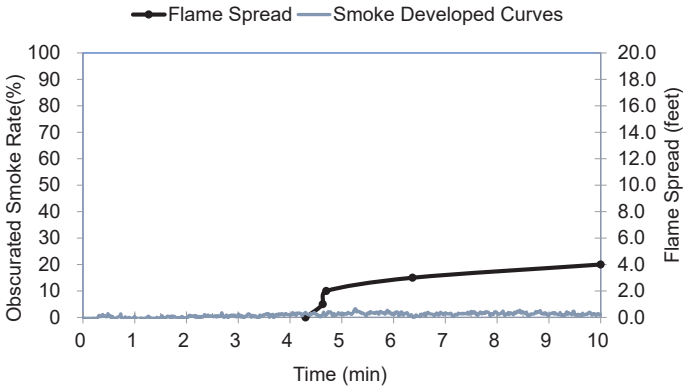

Figure 3. Flame spread and smoke suppression characteristics of the flame-retardant-treated cedar siding under the ASTM E84-24 test (ASTM International 2024).

These visual observations aligned with the quantitative data shown in Figure 4, where the flame spread remained limited (rising gradually from 2.5° to 5° over 10 min), and the smoke development was minimal throughout the test. Photographic and graphical evidence both demonstrated that the flame-retardant treatment mitigated fire propagation and smoke emission, producing a quasi-noncombustible material suitable for exterior applications.

Table 2 presents the FSD and SDI values obtained in this study, which satisfied the ASTM E84 Class A rating. These results indicated that the cedar siding material performed well in terms of securing visibility and safety in actual fire situations. The above results confirmed that cedar siding qualifies as a Class A fire-retardant material according to ASTM E84 standards (ASTM International 2024) and has sufficient quasi-

Table 2. FSI and SDI results for the cedar siding material subjected to the ASTM E84 Steiner tunnel test.

Index	Value	ASTM E84 Classification Criteria
FSI	10	Class A: 0–25 Class B: 26–75 Class C: 76–200
SDI	10	Class A: <450

Figure 4. Photographs of cedar siding specimens before (a) and after (b) Steiner tunnel testing.

noncombustible performance as an exterior building material. However, further weathering tests will be required to verify the ability of this system to perform in outdoor exposures.

Taken together, these results demonstrate that the treated cedar siding exhibited stable combustion behavior, suppressed rapid flame propagation, and significantly limited smoke emissions. These characteristics confirm its suitability as a quasi-noncombustible exterior material compliant with the ASTM E84 Class A standards (ASTM International 2024). In future work, we plan to conduct durability testing on flame-retardant-treated cedar siding exposed to weathering.

Conclusions

This study evaluated the fire safety performance of a cedar exterior siding material manufactured via vacuum/pressure impregnated with a flame retardant. Cone calorimetry tests based on KS F ISO 5660-1 (Korean Agency for Technology and Standards 2015) indicated that the flame-retardant-treated cedar siding material met the THR and HRR standards, confirming its applicability as a quasi-noncombustible material. In addition, it received a Class A rating in the ASTM E84 test (ASTM International 2024), which simulates real-world fire conditions. This indicates that flame-retardant-treated cedar siding is a reliable building material that can ensure occupant safety, even in emergency fire situations. This research provides a crucial technical foundation for the development of eco-friendly, high-performance exterior materials and can contribute to sustainable building designs. Further tests to assess performance of the system in exterior exposures are planned.

Acknowledgments

This research was funded by the R&D Program for Forest Science Technology in Korea (FTIS-RS-2024-00400728).

References

ASTM International (2024) ASTM E84-24: Standard Test Method for Surface Burning Characteristics of Building Materials. American Society for Testing and Materials, West Conshohocken, PA, USA. https://doi.org/10.1520/E0084-24

Blanchet P, Perez C, Cabral MR (2024) Wood building construction: Trends and opportunities in structural and envelope systems. Curr For Rep 10(1):21–38. https://doi.org/10.1007/s40725-023-00196-z

Bray RJ, Tretsiakova-McNally S, Zhang J (2023) The controlled atmosphere cone calorimeter: A literature review. Fire Technol 59(5):2203–2245. https://doi.org/10.1007/s10694-023-01423-6

Chen Z, Zhang S, Ding M, Wang M, Xu X (2021) Construction of a phytic acid–silica system in wood for highly efficient flame retardancy and smoke suppression. Mater 14(15):4164. https://doi.org/10.3390/ma14154164

Emre Ilgin H, Karjalainen M (2022) Massive wood construction in Finland: Past, present, and future. In Wood Industry - Past, Present and Future

Outlook, ed. G Du and X Zhou. InTech Open. https://dx.doi.org/10.5772/intechopen.104979

Gao Y, Feng S, Yan L, Chu T, Wang Z, Xiao J, Xie H, Zhang J, Wang Z (2024) Flame retardancy of densified wood modified by bio-material based flame retardant. Fire Technol 60(5):3671–3688. https://doi.org/10.1007/s10694-024-01594-w

Hansen-Bruhn I, Hull TR (2023) Flammability and burning behaviour of fire protected timber. Fire Saf J 140:103918. https://doi.org/10.1016/j.firesaf.2023.103918

Holeček T, Šedivka P, Sahula L, Berčák R, Zeidler A, Hájková K (2025) Investigation of pressure vacuum impregnation using inorganic, organic, and natural fire retardants on beech wood (*Fagus sylvatica*) and its impact on fire resistance. Fire 8(8):318. https://doi.org/10.3390/fire8080318

Jang E-S, Anno Y, Park W-C, Park H-J (2025a) Optimal impregnation amounts of flame retardant for semi-combustible hinoki cypress (*Chamaecyparis obtusa*) plywood. BioResources 20(4):9595–9605. https://doi.org/10.15376/biores.20.4.9595-9605

Jang E-S, Jo S-U, Park H-J (2024a) Effect of grooving pretreatment on flame retardant vacuum-pressure impregnation performance of full-size timbers. J Wood Sci 70(1):57. https://doi.org/10.1186/s10086-024-02172-y

Jang E-S, Kang C-W (2022) Can the physical properties of wood samples be predicted from photographs displayed on a monitor? Wood Res 67(5):888–893. https://doi.org/10.37763/wr.1336-4561/67.5.888893

Jang E-S, Kang XJ, Jo S-U, Park H-J (2024b) Preliminary investigation on the vacuum pressure impregnation performance of flame retardant for larch (*Larix kaempferi*) depending on grooving type. BioResources 19(4):9606–9615. https://doi.org/10.15376/biores.19.4.9606-9615

Jang ES, Lim G-T, Park H-J (2025b) Impregnation efficiency of flame retardants in hinoki cypress (*Chamaecyparis obtusa*) plywood using the vacuum-pressure method. Wood Res 70(3):470–477. https://doi.org/10.37763/wr.1336-4561/70.3.470477

Jo S-U, Chae H-B, Park H-J, Jang E-S (2024) The optimal impregnation amounts of flame-retardant for Korean larch and Japanese cedar building materials. Wood Res 69(1):179–186. https://doi.org/10.37763/wr.1336-4561/69.1.179186

Korean Agency for Technology and Standards (2015) KS F ISO 5660-1: Reaction-to-fire tests—Heat release, smoke production and mass loss rate—Part 1: Heat release rate (cone calorimeter method) and smoke production rate (dynamic measurement). Korean Agency for Technology and Standards, Seoul, Korea.

Lardet P, Coimbra A, Terrei L, Koutaiba E, Mole-Antoniazza R, Giovannelli G (2024) An empirical correlation for burning of spruce wood in cone calorimeter for different heat fluxes. Fire Technol 60(6):3883–3902. https://doi.org/10.1007/s10694-024-01603-y

Leszczyszyn E, Heräjärvi H, Verkasalo E, Garcia-Jaca J, Araya-Letelier G, Lanvin J-D, Bidzińska G, Augustyniak-Wysocka D, Kies U, Calvillo A (2022) The future of wood construction: Opportunities and barriers based on surveys in Europe and Chile. Sustainability 14(7):4358. https://doi.org/10.3390/su14074358

Liang Y, Jian H, Deng C, Xu J, Liu Y, Park H, Wen M, Sun Y (2023) Research and application of biomass-based wood flame retardants: a review. Polym 15(4):950. https://doi.org/10.3390/polym15040950

Lowden LA, Hull TR (2013) Flammability behaviour of wood and a review of the methods for its reduction. Fire Sci Rev 2(1):4. https://doi.org/10.1186/2193-0414-2-4

Mergel C, Menrad K, Decker T (2024) Which factors influence consumers' selection of wood as a building material for houses? Can J For Res 54(4):467–478. https://doi.org/10.1139/cjfr-2023-0197

MOLIT 2020-1053 (2020) Fire Retardant Performance of Building Finishing Materials and Fire Spread Prevention Structural Standards. Ministry of Land, Infrastructure and Transport (MOLIT), Sejong, Korea

Park H-J (2013) Flame-retardant resin for wood impregnation. Korean Patent KR10-2014-0023853A.

Wu Z-g, Deng X, Li L-f, Yu L-p, Chen J, Zhang B-g, Xi X-d, Zhang Q-y (2021) Investigation the fire hazard of plywoods using a cone calorimeter. Wood Res 66(6):933–942. https://doi.org/10.37763/wr.1336-4561/66.6.933942

Zhang X, Joseph P, Guerrieri M, Moinuddin K, Arun M (2025) Experimental study of pinewood samples incorporating multiple flame-retardant additives under varied heat fluxes in a cone calorimeter. Eur J Wood Wood Prod 83(1):13. https://doi.org/10.1007/s00107-024-02168-x

[This page is intentionally left blank.]